THREE ESSAYS IN COMPUTABLE EQUILIBRIUM ANALYSIS: TARIFF, PRICING, AND SHIPPING

ZHANG LINGGE

PhD

The Hong Kong Polytechnic University

2022

The Hong Kong Polytechnic University

Department of Logistics and Maritime Studies

Three Essays in Computable Equilibrium Analysis: Tariff, Pricing, and Shipping

ZHANG Lingge

A thesis submitted in partial fulfilment of the requirements for the degree of Doctor of Philosophy

December 2021

CERTIFICATE OF ORIGINALITY

I hereby declare that this thesis is my own work and that, to the best of my knowledge and belief, it reproduces no material previously published or written, nor material that has been accepted for the award of any other degree or diploma, except where due acknowledgement has been made in the text.

_____ (Signed)

_____ ZHANG Lingge_____ (Name of student)

ABSTRACT

This thesis consists of three studies on developing computable equilibrium models in international trade research. In the first study, we apply a computable general equilibrium model to analyze the impact of import tariff reduction on national economies in China. Under the Belt & Road initiative, China will conclude more Free Trade Agreements with other counties, and establish more Free Trade Zones. It is expected that the Chinese import tariff rate may continue to decrease. Based on the social accounting matrix of 2012, the model results show that, with the equilibrium of international balance of payment, such a tariff reduction can increase imports, exports, GDP, and resident consumption. In particular, the tariff reduction can bring down the trade surplus and price of GDP. It indicates that the tariff reduction can release the pressure of currency appreciation and resist inflation.

In the second study, we develop an equilibrium model to investigate the pricing mechanism in the Asian liquified natural gas (LNG) market. The market is experiencing a heated debate on whether to retain the oil-indexed pricing mechanism. As the spot gas prices in Asia decoupled from the oil prices, more researchers argued that the oil-indexed pricing mechanism failed to reflect the market fundamentals of Asian LNG. A more efficient pricing benchmark is needed to replace the oil-indexation in pricing LNG. To solve the problem, we investigate the possibility of using the Japan-Korea-Marker (JKM) price as the Asian LNG pricing benchmark. The model incorporates the risk-averse importer and exporter, who optimize their risk-profit tradeoffs by deciding their portfolios composed by long-term contract (LTC) and spot trade. Based on the model, we are able to compare the pricing efficiency and the risk-profit tradeoff of importer/exporter under different benchmarks (the oil price versus the JKM price). The

results suggest that the JKM price is more efficient than the oil price as being the pricing benchmark. In particular, the JKM benchmark is favored for both exporters and importers when they are low risk-averse.

The third study explores whether shipping can affect the international iron ore trade. For this purpose, we establish an equilibrium model with endogenous shipping freight rates. This model captures the strategic behaviors and the interactions among importers, exporters, and carriers. Different from models in literature focusing on other resource trades, this model considers the heterogeneity of iron ores and the production capacity allocation of exporters. In this three-party equilibrium model, importers and exporters are described as a Cournot fashion, incorporating the endogenous freight rates derived from a carrier module. The result proves that the proposed model performs better compared with those with exogenous shipping freight rates and production capacity constraints. Using the model, we simulate a scenario of importers' budget reduction. The results show that shipping can slightly dampen the decline of iron ore trade volumes caused by the importers' budget reduction. This dampening effect varies by freight rates.

Keywords: computable equilibrium model; international trade; sea transportation; trade policy, sea freight rate

PUBLICATIONS ARISING FROM THE THESIS

Yang, Dong, Lingge Zhang, Meifeng Luo, and Feng Li. "Does shipping market affect international iron ore trade?–An equilibrium analysis." *Transportation Research Part E: Logistics and Transportation Review* 144 (2020): 102107.

Zhang, Lingge, Dong Yang, Shining Wu and Meifeng Luo. "Revisiting the pricing benchmarks for Asian LNG — An equilibrium analysis." *Energy Economics* (under review).

Zhang, Lingge, Meifeng Luo, Dong Yang, and Kevin Li. "Impacts of trade liberalization on Chinese economy with Belt and Road initiative." *Maritime Policy & Management* 45, no. 3 (2018): 301-318.

ACKNOWLEDGEMENT

I would like to express my gratitude to my primary supervisor, Dr. Dong Yang. Throughout my Ph.D. program, Dr. Yang has been giving me careful guidance. It was of great help to improve my academic ability. In the selection of my research direction, he always respected my interest. Even though some ideas were immature, he firmly supported me and provided abundant academic resources. His patience and encouragement dispel my self-doubt in those difficult times. The cooperation with Dr. Yang was a memorable journey. I will treasure this period.

I wish to show my appreciation to my co-supervisor, Dr. Meifeng Luo. From him, I learned the qualities that should be possessed as a researcher. The cooperation with Dr. Luo was an experience full of challenges. He was a perfect questioner in the discussion of my research. The questions proposed by him always stumped me. While struggling with these questions, I gradually realized that finding answers to these questions was of constructive significance to elaborate my studies.

I would like to thank Dr. Shingning Wu and Dr. Feng Li. As co-authors, they have made tremendous contributions to the publication of our papers. I have learned a lot from their distinguished academic abilities. I expect more cooperation opportunities with them in the future.

I would like to thank my colleagues and schoolmates, in particular, Dr. Mengchi Li, Dr. Yujie Wang, and Miss Jing Zhang. Thanks for your help in many ways. It was my great honor to work with you all.

My special thanks go to my family. Thanks for your understanding and support. The company of my family is always the driving force of my efforts.

TABLE OF CONTENTS

Chapter 1. Introduction

International trade is one of the most important economic activities that drive economic growth and development in the world. In 2019, the value of global trade was 18.89 trillion US $, accounting for 56.42% of global GDP[1]. The research on international trade devotes to exploring determinants and mechanisms related to international trade, as well as extensive linkages of international trade with other economic issues. As a consequence, it provides vital information for trade and economic policy making. To give a glance at the recent studies of international trade, we firstly retrieve the literature for international trade research on the Web of Science. Using "international trade" and "global trade" as topics, we find 8,435 records of articles and review papers from 2015 to 2020[2]. Based on this literature sample, we conduct a term co-occurrence analysis to examine hot topics and mainstream methodologies in recent international trade research. Figure 1-1 shows a network of co-occurrence terms, where the circle size represents the occurrence frequency of a co-occurrence term. According to the information described in Figure 1-1, we can provide an overview for the research on international trade published in past six years. First, traditional concerns in international trade, such as economic growth, foreign direct investment, trade flows, trade policies, comparative advantages between developed and developing countries, trade costs, trade agreements, global value chains, and trade liberalization were still the research focuses. Second, the research has extended to include the interactions between international trade and non-

[1] Data source: data of world bank. Available at https://data.worldbank.org/indicator/NE.TRD.GNFS.ZS

[2] Based on the topic search of "international trade" and "global trade", we have retrieved academic articles and review papers in the period of 2010-2020. The retrieved results include 12,115 records. Among them, 8,435 papers were published between 2015 and 2020. It indicates that 2015-2020 is the most productive period for international trade research. We therefore select the papers in the period between 2015-2020, as they are more representative for the recent trend of international trade research.

trade issues, e.g., climate changes, carbon emission, energy consumption, sustainable development, food security, and endangered species protection.

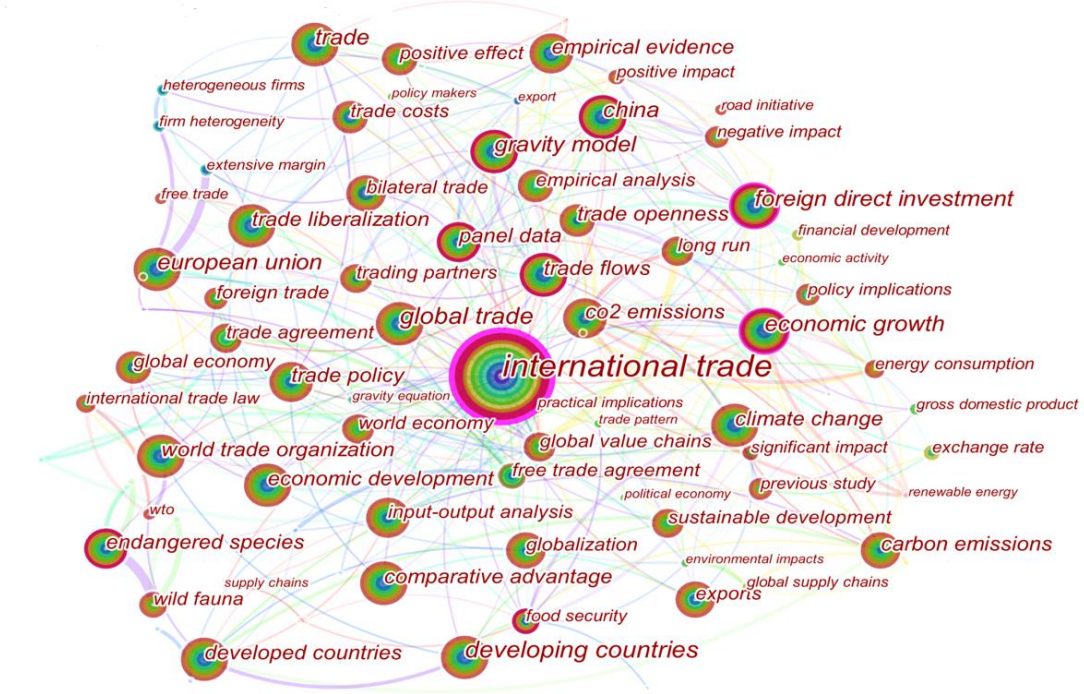

Figure 1-1. The network of co-occurrence terms in international trade research

The research diversity motivates our interests in the methodology applied in international trade research. Traditionally, international trade research emphasizes more on the theoretical explanation (Sen, 2010). However, the frequency of terms "empirical analysis" and "empirical evidence" indicates that empirical studies have widely applied in the study of international trade in the past six years. As an explanation, the development of information technology lowered the barrier to access trade data, thereby driving the methodology in trade studies into empirical approaches (Chen and Chen, 2019). Notably, Figure 1-1 shows high frequency and extensive links of the term "gravity model." It indicates that the gravity model has been the workhorse in international trade research (Yotov et al., 2016). Out of the blue, trade researchers seem

to lose interest in computable equilibrium models, for example, the Global Trade Analysis Project (GTAP) model.

The gravity model has theoretical consistency with the computable equilibrium model, as many researchers has derived the gravity specifications from various theoretical equilibrium models (e.g., Deardoff, 1998; Anderson and van Wincoop, 2003; Eaton and Kortum, 2002; Caliendo and Parro, 2015). What makes the gravity model widely applied in the international trade research? According to the discussion of Yotov et al. (2016), there are two possible reasons:

a) From the modeling standpoint, the trade gravity model is an analogy of Newton's gravity equation. It provides an intuitive and tractable formation which connects the trade volume between arbitrary two countries with their economic sizes and distance. Enormous studies have verified that it has a good empirical explanation of trade volume. For the computable equilibrium model, it is an extension of a theoretical equilibrium model by incorporating more settings of realistic details. Due to the complex relationships endogenized in the model, it is difficult to explain the trade volume directly.

b) **From the policy analysis standpoint**, the gravity model was once regarded as an empirical model lacking theoretical foundations. It can only take the ex-post analysis (e.g., evaluating the impact of an existing trade policy). For the ex-ante analysis (e.g., quantifying the future impact of a new policy), the computable equilibrium model is an efficient tool because of its capability in simulating possible policy scenarios. However, the gravity model has equipped solid theoretical foundations via its nexus with theoretical equilibrium models. It implies that the gravity model has shifted into a structural model that can also conduct the ex-ante

analysis as the computable equilibrium model does.

In facing the advantages of the gravity model, is there any application potential for the computable equilibrium model in international trade research? To answer this question, we focus on those limitations of the gravity model. Specifically, the aim of thesis is to investigate whether the computable equilibrium model can overcome those limitations. Since the gravity model has been the major tool in trade studies, its limitations naturally reflect some undiscovered impacts and linkages of trade determinants. If we can overcome them via the computable equilibrium model, we can proof the value of computable equilibrium model in uncovering those potential impacts and linkages.

We start from the limitations of the gravity model. As we mentioned, the gravity model is distinguished by its stability in explaining the stylized facts related to the trade volume. Emphasizing trade volume as the explained variable of the model, however, leads to the following limitations of the gravity model in the international trade research:

a) For a given trade policy, the gravity model performs well in analyzing its trade flow-related impacts (e.g., trade diversion or trade creation), but it cannot directly capture its wider economic impacts, such as revenue, consumption, and welfare in the trade counties (Ivus and Strong, 2007).

b) The gravity model is not a powerful tool for pricing analysis. The trade types are diversified. Even for a single commodity, there are various trade types in practice, for example, spot markets, forward contracts, and auctions. Each trade type has its independent pricing mechanism constructed by the complex pricing clauses. However, the price variable in the gravity model is an index to reflect the aggregate price level (Anderson, 2011). This results in the loss of valuable information related to the pricing process.

c) The endogeneity problems exist in the gravity model. Nearly all of the typical variables in the gravity model can simultaneously influence trade, and be influenced by trade (Kleinert and Spies, 2011). As these potential interactions are difficult to be captured via the gravity model, the reliable estimation of the policies' impacts is challenged.

Next, we showcase how to overcome these limitations using computable equilibrium models. To this end, we present three studies in this thesis. In each study, we will develop an individual computable equilibrium model to address one of the forementioned limitations. Based on the model, we will investigate a real trade issue to show the practical significance of overcoming this limitation.

In the first study, we study the tariff reduction's impacts on Chinese national economy in the context of the Belt and Road Initiative (BRI) and the development of free trade agreement. This is an example of exploring a trade policy's wider economic impacts. The gravity model can estimate the impacts of tariff reduction on imports and exports, but it is unable to examine the impacts on other economic indicators (i.e., exchange rate, resident consumption, and government revenue). We, therefore, apply a computable general equilibrium (CGE) model to represent the Chinese national economy. Compared to gravity model, the CGE model modularly describes the production, consumption, factor and investment. We can capture either the aggregation of these modules, or their allocation among social accounts (e.g., residents, enterprise, and government). The wider economic impacts of tariff reduction, thus, can be estimated. Using the real data of 2012, we simulate a series of national economic indices, including aggregate ones (e.g., GDP, GDP price) and disaggregate ones (e.g., resident consumption, government revenue). Under the assumption of equilibrium in

international balance of payment, the results ease the concern that further import tariff reduction may harm the domestic production. Rather, it points out that there is still room to improve national economy and increase the consumer utility by trade liberation.

In the second study, we show how to address pricing issue using equilibrium models. The background of this study relates to the reformation of pricing mechanism in Asian liquified natural gas (LNG) market. The market has long been dominated by the long-term contracts between gas exporters and importers, which use the oil price as the pricing benchmark. As the spot gas prices in Asia decoupled from the oil prices, many researchers argued that the oil-indexed pricing mechanism failed to reflect the market fundamentals of Asian LNG. Therefore, we set the long-term contract (LTC) as the example to investigate the possibility of using the Japan-Korea-Marker (JKM) price (i.e., a spot LNG price) as the Asian LNG pricing benchmark. For this purpose, we need to highlight: a) the complex pricing clauses ruled in the LTC; b) the intertemporal arbitrage and hedging due to the existence of both spot trade and LTC; c) the different freight rates and corresponding risks between the spot trade and LTC. As the gravity model cannot incorporate these complexities in its price variables, we develop an equilibrium pricing model under the price uncertainties. The model is built upon the mean-variance expected utility framework. It allows the risk-averse importer and exporter to optimize their risk-profit tradeoffs by deciding their LTC-spot trade portfolios. Using the model, we compared the pricing efficiency and the risk-profit tradeoff of importer/exporter under different benchmarks (the oil price versus the JKM price). The results show that the JKM price is more efficient than the oil price as being an LTC pricing benchmark. In addition, we consider the possible impact of freight liability ascription. The freight liability ascription determines whether to trade at cost-insurance-freight (CIF) price (exporter affords the freight rate) or free-on-board (FOB)

price (importer affords the freight rate). In the gravity model, there is no specified distinction between these two prices, as the demand side (importer) is the final undertaker of all trade cost. The trade volume that the gravity model concerns cannot be affected by the difference between CIF and FOB prices. Even so, the intuition tells us that the two prices may have the difference in efficiency as being pricing benchmarks. This is because the FOB price is more transparent than the CIF as it excludes the freight rates that the importer may not observe. We compare the performance of the JKM CIF benchmark and that of the JKM FOB benchmark. Unfortunately, the result rejects our intuition. The two benchmarks make little difference in pricing efficiency.

In the third study, we focus on the endogenous transport cost in international trade. In quantitative trade modeling, the transport cost is accustomed to setting as a component of the exogenous trade cost (Asturias,2020). The exogenous transport cost (i.e., the iceberg-type cost) stresses the impact of transport cost on the trade volume, while ignoring the trade volumes acting as the demand of transportation market can in turn affect the price level of transport service. Such an interactions between the transport cost and the trade volume is a typical example of gravity model's endogeneity problem. Modeling endogenous transport cost, is an approach to capture this interaction. Some researchers have attempted to endogenize the transport cost in the gravity specification via incorporating modelling transport sector from market power (Rudolph, 2009), investment decision (Kleinert and Spies, 2011) and round-trip behavior (Wong, 2018). These gravity models only describe the transport cost in a bilateral trade, but fail to consider the fact that the third parties' transport costs can affect the bilateral trade, i.e., the network effect of transport cost. We address this problem via developing a mixed complementarity-based equilibrium model including importers, exporters, and ship carriers. This model is built upon: a) heterogenous products; b) a constant elasticity

of substitution framework in demand side; c) a Cournot fashion in supply side; d) production capacity allocation; e) a two-stage minimal-cost shipping network with endogenous transport costs; f) shipping market segments that are characterized by two dimensions of the sea route and the ship type. We applied this model to investigate the international iron ore trade. Based on the real data, we compare this model to its two variants. One variant assumes exogenous transport costs. The other one assumes exogenous transport costs and no production capacity allocation. We have two findings: a) production capacity allocation can make up for profit losses brought by competition among iron ore exporters; b) the shipping network can dampen the reduction of iron ore trade volumes due to a sudden negative shock (e.g., an unexpected reduction in importers' purchasing budget).

The rest of this thesis is organized as follows. Chapter 2 studies the impacts of tariff reduction on national economy via a CGE model. Chapter 3 develops an equilibrium pricing model to investigating the pricing mechanism in Asian LNG market. Chapter 4 proposes a computable equilibrium model with endogenous transport cost to explore the interactions between transport and trade sectors. Chapter 5 draws conclusions and further studies related to this thesis.

Chapter 2. Analyzing the impact of tariff reduction policy on Chinese national economy — An CGE approach

2.1 Introduction

Since joining WTO in 2001, China has been implementing an open door policy and keep reducing its import tariff for fifteen years. According to the statistics published by

the Chinese government, the general tariff has been reduced from 15.3% in 2001 to 9.8% in 2010 and remained at that level since then. Compared with the major importing countries in the world, the Chinese import tariff is relatively low. With the Belt and Road initiative (BRI) proposed by the Chinese government in 2013 and the free trade agreement (FTA) signed with many countries along the Belt and Road, it is expected that the effective import tariff of China may continue to reduce such that further lower the barrier of international trade and accelerate the trade liberalization.

It is a common understanding that import tariff is an important measure in protecting domestic industries when they are facing competition from other countries. In considering import tariff, policymakers should also consider its impact on the whole national economy to avoid its potential negative impact on other economic indicators out of trade.

Currently, the import tariff rate in China is considered moderate. Nevertheless, the domestic industries are already having a difficult time to survive, due to the slowdown of world economic growth and increase in domestic labor costs. It is concerned that the continuing reduction in import tariffs may reduce the competitiveness of Chinese products in the domestic market, which may have negative impacts on the national economy. Chinese domestic industries may undertake risks of losing competitive advantage in the long term since they are facing structure reform and declining competitiveness. Under this background, this chapter aims to explore the national economic performance of China after further reducing the import tariff rate.

The impacts of tariff rate reduction on national economic is subjected to the interactions among the production sectors, commodity markets, and cash flows of economic agents. Empirical approaches considering the interactions between trade and

aggregate economic indices, for example, gravity models, are not appropriate for our research purpose. Therefore, we apply a Computable General Equilibrium (CGE) model in this chapter, as it allows us to a) incorporate the complex interactions in the national economy; and b) estimation both aggregate economic indicators (i.e., GDP) and disaggregate ones (i.e., resident consumption).

Using the model, we simulate different scenarios of tariff rate reduction in China. The results do not show any significant negative impacts of tariff rate reduction on Chinese economy. In particular, we find that such a reduction of tariff rate is efficient to alleviate currency appreciation and domestic inflation. Practically, these results provide evidence to support the further trade openness of China along development of the BRI.

The rest of this chapter is arranged as follows. Section 2.2 reviews the existing relevant literature. Section 2.3 describes the data collection. Section 2.4 presents the modeling framework. Section 2.5 shows the results of the model in simulating scenarios of import tariff reduction. In Section 2.6, we conduct a sensitivity analysis for calibrated parameters to examine the model stability. Section 2.7 draws the conclusion.

2.2 Literature review

The primary aim of BRI is to develop six economic corridors covering Asia, Europe, and Africa. To achieve this purpose, two major issues need to be addressed. One issue is the transport facilitation among countries along the BRI to promote their connectivity. The other one is the development of free trade agreements (FTAs) and free trade zones (FTZs) for further trade liberalization among those countries.

Numerous research has concentrated on connectivity-related issues under the BRI

from various perspectives (Wang et al., 2021). Researchers investigated the relationships between transportation infrastructure and economic growth in BIR countries (Chhetri et al., 2018; Li et al., 2018; Yii et al., 2018). They highlighted that facilitating transportation is the priority in promoting coordination of development along with BRI countries. The competition between emerging BRI corridors and traditional transportation routes is also a hot-button concern. For example, Yang et al. (2018) applied a multi-criteria decision method to compare the stakeholders' preferences in considering whether to select the traditional sea-land routes or the emerging BRI routes. The result indicated that the policymaker and the industrial practitioner have different preferences in route selection. Wen et al. (2019) developed a route utility function to investigate the route alternatives between China and Europe. The result showed the advantages of BRI corridors to traditional sea-land routes.

Also, some studies focused on the trade policies in development of the BRI (e.g., FTA and FTZ). For example, Yang and Martinez-Zarzoso (2014) analyzed the impacts of the ASEAN-China FTA on the trade between ASEAN and China based on a gravity model. The result indicated that the FTA had a significant effect on promoting trade increase among FTA members. Lu et al. (2020) applied a game theory model to investigate the competition between BRI FTA and US-Europe-Japan FTA. They found that the potential member countries prefer to choose the FTA with the larger organization, as it can bring higher welfare. Cai et al. (2021) proposed a dynamic panel data approach to estimate the impact of FTZ in China (Shanghai) on local economic growth. The result revealed that the development of FTZ is effective to increase both GDP and GDP per capita in the Shanghai region. Bao et al. (2021) built a difference-to-difference model to analyze the impact of FTZ on imports, exports, and capital flows. The result showed that FTZ is significant to improve foreign direct investment, but that

is limited to promoting trade growth.

Existing studies on the BRI have well explored the effect of enhancing connectivity and deepening trade liberation on promoting trade creation and economic growth. However, these studies draw less attention to the wider economic impacts of BRI. Specifically, we cannot obtain the systematic impact of a BRI policy (e.g., the tariff rate reduction) on a country's national economy. In this chapter, we will set the Chinese national economy as an example to fill this gap.

Although empirical approaches in existing studies on BRI FTA and FTZ are good at estimating relationships and interactions between factors, they are not designed to simulate a national economic system. The CGE model is more appropriate to perform such a task. It firstly appeared in Johansen (1960) in a study of the Norwegian national economy. The most successful CGE model should be the GTAP model. It has been an important policy simulation tool to analyze various economic issues, such as trade war (Rosyadi et al., 2018), FTA (Siriwardana and Yang, 2008; Nag and Sikdar, 2011; Zhao, 2020), energy consumption (Chepeliev and McDougall, 2018), and regional differences (Van et al., 2017). In addition to GTAP model, some researchers develop CGE models driven by their research issues. For example, Devarajan et al. (2011) proposed a disaggregated CGE model to study the tax policies of South African. This model highlighted the circulation in domestic commodity and capital markets. Naranpanawa and Arora (2014) built a single-country CGE model at the regional level to study the link between trade liberalization and regional disparities in India. Qi et al. (2016) extended a CGE model by incorporating the description of an energy sector, to analyze the Chinese CO2 emission plan and even the whole Chinese climate policy up to 2050. We aim to simulate the impact of tariff rate reduction on national economy. Therefore,

the CGE model in this chapter focuses more on the descriptions of the cash flow relationships among different economic agents.

This chapter fill the gap for studying the systematic impacts of BRI on national economy of member countries. Empirically, it contributes to the understanding of the possible domestic impacts of further opening up of the Chinese economy with development of the BRI.

2.3 Data collection

We group the national economic system into 17 industrial sectors following the classification in the Input-Output Table (2012) from National Bureau of Statistics of China. Each sector has two accounts to store production and commodity data. The production and commodity data of the 17 sectors are the basis to generate the social accounting matrix (SAM) table which is the database of the CGE model. The specification of these 17 sectors is shown in Table 2-1.

Table 2-1. Sectors in the CGE model

No.	Sector
1	farming, forestry, animal husbandry and fishery
2	Mining industry
3	Food, beverage and tobacco manufacture
4	Textile, clothing and leather manufacture
5	Coking, fuel gas and petroleum industries
6	Chemical industry
7	Non-metallic mineral manufacture
8	Metallic mineral manufacture
9	Mechanical equipment manufacture
10	Other manufacture
11	Electricity, heat and Hydraulic industries
12	Architecture industry
13	Transport, warehousing, postal service and IT industries
14	Retail & wholesale trade, hotel & food industries
15	Real estate, leasing and commercial service
16	Financial service
17	Other service industries

The explanations of SAM table are given in Appendix A-1. The data sources of this table are input-output Table of 2012 (China Statistical Yearbook-2015), the Flows-of-Funds Table of 2012 (China Statistical Yearbook-2014), Balance of Payments Statement of 2012 (China Statistical Yearbook-2013), and Fiscal Yearbook of China-2013. The principle of generating such a table can be found in Keuning and Deruijter (1988).

In preparing the SAM, the import tariff rate is not sector or commodity-specific. Rather, it is a weighted average import tariff rate calculated using the following equation:

$$\text{import tariff rate} = \frac{\text{import tariff}}{\text{import value} + \text{import tariff}}$$

where the total import tariff is from Fiscal Yearbook of China-2013 and total import value is from Input-Output Table of 2012.

There are several assumptions for the design of the SAM table. First, the net production tax is assumed as the total value-added tax subtracting the production subsidies from the government. Since we just consider two production inputs (i.e., labor and capital), the total value-added tax is the sum of value-added tax from labor and capital. Second, both labor and capital are assumed to be taxed at the same rate. Third, treasury's liability revenue is defined as the cash flow from the "Investment & saving" account to the "Government" account. It is simplified as the government's earning from treasury bonds. We assume that the purpose of the government to issue the treasury bond is only to make up the fiscal deficit. Thus, the treasury's liability revenue should numerically equal the financial deficit in the SAM table.

2.4 Modeling framework

Our CGE model includes three base modules: a) the input-output module; b) the cash flow module; c) the market equilibrium module. The input-output module describes the supply and demand relationships between producers and consumers. Producers maximize their profits by taking inputs from the factor market and commodity market. Consumers maximize their utility subject to the budget constraint. The budgets are derived from their incomes via providing labor or capital in the factor market. The cash flow module describes the relationships between incomes, expenditures, and savings in the four social accounts (i.e., resident, enterprise, government, and the rest of world). The market equilibrium module describes the market clearing and closure conditions to

ensure the general equilibrium.

2.4.1 Input-output module

We use a nested Constant Elasticity of Substitution (CES) function to describe the production process. In each sector, the producer uses value-added input and intermediate input to produce output. The value-added input is generated from capital and labor through a CES function. The output is either supplied in the domestic market or exported to the rest of world. The total consumption is determined by an Armington function with two inputs: the outputs supplied in the domestic market and the import. The total consumption is partly used as intermediate inputs in domestic production. The rest acts as the final goods for the consumption of the resident and the government. Figure 2-1 shows the intuitive structure of this module.

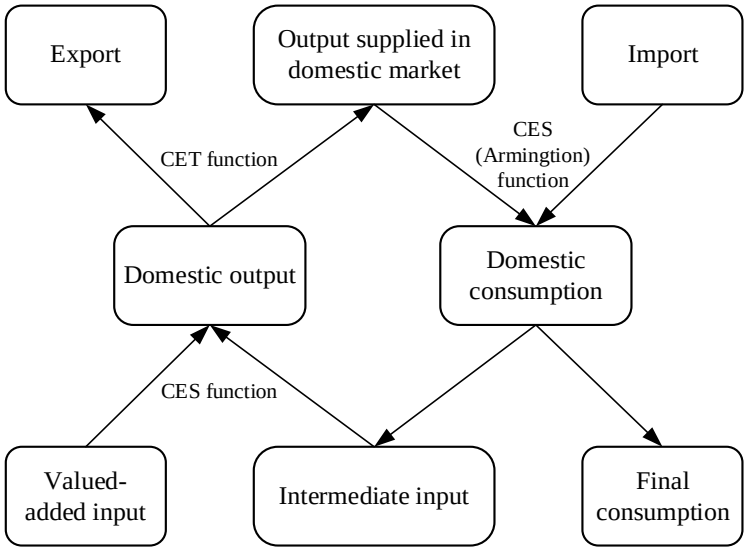

Figure 2-1. The structure of input-output module

2.4.2 Cash flow module

In this module, we model the incomes and expenditures of the four accounts: resident, enterprise, government, and the rest of the world. For the resident account, the income

is from three sources: wage income, domestic capital earning, and transfer payment. The transfer payment may come from government, foreign (the rest of world) accounts, and enterprise. Resident expenditure includes income tax and expenses on commodity consumption. The leftover after the expenditure is the resident's savings. Since this study is conducted at the national level, it is appropriate to assume that the resident consumption propensity is consistent.

For the enterprise account, its earnings are derived from capital input. Its expenditure includes income tax and transfer payments to residents. Enterprise also invests. The propensity to invest in each sector is assumed exogenous.

Government earnings come from tax revenue, transfer payments from the foreign account, and debt or financial deficit. Its expenditures include commodity expenditures and transfer payments to resident and foreign accounts. The difference between these two is the government saving.

Foreign (the rest of world) account is applied to model the balance of international payments. The income of this account mainly comes from imports to China, Chinese capital investment in the international market, and transfer payments from the Chinese government. The expenditure consists of Chinese exports, transfer payments to the resident account, and the government account in China. The difference between income and expenditure is still the saving. In addition, we use both GDP and the price of GDP, or GDP deflator, to represent the condition of the national economy.

2.4.3 Market equilibrium module

In this module, four market clearing conditions are considered to ensure the existence of general equilibrium. First, in the commodity market, the aggregate supply of every

sector should be equal to the sum of intermediate input of production in all sectors, consumption of the resident, consumption of the government, and investment. Second, the demand for labor in production should be equal to its supply by the resident in the labor market. Third, the capital supply should equal its demand; Finally, the investment (including the revenue from holding government bonds) should balance with total savings from the resident, enterprise, government, and foreign account.

In addition to the market clearing conditions, it is also necessary to specify the closure conditions by setting the key exogenous variables, such as wage rate, capital return, resident income, and saving in the foreign account, to ensure that the model can fit the real macroeconomic foundations. The base year in this study is 2012. In that year, the unemployment rate in China was at a high level (4.1%). It indicates that the Chinese economy in 2012 had not recovered from the financial crisis of 2008. Therefore, we adopt the Keynesian closure conditions which highlight the nonnegligible unemployed labor and capital in a sluggish economy.

We present the detailed expression of this CGE model in Appendix A-2. The value of relevant parameters in the model is shown in Appendix A-3.

2.5 Results of simulating tariff reduction

With the Road Initiative, it is expected that the overall import tariff of China will further decrease. In this section, we applied the CGE model to simulate the import tariff reduction. The initial value of the import tariff rate is 2.3%, which is the average import tariff rate in 2012. We reduce this tariff rate to 0 with five equal intervals, each by 0.46%. We examine the comprehensive impacts of tariff reduction based on a broad indicator selection. These indicators can be classified into three categories: a) trade indicators

represented by import and export; b) disaggregate indicators represented by resident consumption (RC) and government revenue (GR); c) aggregate indicators represented by GDP and price of GDP.

In the first place, we examine the trade indictors as the tariff reduction essentially is a trade policy. As shown in Table 2-2, the reduction of tariff rate can increase both imports and exports of China. The reason for export growth is the assumption of the international balance of payments. In the foreign account (i.e., rest of world account, see Appendix A-2), the income comes from the Chinese imports and the transfer payment from China to the foreign account. The expenditure consists of Chinese exports and the transfer payment from the foreign to China. In the CGE model, these transfer payments are fixed as exogenous variables. Due to the Keynesian Closure, the net saving (i.e., income minus expenditure) in the foreign account is also fixed. Therefore, when the imports increase, the exports increase to keep the international balance of payments. Notably, the trade surplus decreases with the tariff reduction, since the imports increase faster than the exports. The smaller trade surplus is good for China, as it can alleviate the long-term pressures on currency appreciation. As shown in Table 2-2, the exchange rate keeps at a stable level with the tariff reduction. This finding has an important implication for China to use the trade policies to stabilize the exchange rate.

Table 2-2. Imports and exports

Import tariff %	Imports	Exports	Trade surplus	Exchange rate
2.3	12210.98	13674.62	1463.64	1.000
1.84	12321.51	13782.27	1460.76	1.000
1.38	12434.09	13891.93	1457.84	1.000
0.92	12548.79	14003.66	1454.87	1.000
0.46	12665.65	14117.52	1451.87	1.001
0	12784.76	14233.57	1448.81	1.001

Note: The unit of imports, exports and trade surplus is billion ¥.

Next, we discuss the impacts of tariff reduction on resident consumption and government revenue. As shown in Table 2-3, a reduction in tariff results in the growth of resident consumption, as it lowers the price level in the domestic market. It indicates that the tariff reduction is beneficial to the domestic consuming market expansion, which can further motivate the increase of domestic production in China. Government revenue declines because of the reduction of import tariffs. Nevertheless, the import tariff is just a small component in the government revenue, thereby affecting a little on the purchasing power of the Chinese government. It is noted that both value-add and income taxes increase with the reduction of import tariffs. This further proves the effect of reducing tariffs on promoting the domestic production of China. However, such an effect is not significant enough to allow the growth of value-add and income taxes to offset the reduction of tariffs.

Table 2-3. Resident consumption and government revenue

Tariff %	RC	GR		Value-added tax		Income tax		Import Tariff	
		Value	Change	Value	Change	Value	Change	Value	Change
2.3	19854.97	17919.21	0	7360.80	0	2551.38	0	274.45	0
1.84	19871.94	17869.49	-49.92	7363.31	2.51	2552.02	0.64	221.58	-52.87
1.38	19889.12	17818.94	-100.27	7365.94	5.14	2552.69	1.31	167.72	-106.73
0.92	19906.49	17767.52	-151.69	7368.70	7.9	2553.38	2	112.86	-161.59
0.46	19924.08	17715.23	-203.98	7371.59	10.79	2554.1	2.72	56.96	-217.49
0	19941.88	17662.04	-257.17	7374.61	13.81	2554.85	3.47	0	-274.45

Note: The unit is billion ¥.

Table 2-4 shows that the impacts of tariff reduction on the national economy of China at the aggregate level. As displayed in the table, the GDP increases with the declining tariff rate. This is majorly attributed to the domestic production growths promoted by the tariff reduction indirectly. Notably, the decline of the price of GDP

implies that the nominal GDP converges to the real GDP. This result indicates that reducing import tariffs is also efficient to tame inflation.

Table 2-4. GDP and price of GDP

Import tariff %	GDP	Price of GDP
2.3	53681.12	1.005
1.84	53695.22	1.004
1.38	53709.47	1.003
0.92	53723.88	1.002
0.46	53738.45	1.001
0	53753.20	1.000

Note: 1) The unit of GDP is billion ¥. 2) Price of GDP is the ratio of nominal GDP to the real GDP.

We summarize the impacts of import tariff reduction on the national economy of China from these results. Briefly, reducing the import tariff can: a) promote both imports and exports; b) motivate the growths of domestic consumption and GDP; c) maintain the stability of exchange rate combined with the balance of international payments; d) resist the currency inflation; e) decrease the revenue of the government.

2.6 Sensitivity analysis for elasticity of commodity substitution

The CGE model includes many parameters (e.g., elasticities of substitution and transformation) which need to be estimated via regression. Restricted by the data availability, the parameter value that we apply for this study are the results from Zhai and Hertel (2005), Glendinning et al. (2002), and Glomsrød and Taoyuan (2005). As these parameters are estimated via an outdated database, we conduct a sensitivity analysis based on the Monte Carlo approach to examine the impacts of possible parameters' bias on the model results. As the focus of this study is the import tariff reduction, we select the elasticity of substitution between imported goods and domestic produced commodities for the analysis.

Table 2-5 lists the assumptions for the sensitivity analysis, including the initial value for the elasticities of substitution for the 17 sectors, their possible value ranges, and the assumption of distributions.

Table 2-5 the elasticity of substitution between imported and domestic commodities

Commodity	Sectors	Initial values	Uniform distribution
c_1	Farming, forestry, animal husbandry and fishery	0.6	[0.3, 0.9]
c_2	Mining industry	0.7	[0.35, 1.05]
c_3	Food, beverage and tobacco manufacture	0.7	[0.35, 1.05]
c_4	Textile, clothing and leather manufacture	0.7	[0.35, 1.05]
c_5	Coking, fuel gas and petroleum industries	0.5	[0.25, 0.75]
c_6	Chemical industry	0.5	[0.25, 0.75]
c_7	Non-metallic mineral manufacture	0.5	[0.25, 0.75]
c_8	Metallic mineral manufacture	0.5	[0.25, 0.75]
c_9	Mechanical equipment manufacture	0.5	[0.25, 0.75]
c_{10}	Other manufacture	0.7	[0.35, 1.05]
c_{11}	Electricity, heat and Hydraulic industries	0.5	[0.25, 0.75]
c_{12}	Architecture industry	0.3	[0.15, 0.45]
c_{13}	Transport, warehousing, postal service and IT industries	0.9	[0.45, 1.35]
c_{14}	Retail & wholesale trade, hotel & food industries	0.6	[0.3, 0.9]
c_{15}	Real estate, leasing and commercial service	0.6	[0.3, 0.9]
c_{16}	Financial service	0.6	[0.3, 0.9]
c_{17}	Other service industries	0.6	[0.3, 0.9]

We analyze the sensitivity of substitution parameter to the result based on the simulation of 30% tariff rate reduction[3], i.e., the tariff rate is equal to 1.61%. We repeat the simulation two thousand experiments. For each of them, a new set of elasticities with be generated randomly according to their distributions. The simulation results are summarized in Table 2-6.

[3] From joining WTO in 2001 to launching BRI in 2013, the tariff rate in China has been reduced by 36% (see, Fiscal Yearbook of China-2013). Based on this experience, a 30% reduction in tariff rate should be a reasonable assumption for ten years after launching BRI.

Table 2-6 Sensitivity analysis results based on the 30% reduction in import tariff

Variables	Initial values	Average values	Standard deviation	Relative error (%)	Confidence interval (95%)
GDP	537023.21	537622.36	525.63	0.11	[535271.67, 539973.05]
Price of GDP	1.004	1.00398	2.44E -5	0	[1.003, 1.005]
Imports	123775.43	122633.40	19327.09	0.92	[36200.01, 209066.79]
Exports	138368.50	138079.14	18552.10	0.21	[55111.60, 221046.67]
GR	178443.20	178549.13	186.13	0.06	[177716.73, 179381.53]
RC	198805.04	198551.52	249.37	0.13	[197436.32, 199666.73]

In Table 2-6, we can see that the values of sensitivity analysis for selected variables have little change compared with their initial values. The two maximal relative errors are 0.92% and 0.21% for imports and exports, respectively. The two minimum relative errors are 0 and 0.06% for the price of GDP and revenue of the government, respectively. Furthermore, Table 2-6 also provides the 95% confidence interval for the simulated value. It shows that the initial value of each variable lies within the range of confidence interval. This sensitivity analysis indicates that the results from the CGE model are accepted at the 95% confidence level. Thus, the elasticities we applied in the model should be reliable.

2.7 Conclusion

The import tariff rate is an important policy instrument for a government to adjust the structure of foreign trade and spark domestic production. The implementation of the BRI may further reduce the tariff rate. In this research, we investigated the impact of import tariff rate reduction on the major economic variables of the Chinese national economy. A CGE model was applied to describe the relationships among production, consumption, imports, and exports for 17 sectors of the national economy. This model

allows us to study the impacts of the major economic variables through complex interactions among different factors.

With the decrease of import tariff rate, our results show that imports can increase. Due to the assumption of balanced international payments, exports also increase. Although the export increase is not as fast as that in imports, the trade surplus still keeps on a considerable scale. Besides, the smaller trade surplus is helpful to alleviate the pressure of currency appreciation. For the wider economic impacts, the tariff reduction is positive to resident consumption, GDP, and price of GDP. It is negative to government revenue, but this effect is not significant.

Chapter 3. Revisiting the pricing benchmarks for Asian LNG — An equilibrium analysis

3.1 Introduction

The global natural gas market is regarded as a composite of three relatively independent regional markets (North America, Europe, and Asia), each with significant price differentials. In the Asian market, the gas price over the last ten years has generally been higher than that in Europe and North America, a phenomenon often called the "Asian premium" (as shown in Figure 3-1).

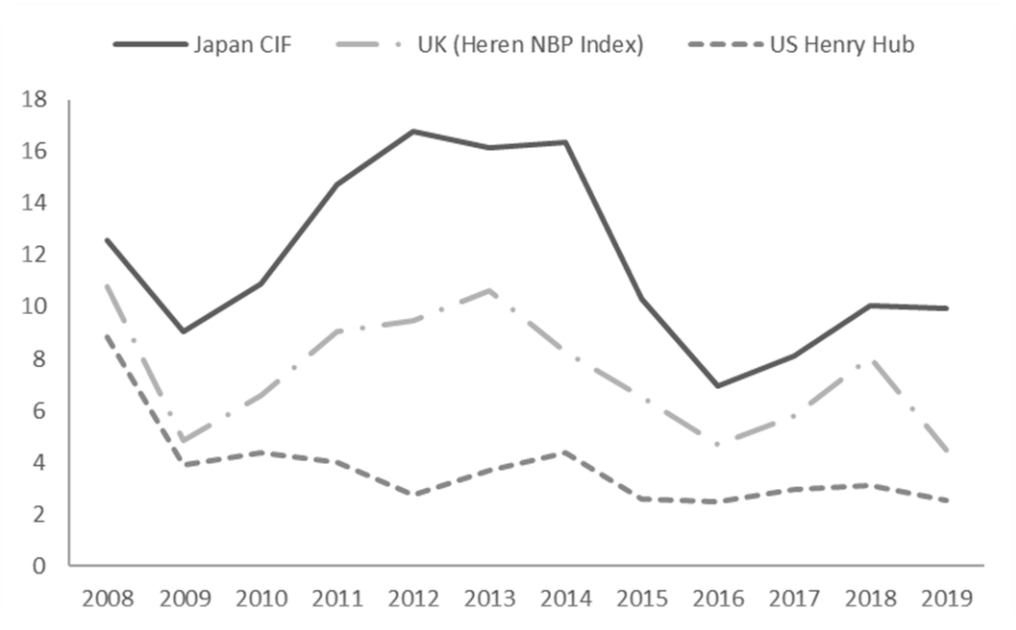

Figure 3-1. Natural gas prices in Asia, Europe and North America from 2008 to 2019 (unit: US$/MMBtu). *Source*: *British Petroleum (BP) Company, 2020.*

The high price of LNG in the Asian market has once been attributed to the market fundamentals of Asian natural gas, namely, supply, demand, and transportation cost (Neumann and Hirschhausen, 2015). As Vivoda (2014) explained, the major gas-consuming countries in Asia are highly dependent on liquified natural gas (LNG) imports from distant gas sources. In 2019, Asia was the largest gas-importing region: it accounted for 39.3% of the global gas trade, of which 86.26% was in the form of LNG (BP, 2020). The high importing demand with the expensive transportation cost (freight rate of LNG is traditionally higher than transmission fee of the pipeline) eventually results in high gas prices.

However, recent studies have found that the oil-indexed pricing mechanism that dominates in the Asian LNG trade, rather than the market fundamentals, is the determinant of high LNG prices in Asia (Zhang et al., 2018a; Shi and Shen, 2021; Li et al., 2020). Therefore, doubts about the rationality of the oil-indexed pricing mechanism

are growing in the Asian LNG market. Essentially, the oil-indexed pricing mechanism is founded on the assumption that the oil and natural gas are substitute fuels. Some argue these two fuels are not perfect substitutes and have different driving factors of market fundamentals (Zhang et al., 2018b). It implies that the oil-indexed pricing mechanism is inefficient to reflect the supply and demand of the Asian LNG market. Stern (2014) noted that some exogenous shocks, e.g., the shale gas revolution, Fukushima nuclear accident, had a profound impact on the gas supply and demand, while this impact was not reflected in the oil-indexed gas price. In practice, price decoupling between the oil price and the LNG spot price in the Asian LNG market makes it more conceivable that the oil-indexed pricing mechanism is inefficient (Zhang and Ji, 2018). In particular, the COVID-19 crisis exacerbated gas oversupply by dampening gas demand. This led to the record-low LNG spot price, which intensified Asian LNG price decoupling (Ason, 2020). This phenomenon suggests that LNG market fundamentals are less correlated with oil prices and thus that oil-indexed pricing has become untenable (Stern and Imsirovic, 2020).

Given this, creating an Asian LNG spot trading hub has been proposed as a solution for efficiently pricing LNG (Shi and Variam, 2017). As other gas trading hubs (e.g., the Henry hub for the United States) determine the price of natural gas based on gas-to-gas competition within a market, it is possible that the hub price can be an efficient benchmark for reflecting LNG demand and supply in pricing long-term contracts (LTCs), futures, and other derivatives (Zhang et al., 2018a). As there currently exists no LNG trading hubs in Asia, it is more practical for Asian gas importers to find an existing benchmark to improve the pricing efficiency. Recently, the Japan-Korea Marker (JKM) price published by Platts is gaining attraction, with the rapid expansion of the LNG spot trade in Asia (Stern and Imsirovic, 2020).

This Chapter, therefore, aims to investigate whether using the JKM price as the pricing benchmark is a feasible solution to improve the LNG pricing efficiency in Asia. In order to answer this question, two basic conditions need to be evaluated. First, we must ascertain whether the JKM price performs better than the oil price in reflecting LNG supply and demand in Asia. Second, we must determine whether both gas importers and exporters are willing to accept the new benchmark. Furthermore, we have to address the concerns of industry veterans regarding the low transparency of the JKM benchmark (due to its daily, inquiry-based price formation). The inquiry only provides a final price to gas importers, and the opacity of the trade cost thus leaves exporters room for hidden margins (Palti-Guzman, 2018). In comparison to the current JKM cost-insurance-and-freight (CIF) price, the free-on-board (FOB) price transfers the transportation costs from exporters to importers, thereby increasing transparency. Inspired by this, we will also explore whether the JKM FOB performs better than the JKM CIF as an LNG pricing benchmark.

Some empirical studies have illustrated that the JKM price is more efficient than the oil price in serving as a benchmark for LNG pricing (e.g., Alim et al., 2018). These studies, however, fail to evaluate the reactions of importers and exporters, as empirical methods are unable to look into the black box of market mechanisms. In order to fill this gap, we build an equilibrium model for LTC pricing in the Asian LNG market. This model is built upon a mean-variance expected utility framework. This framework is commonly used in equilibrium analysis of the electric power market (Bessembinder and Lemmon, 2002; Gersema and Wozabal, 2017). In order to apply it in the LNG market, we modify the model by considering following two characteristics of the Asian LNG market. First, natural gas is a storable commodity, while electricity is not. For electricity, it is impossible to buy a certain amount of electricity in one period and then

hold it for the next-period sale. In our model, therefore, we add a non-negative inventory constraint so as to retain the possibility that the importer conducts intertemporal arbitrage in the LNG spot market. Second, based on the fact that Asian LNG trades at the CIF price, our model considers freight fluctuations. This modification allows us to explore the feasibility of using the JKM FOB benchmark, via analysis of the impact of freight rate transfers between importers and exporters on natural gas pricing.

Based on the proposed equilibrium model, we can investigate and compare the pricing efficiency of possible benchmarks (i.e., oil prices, the JKM CIF price, and the JKM FOB price) via the LTC's risk sharing function. The risk sharing of an LTC is reflected in its take-or-pay (TOP) clause. This clause stipulates that the importer bears the LNG volume risk and the exporter takes the price risk (Abada et al., 2017). This risk sharing by means of the TOP clause is effective, if the pricing benchmark of an LTC is efficient in reflecting the supply and demand for natural gas within a market. Additionally, the model allows us to estimate the risk-profit tradeoff of importers and exporters, based on their LTC-spot trade portfolio. By comparing the risk-profit tradeoff under different benchmarks, we can directly judge the benchmark that a given importer or exporter would be likely to accept.

Based on historical data, we forecast the future dynamics of candidate benchmarks which are input into the model. The results of numerical study show that the JKM CIF/FOB price is more efficient than the oil price as a pricing benchmark of LNG LTC. This is due to the fact that the JKM pricing benchmark can help importers to create more effective hedging positions in their LTCs. This benchmark is favored for exporters and importers if both of them are low risk-averse. In addition, the JKM

pricing benchmark can effectively prevent the transfer of price risk from an LNG exporter to the importer in the high-risk-aversion case.

The rest of this chapter is organized as follows: Section 3.2 reviews the existing literature on the topic, and summarizes the contributions of this study. Section 3.3 describes the equilibrium pricing model constructed for the Asian LNG market. Section 3.4 simulates the random inputs of the equilibrium model based on real data. Section 3.5 compares the model results of different pricing benchmarks. Section 3.6 presents the conclusions of this Chapter.

3.2. Literature review

With the growth of spot trading and gas-oil price decoupling in Asia, the so-called "Asian premium" is attracting attention from studies on Asian LNG prices. Recently, researchers have explored the origins of this phenomenon. Zhang et al. (2018a) compared the price determinants of gas markets in the US, Germany, and Japan. Shi and Shen (2021) followed Zhang et al. (2018a), and put their focus on the macroeconomic uncertainties surrounding the gas market. Using a vector autoregressive (VAR) model, these two studies indicated that the oil-indexed pricing mechanism was accountable for the "Asian premium." Another group of literature on the origins of the "Asian premium" investigated price bubbles within regional natural gas markets. Zhang et al. (2018b) adopted a generalized sup augmented Dickey-Fuller test to explore gas price bubbles in the US, Europe, and Japan. Taking the same approach, Li et al. (2020) further identified the periodicity of gas price bubbles in these three markets. Both studies concluded that the price differential in the Asian LNG market was a spillover effect from the oil market. The aforementioned studies also proposed policies to address the pricing inefficiency, such as building an LNG trading

hub (Zhang et al., 2018a; 2018b), and using the JKM price as the pricing benchmark (Alim et al., 2018). The effectiveness and feasibility of these policies, however, have not yet been evaluated.

An evaluation of these policies directed toward the Asian premium is an investigation of whether to retain the oil-indexed pricing mechanism for the natural gas trade. Numerous studies have provided empirical evidence on this point by exploring the relationship between the gas spot price and the oil price. Early studies focused on cointegration analysis of these two prices. Brown and Yücel (2008), and Hartley et al., (2008) concluded that the oil-indexed gas price was reliable, as they found the long-term equilibrium between the two prices. Doubts about the reliability of this conclusion emerged, however, with the finding that the cointegration of these prices was volatile over time (Erdős, 2012; Ramberg and Parsons, 2012). In order to capture the time-varying characteristics of prices, Brigida (2014) and Asche et al. (2017) applied regime-switching models to investigate the US and UK gas markets, respectively. Both of them verified that price cointegration existed, but with instability. Geng et al. (2016) applied the same approach in order to explore the impact of the shale gas revolution on natural gas prices. They found that the shale gas revolution intensified the gas-oil price decoupling within the US market.

With the advent of novel empirical approaches and the availability of sophisticated databases, some literature began to incorporate more of the complexities related to the dynamic and nonlinear features of the gas-oil nexus. Batten et al. (2017) employed time- and frequency-domain causality tests so as to analyze the time-varying spillover effect between the gas spot price and the oil price. They concluded that the two prices in the US have been almost independent after the 2008 financial crisis. Zhang and Ji

(2018) applied a long-memory approach, and showed strong evidence of price decoupling in the US; meanwhile, the gas-oil price nexus still held in Europe and Asia. Wang et al. (2019) applied a dynamic model averaging (DMA) approach in order to explore the driving factors of gas prices in the US market. The results suggested that the effect of supply and demand was more significant than that of the oil price on the gas spot price. Lovcha and Perez-Laborda (2020) also analyzed the oil-gas price volatility spillover via the framework of dynamic frequency connectedness. They found that the magnitude of the spillover effect varied over time, but that the volatilities of the two prices were not decoupled. Ftiti et al. (2020) examined the dynamic gas-oil relationship via both linear and nonlinear machine learning models. They found that the gas-oil relationship more closely resembled a nonlinear one, which depended on the existence of extreme price movements in the tested time scales. It is clear that these empirical studies did not arrive at a consensus on the gas-oil price relationship, due to the differences in methodologies, markets analyzed, and data sample periods. More importantly, these studies cannot explicitly showcase the impact of either retaining or abandoning this pricing mechanism on participants in the natural gas trade.

The equilibrium model proposed in this study is built upon the decision-making of market participants, which allows us to excavate the mechanism that underlies the effects of the proposed policies. There are many deterministic and stochastic equilibrium models for natural gas market (e.g., Zhuang and Gabriel, 2008; Egging et al., 2010; Guo and Hawkes, 2018). These models have been successfully applied to evaluate the implications of various policies, including market entrance (Feijoo et al., 2016), energy structure transition (Holz et al., 2016), and pricing schemes (Shi and Variam, 2017). For instance, Egging et al. (2017) proposed an equilibrium model that considered risk-averse agents within the European gas market. This model was applied

to analyze the effects of uncertain shale gas exploration on the investment choices of gas suppliers. The results suggested that the high risk-averse disposition of suppliers leads to lower investment, thereby causing gas prices to rise. Abada et al. (2017) presented an equilibrium model that endogenized the long-term contract behavior of risk-averse gas producers and midstreamers. This study is a typical example of using an equilibrium model to analyze the gas pricing mechanism. Using the model, they showed that the oil-indexed LTC is still attractive in the European gas market, as it provides financial security for European producers (who bear expensive investment costs). There exist few studies, however, that apply the equilibrium model to studying risk management and risk aversion (which also affect the gas trade), and none of the existing studies focus on the Asian market.

The contribution of this study is thus threefold. First, through building an equilibrium pricing model that accounts for risk aversion, we provide a new perspective for analyzing the pricing mechanism in the Asian LNG market. We examine not only the efficiency of different pricing benchmarks, but also their effects on the risk-profit tradeoff calculations of market participants. This is a crucial consideration for implementing a pricing mechanism. Second, we enrich the equilibrium model and its incorporation of risk aversion by considering the particular characteristics of the LNG market. We compare the FOB-based pricing with CIF-based pricing in order to explore the effects of freight rate transfers on improving the performance of pricing benchmarks. Third, we find that using the JKM price as the pricing benchmark can improve the pricing efficiency for LTCs. This finding has important practical significance for the selection of pricing benchmarks in the Asian LNG market.

3.3 Model

In this section, we construct an LTC equilibrium pricing model. In particular, Section 3.3.1 provides the assumptions and nomenclature of the model. We define the agent's profits in Section 3.3.2. In Section 3.3.3, we display the optimization problems for both exporters and importers, and the market clearing conditions.

3.3.1 Model assumption and nomenclature

In this study, we assume that all participants in the LNG trade are homogenous, and that they can be represented by two representative agents, namely exporter and importer. We focus on a bilateral transaction between an exporter and an importer. The exporter sells LNG to the importer, either via LTC or spot market. The importer purchases LNG so as to meet the consumption within a market, or to resell it in a spot market. The importer cannot directly resell the gas in LTC, due to the restriction of destination clause (Shi and Variam, 2016). Competition within the market is assumed to be perfect, which implies that the importer and the exporter alike are both price takers. In addition, we assume that both the exporter and the importer have the same expectations of prices, as the market information (e.g., futures prices of oil and LNG) is consistent for each of them.

In general, a standard LTC of LNG has a 20-year contract period, which is too long a period for us to make a persuasive forecast of LNG market trends. Alternatively, we divide the whole LTC period into several trading periods (e.g., one year) and focus our study on one of those periods. The rationality of this setting is supported by examples of LTC price renegotiation in reality, for example, the renegotiation between India and Australia in 2017. Through the renegotiation, Australia reduced the LTC price for India

from 14.5% of the Japanese crude import price to 13.9% of the Brent oil price[4]. Due to the change in the LTC price, the contract before and after the renegotiation can be regarded as separated trading periods.

As an example, Figure 3-2 showcases the dynamics of the first trading period after entering into an LTC. At initial time 0, an LTC for LNG is concluded between the exporter and importer. In addition to total trade volume and the pricing benchmark throughout the whole contracting period, the LTC specifies the delivery volume in each trading period, and the base price in the first trading period. In the trading period between time 0 and T, the LNG is delivered in batches at specified delivery times $(1, 2, \dots, T)$. The interval of two adjacent times constitutes one delivery period of LNG. For example, the interval between time 0 and time 1 is the first delivery period, marking the commencement of the contract. At each delivery time t, the corresponding batch of LTC delivery is completed, and the spot trade of both the exporter and the importer finishes clearing. For the purpose of simplification, we assume that the delivery volume of LTC is equal at every delivery time. At the ending time T, with the completion of the last batch of LTC delivery, the contract settlement for the first trading period is finished. After finishing the first-period trade of LTC, the contract parties will review the contract in order to determine the base price for the next trading period. The contract will continue by following the above process, but with a new base price. Each trading period is also accompanied by market uncertainty, we assume that the market uncertainty only comes from the volatility of the LNG spot price, the price benchmark, and spot freight rates.

[4] Detailed information was reported by LiveMint in 2017, and available at https://www.livemint.com/Money/MpJAxVSQwMExq5KmfpYGJL/The-gains-from-the-Gorgon-LNG-contract-renegotiation.html

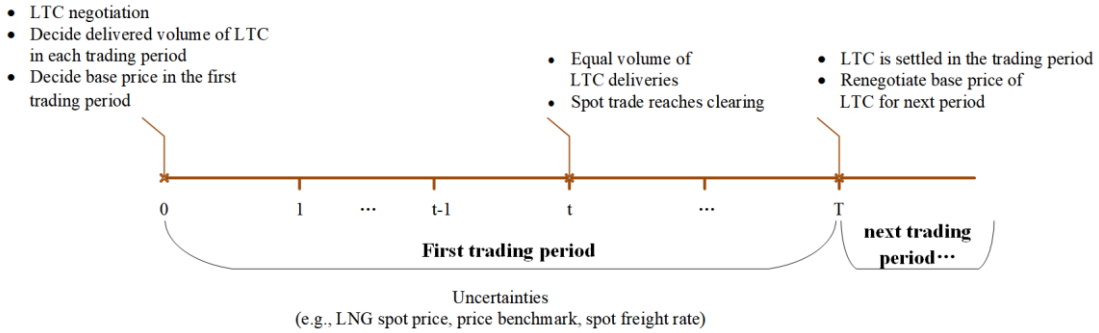

Figure 3-2. Dynamics of a trading period under an LNG long-term contract

We define the mathematical notations of the model, as follows:

Indices	
h	Superscript denoting agent, $h \in H = \{s, b\}$, where s denotes the LNG exporter, and b denotes the LNG importer.
t	Subscript denoting the discrete time in a trading period (e.g., one year), $t \in \{0, \dots, T\}$. When $t = 0$, it indicates the initial time of the trading period. When $t \in \{1, \dots, T\}$, it indicates a delivery time within the trading period.
LTC	Superscript denoting Long-term contract (for both LNG trade and shipping).
SPM	Superscript denoting spot market (for both LNG trade and shipping).
OIL	Superscript denoting oil market.
CPM	Superscript denoting gas consumption market.
Variables	
q	Trade volume of LNG
p	Price of LNG or oil
f	Freight rate of LNG
π	Profit of agent
w	Revenue of agent
ϕ	Cost of agent
Parameters	
γ^h	Attitude of the agent towards risks, if $\gamma^h = 0$, the agent is risk neutral; if $\gamma^h > 0$, the agent is risk averse.
κ	Binary parameter indicating whether exporter or importer pays for freight rate.
δ	Binary parameter indicating the pricing benchmark.
d	LNG consumption demand.
Q	LNG production/regasification capacity of agent.

In this study, we clarify that a tilde on a variable $\tilde{x}$ indicates that the variable is

random, while a bar on a variable $\bar{x}$ indicates that the variable is exogenous, and acting as a parameter. Additionally, variables in the model are nonnegative unless otherwise stated.

3.3.2 Definition of agent profits

For an exporter, its total profit is obtained from LNG sales, via both spot market and LTC.

$$\tilde{\pi}^{s} = \tilde{\pi}^{s,SPM} + \tilde{\pi}^{s,LTC}, \tag{3.1}$$

where $\tilde{\pi}^{s}$ is the total profit of the exporter, and $\tilde{\pi}^{s,SPM}$ and $\tilde{\pi}^{s,LTC}$ are the profits from LTCs and spot trades, respectively. The spot profit of an exporter is defined as follows:

$$\tilde{\pi}^{s,SPM} = \sum_{t=1}^{T} \left(\tilde{p}_t^{SPM} - \tilde{f}_t^{SPM}\right) q_t^{s,SPM}, \tag{3.2}$$

where $\tilde{p}_t^{SPM}$ and $\tilde{f}_t^{SPM}$ are the spot CIF price of LNG, and the spot freight rate at delivery time t, respectively; $q_t^{s,SPM}$ indicates the LNG spot sales at t. We only consider the freight rate in formulating the exporter's profit. The reason for this is that the trading period set in this model is a relatively short term (one year). Other costs (namely, production costs) in that period can be regarded as constant, and thus have no effect on the market risks that the exporter takes.

The key to defining the LTC profit of an exporter is the LTC pricing function. We formulate the LTC price as the sum of the base price and the variation of the pricing benchmark, which is shown in following equation:

$$\begin{aligned} \tilde{p}^{LTC} = p_0^{LTC} &+ \delta(\tilde{p}_T^{OIL} - \bar{p}_0^{OIL}) \\ &+ (1-\delta)\left[\left(\tilde{p}_T^{SPM} - \kappa \tilde{f}_T^{SPM}\right) - \left(\bar{p}_0^{SPM} - \kappa \bar{f}_0^{SPM}\right)\right], \end{aligned} \tag{3.3}$$

where $\tilde{p}^{LTC}$ is the settlement price of the LTC, $\bar{p}_0^{OIL}$ is the LTC base price negotiated at time 0, $\bar{p}_0^{OIL}$ and $\tilde{p}_T^{OIL}$ denote the oil price at initial time 0 and ending time T, respectively. All prices at the beginning of the trading period ($t = 0$) can be observed by both the importer and the exporter, thereby rendering them exogenous. As our assumption on LTC execution only allows the LTC to be settled at the end of the trading period ($t = T$), the benchmark variation is the price difference between time 0 and time T. When the binary parameter δ equals 1, the LTC is benchmarked according to the oil price. Otherwise, it is benchmarked by the LNG spot price. For the case of the LNG spot pricing benchmark, we further split our price analysis into CIF-indexed and FOB-indexed benchmarks via binary parameter κ. When κ equals 0, the LNG spot pricing benchmark is the CIF. Otherwise, it is an FOB-based benchmark.

We describe the LTC profit of a given exporter as follows:

$$\tilde{\pi}^{s,LTC} = \left(\tilde{p}^{LTC} - \kappa \bar{f}^{LTC}\right) q^{s,LTC}, \tag{3.4}$$

where $q^{s,LTC}$ denotes the LNG volume that the exporter sells through the LTC during the trading period. We assume that the LTC binds a long-term chartering contract (LCC) with LNG tankers. Our rationale is that the long-term chartering contract can provide a stable fleet capacity so as to ensure that the LTC volume can be delivered during a given trading period. In order to simplify it, we assume the long-term freight rate $\bar{f}^{LTC}$ is fixed. The parameter κ in equation (3.4) is consistent with that in equation (3.3). The implication of this is that, if the pricing benchmark is CIF/FOB, $\tilde{p}^{LTC}$ is a CIF/FOB price. It should be noted that $\tilde{p}^{LTC}$ is a CIF price ($\kappa = 1$) when the oil-indexed benchmark ($\delta = 1$) is adopted.

An importer purchases LNG from the exporter, both through LTCs and spot market

trades. A given importer's purchasing cost is described as equation (3.5):

$$\tilde{\phi}^b = \left[\tilde{p}^{LTC} + (1-\kappa)\bar{f}^{LTC}\right] q^{b,LTC} + \sum_{t=1}^{T} \tilde{p}_t^{SPM} q_t^{b,SPM+}, \tag{3.5}$$

where $\tilde{\phi}^b$ is the total purchasing cost of the importer within the trading period, $q^{b,LTC}$ is the LNG volume that the importer purchases via LTC, and $q_t^{b,SPM+}$ denotes the spot LNG volume that the importer purchases at delivery time t. $(1-\kappa)$ in equation (3.5) ensures that the type of $\tilde{p}^{LTC}$ (CIF or FOB) is consistent with that in equation (3.4). The importer can either sell the purchased LNG in the gas consumption market, or resell it in a spot market. The revenue that the importer obtains can be described as follows:

$$\widetilde{w}^b = \bar{p}^{CPM}\left(q^{b,LTC} + \sum_{t=1}^{T} q_t^{b,SPM+} - \sum_{t=1}^{T} q_t^{b,SPM-}\right) + \sum_{t=1}^{T} \tilde{p}_t^{SPM} q_t^{b,SPM-}, \tag{3.6}$$

where $\widetilde{w}^b$ is the total revenue of the importer, and $\bar{p}^{CPM}$ indicates the gas price in the consumption market. We assume that this price is fixed during the trading period. $q_t^{b,SPM-}$ is the LNG volume that the importer resells in a spot market. According to equations (3.5) and (3.6), we can define the importer's profit as:

$$\tilde{\pi}^b = \widetilde{w}^b - \tilde{\phi}^b - \sum_{t=1}^{T} \tilde{f}_t^{SPM} q_t^{b,SPM-}, \tag{3.7}$$

where $\tilde{\pi}^b$ is the total profit of the importer, $\tilde{\pi}^b$ is not solely the revenue after subtracting the purchasing cost: as the spot market in Asia is still dominated by bilateral physical trade, transportation costs are inevitable (Abada et al., 2017). Therefore, freight charges for reselling LNG (i.e., the last portion of equation (3.7)) also need to be deducted in order to determine total profit.

3.3.3 Market equilibrium model

As we mentioned in Section 3.3.1, our model is based on the mean-variance expected utility framework. The expected utility function is displayed as follows:

$$\mathbb{E}[U(\tilde{\pi}^h)] = \mathbb{E}(\tilde{\pi}^h) - \frac{\gamma^h}{2} Var(\tilde{\pi}^h), \quad \forall h \in H = \{s, b\}, \tag{3.8}$$

The expected utility $\mathbb{E}[U(\tilde{\pi}^h)]$ of an agent h is linearly correlated with its expected profit, and the profit-related risk is measured by the variance of profit. γ^h denotes the willingness of each agent to accept risks. In this study, we assume that both the importer and the exporter are risk-averse, so γ^h is a positive parameter. Through utility maximization, each of the two agents can achieve a balance between their profits and the corresponding risks. The equilibrium model, therefore, is assembled by integrating the utility maximization problems of each agent, together with the market clearing conditions in both LTC and spot trade transactions.

The utility maximization of the importer is shown as:

$$\max_{q^{b,LTC}, q_t^{b,SPM+}, q_t^{b,SPM-}} \mathbb{E}[U(\tilde{\pi}^b)] \tag{3.9}$$

Subject to

$$\frac{q^{b,LTC}}{ord(T)} + q_t^{b,SPM+} \leq Q^b \quad (\lambda_t^b), \quad \forall t \in \{1,2,\dots,T\}, \tag{3.9.a}$$

$$\begin{aligned} &\frac{q^{b,LTC}}{ord(T)} + q_t^{b,SPM+} - q_t^{b,SPM-} + (ord(t)-1)\frac{q^{b,LTC}}{ord(T)} \\ &\qquad + \sum_{t'<t} \left(q_{t'}^{b,SPM+} - q_{t'}^{b,SPM-} - d_{t'}\right) - d_t \\ &\qquad \geq 0 \quad (\mu_t^b), \quad \forall t, t' \in \{1,2,\dots,T-1\}, \end{aligned} \tag{3.9.b}$$

$$q^{b,LTC} + \sum_{t=1}^{T}\left(q_t^{b,SPM+} - q_t^{b,SPM-}\right) - \sum_{t=1}^{T} d_t = 0 \quad (\rho^b), \tag{3.9.c}$$

where Q^b represents the importer's regasification capacity, which is constant at each delivery time t. $ord(T)$ denotes the ordinal number of T in the sequential set $\{1,2,\dots,T\}$. $\frac{q^{b,LTC}}{ord(T)}$ represents the LTC LNG delivered at each t. d_t indicates the demand of gas consumption at t. λ_t^b, μ_t^b and ρ^b are the shadow prices of corresponding constraints. As the importer is a price taker, $\tilde{p}_t^{SPM}$, $\tilde{p}^{LTC}$ and $\tilde{f}_t^{SPM}$ (contained in $\tilde{\pi}^b$—see Section 3.2) can be regarded as given. The decision variables in this optimization problem are $q^{b,LTC}$, $q_t^{b,SPM+}$ and $q_t^{b,SPM-}$. Constraint (3.9.a) expresses that the total import volume of LNG should be restricted by the importer's regasification capacity. In constraint (3.9.b), the term $\frac{q^{b,LTC}}{ord(T)} + q_t^{b,SPM+} - q_t^{b,SPM-}$ indicates the net procurement volume of importer at t. $(ord(t)-1)\frac{q^{b,LTC}}{ord(T)} + \sum_{t'<t}\left(q_{t'}^{b,SPM+} - q_{t'}^{b,SPM-} - d_{t'}\right)$ indicates the LNG inventory up to t. Constraint (3.9.b) ensures that, at each delivery time t before settlement of the LTC, the sum of net procurement and inventory should at least satisfy gas consumption. Constraint (3.9.c) is the special case of Constraint (3.9.b), when t equals T. Constraint (3.9.c) is stricter, however, so as to ensure market clearing within the gas consumption market. This constraint implies that the total net LNG procurement of the importer should be equal to consumption during the trading period.

The utility maximization of the exporter is given as:

$$\max_{q^{s,LTC}} \mathbb{E}[U(\tilde{\pi}^s)] \tag{3.10}$$

Subject to

$$q^{s,LTC} + \sum_{t=1}^{T} q_t^{s,SPM} \leq Q^s \ \ (\lambda^s), \tag{3.10.a}$$

where Q^s is the exporter's production capacity during the trading period, and λ^s is the shadow price of constraint (3.10.a). As the exporter is also a price taker, $\tilde{p}_t^{SPM}$ and $\tilde{p}^{LTC}$ (contained in $\tilde{\pi}^s$) are treated as given. In this study, we assume that $\tilde{p}_t^{SPM}$ is an equilibrium price, which implies that the spot volume sold by the exporter ($q_t^{s,SPM}$) is dependent on the demand of the importer. Therefore, the decision variable in this optimization problem is only the LTC volume sold by the exporter ($q^{s,LTC}$). Due to oversupply in the LNG market (Sesini et al., 2020), we assume that the exporter can satisfy the demand of the importer at each delivery time t. Hence, we do not impose the restriction on the LNG exports during each delivery period. Constraint (3.10.a) only ensures that the total LNG exports in the trading period are not greater than Q^s.

We introduce the **market clearing conditions** as follows:

$$q^{b,LTC} = q^{s,LTC}, \tag{3.11}$$

which represents the equilibrium in LTC trade between a given importer and exporter. Additionally,

$$q_t^{b,SPM+} = q_t^{s,SPM}, \tag{3.12}$$

which indicates equilibrium in the spot market between the importer and the exporter. In order to solve this model, we transport it into a mixed complementarity problem (MCP), via the KKT conditions and market clearing conditions. A detailed description of the transformed MCP is given in Appendix B-1.

3.4 Simulation of stochastic inputs

Three random variables act as the stochastic inputs in the proposed equilibrium model: a) the oil price $\tilde{p}_t^{OIL}$; b) the LNG spot price (CIF) $\tilde{p}_t^{SPM}$; and c) the spot freight rate $\tilde{f}_t^{SPM}$. In this section, we apply historical data in order to simulate the movements of these three prices over a trading period from November, 2020 to December, 2021. In Section 3.4.1, we present the econometric approach for the simulation. In Section 3.4.2, we show the simulated results.

3.4.1 Simulation procedure of stochastic inputs

The purpose of simulating the aforementioned random prices is to determine the expectation $\mathbb{E}(\tilde{\pi}^h)$ and variance $Var(\tilde{\pi}^h)$ of each agent's profits in the equilibrium model. This requires that our approach not only forecast short-term price trends accurately, but also capture their distribution characteristics. To this end, we apply an approach that combines a mean-reversion model and kernel regression model.

We assume that three prices satisfy the mean reversion process. This model can be described as the following differential equation:

$$dz_t = \mu(m_t - z_t)dt + \sigma dW_t, \quad t = 1,2, \dots, T \tag{3.12}$$

where z_t is the logarithm of a price p_t. μ and σ are positive parameters reflecting the speed and volatility of mean reversion, respectively. m_t is the time-dependent mean of z_t. W_t represents a Wiener process. By following Gersema and Wozabal (2018), we apply a locally constant kernel regression to estimate m_t. The regression function is given as:

$$m_t = E[z|F(t)] = \frac{\sum_{\tau=1}^{T} K_h[F(t) - F(\tau)]z_\tau}{\sum_{\tau=1}^{T} K_h[F(t) - F(\tau)]}, \qquad t, \tau \in [0,1,2, \dots, T] \tag{3.13}$$

where $K_h(\cdot)$ is a Gaussian kernel with h bandwidth, $F(t)$ denotes the time transformation, representing the periodic characteristic of prices, such as seasonality. If there is no clear periodicity in the price series, $F(t)$ can directly equal $ord(t+1)$[5]. In order to estimate the parameters μ and σ, we refer to the approach of Tseng and Barz (2002), who constructed a mean reversion process for a stationary series by removing the periodicity and trends from the price series.

First, we remove the periodicity of z_t, and obtain the logarithm price without periodicity, $\dot{z}_t$. We define the periodicity as monthly. This periodicity can be represented as the difference between the average logarithm price of the month, and the average logarithm price over the sample period. For example, given a sample period from 2010 to 2019, the mean of all January logarithm prices minus the average logarithm price over 10 years is equal to the periodicity of January.

Second, we construct the stationary price series $\ddot{z}_t$ by detrending $\dot{z}_t$. We define the trend of $\dot{z}_t$ as being yearly. The trend is represented by the difference between the annual mean of $\dot{z}_t$ and the mean of $\dot{z}_t$ over the sample period.

Last, we display the mean reversion process for the modified price series $\ddot{z}_t$ as follows:

$$d\ddot{z}_t = \mu(m - \ddot{z}_t)dt + \sigma dW_t, \;\; t = 1,2, \dots, T \tag{3.14}$$

where m is the mean of $\ddot{z}_t$. Note that m is time invariant, since the price series $\ddot{z}_t$ is

[5] $ord(t+1)$ indicates the ordinal number of t in the ordered set $\{0,1,2, \dots, T\}$.

stationary. For the purposes of parameter estimation, we transform equation (3.14) into the following, discrete-time form:

$$\ddot{z}_t - \ddot{z}_{t-1} = [1 - \exp(-\mu)](m - \ddot{z}_{t-1}) + \epsilon_t, \;\; t = 1,2, \dots, T \tag{3.15}$$

where the residual ϵ_t should be subject to $N(0, {\sigma_\epsilon}^2)$. Based on equation (3.15), we fit time series $\ddot{z}_t$, using the maximum likelihood approach. The corresponding maximum likelihood estimators are shown as:

$$\begin{aligned} m &= \frac{1}{ord(T)} \sum_{t=0}^{T} \ddot{z}_t - \frac{1}{ord(T)} \frac{\ddot{z}_0 - \exp(-\mu)\, \ddot{z}_t}{1 - \exp(-\mu)} \\ &\approx \frac{1}{ord(T) + 1} \sum_{t=0}^{T} \ddot{z}_t \,, \;\; for \; \ddot{z}_0, \ddot{z}_T \approx m, \end{aligned} \tag{3.16}$$

$$\mu = -\ln \left[\frac{\sum_{t=1}^{T} (\ddot{z}_t - m)(\ddot{z}_{t-1} - m)}{\sum_{t=1}^{T} (\ddot{z}_{t-1} - m)^2} \right], \tag{3.17}$$

$${\sigma_\epsilon}^2 = \frac{1}{ord(T)} \sum_{t=1}^{T} [(\ddot{z}_t - m) - \exp(-\mu) \cdot (\ddot{z}_{t-1} - m)]^2, \tag{3.18}$$

$$\sigma^2 = \frac{2\mu {\sigma_\epsilon}^2}{1 - \exp(-2\mu)}. \tag{3.19}$$

Note that, in equation (3.16) and (3.18), $ord(T)$ indicates the ordinal number of T in the ordered set.

After estimating parameters μ and σ, we substitute them into the time-varying process. The original logarithm price z_t can then be simulated as:

$$z_t = [1 - \exp(-\hat{\mu})] m_{t-1} + \exp(-\hat{\mu})\, z_{t-1} + \varepsilon_t, \;\; t = 1,2, \dots, T \tag{3.20}$$

where the residual ε_t should be subject to $N(0, \hat{\sigma}^2)$, $\hat{\mu}$ and $\hat{\sigma}$ denote the estimated

results of the parameters via the maximum likelihood approach. As we have determined the distribution characteristics of ε_t, we apply the Monto Carlo approach in order to generate scenarios of p_t. The corresponding steps are shown as:

- First, we generate I ($I = 5000$) scenarios for each ε_t. The scenarios of ε_t can be aggregated as a vector $\boldsymbol{\varepsilon_t} = [\varepsilon_{1t}, \varepsilon_{2t}, \dots, \varepsilon_{it}, \dots, \varepsilon_{It}]^T$.
- Second, the price movement $\boldsymbol{z_i} = [z_{i1}, z_{i2}, \dots, z_{it}, \dots, z_{iT}]^T$ in each scenario i can be simulated using equation (20), via substituting ε_t with ε_{it}.
- Third, repeat the second step for all scenarios. Scenarios of each z_t should be the vector $\boldsymbol{z_t} = [z_{1t}, z_{2t}, \dots, z_{it}, \dots, z_{It}]^T$. Scenarios of p_t are defined as the vector $\boldsymbol{p_t}$, where $\boldsymbol{p_t} = \exp(\boldsymbol{z_t})$.

Within the scenario vector $\boldsymbol{p_t}$, we can further estimate expectations and covariance matrices over the three random prices, which act as the stochastic inputs of the equilibrium model.

3.4.2 Simulated results

In this section, we present the simulated results for each of the stochastic inputs into the equilibrium model, that is, the oil price, the LNG spot price, and the spot freight rate.

The oil price in the equilibrium model represents one choice for an LTC pricing benchmark. In this study, we adopt the Japan Crude Cocktail (JCC) price, which is a commonly used oil-indexed benchmark for LNG LTCs in Asia. The monthly data on JCC prices are published by the Ministry of Economy, Trade and Industry (METI) of Japan. The in-sample period ranges from January 2000 to October 2020. The out-of-sample period ranges from November 2020 to October 2021. The in-sample, real JCC

price is shown as the blue line in Figure 3-3 (a). Since it does not have obvious periodicity, we apply $ord(t+1)$ as the time transformation $F(t)$ for kernel regression. In order to provide a basis for the out-of-sample forecast, we use the observed JCC futures prices on October 29, 2020 to profile the trend of mean reversion from November 2020 to October, 2021. This analysis is shown as a black line in Figure 3-3 (a). By incorporating the in-sample, real JCC price, we form a 2000-2021 time series that acts as the input of kernel regression, so as to keep the continuity of estimation. The estimation result of the time-dependent mean from the kernel regression is shown in Figure 3-3 (a) as a red line. The estimated parameters $\hat{\mu}$ and $\hat{\sigma}$ for the JCC price are 0.390 and 0.094 (see Table 3-1). We use R^2 and Mean Absolute Percentage Error (MAPE) to examine the fit performance of the previously described approach to in-sample data. As shown in Table 3-1, the R^2 and MAPE in the JCC price simulation are 0.974 and 0.025, respectively. This indicates that the estimated result is a good fit for the real data in the in-sample period. Then, we forecast the JCC price over the out-of-sample period. Figure 3-4 (a) displays the forecast result over a 95% confidence level.

The JKM price is an alternative choice for replacing the oil-indexed benchmark. The weekly data is sourced from Thomson Reuters Eikon. The in-sample period ranges from July 31, 2014 to October 29, 2020. The out-of-sample period ranges from November 5, 2020 to October 30, 2021. In Figure 3-3 (b), the blue line shows the real JKM price during the in-sample period. Similar to the JCC price, the JKM price doesn't show obvious periodicity. We therefore set the time transformation $F(t)$ as $ord(t+1)$ for kernel regression. The black line shows the JKM futures prices on October 29, 2020. The JKM futures prices make up a continuous time series together with the real JKM price for the time-dependent mean estimation. The red line in Figure 3-3 (b) represents the estimated, time-dependent mean of the JKM price from kernel regression. The

estimated parameters $\hat{\mu}$ and $\hat{\sigma}$ for the JKM price mean-reversion process are 0.390 and 0.094. R^2 and MAPE are 0.976 and 0.031, respectively, showing that the estimated JKM price during the in-sample period is well fitted to the real data. Then, we forecast the JKM price over the out-of-sample period. Figure 3-4 (b) displays the forecast result over a 95% confidence level.

The spot freight rate is the trade cost item we are most concerned with in the model. In this chapter, we use the spot freight rate from Baltic LNG Route 1 (BLNG1) as an example.[6] The in-sample weekly data between January 5, 2018 and October 29, 2020 is sourced from the Shipping Intelligence Network. The out-of-sample period ranges from November 5, 2020 to October 30, 2021. In Figure 3-3 (c), the blue line shows the real spot freight rate during the in-sample period. Unlike the JCC and JKM prices, the spot freight rate has obvious periodicity. Briefly, the spot freight rate maintains an upward trend from April to October. The freight rate displays a downward trend from October to April of the following year. The periodicity of the spot freight rate leads to a different time transformation $F(t)$, shown as:

$$F(t) = \sin\left(\pi + \frac{ord(t+1)}{26}\pi\right) + ord(t+1), \tag{3.21}$$

where $\sin\left(\pi + \frac{ord(t+1)}{26}\pi\right)$ indicates the stationary periodicity in the long run. The black line shows the BLNG1 futures prices observed in the Thomson Reuters Eikon on October 29, 2020. These prices act as the trend for the mean reversion in the out-of-sample period. The real prices and the related futures prices together construct the time series for the time-dependent mean of sport freight rate. The estimated time-dependent

[6] Baltic LNG route 1 (BLNG1) refers to the route between Gladstone (Australia) and Tokyo (Japan).

mean is shown as the red line in Figure 3-3 (c). The estimated parameters $\hat{\mu}$ and $\hat{\sigma}$ for the spot freight rate mean-reversion process are 0.259 and 0.211. R^2 and MAPE are 0.943 and 0.011, respectively, showing that the estimated spot freight rate during the in-sample period is well fitted with the real data. Figure 3-4 (b) displays the out-of-sample forecast result over a 95% confidence level.

Table 3-1. In-sample fit of estimated prices compared to real data

	$\hat{\mu}$	$\hat{\sigma}$	R-squared	MAPE
JCC	0.390	0.094	0.974	0.025
JKM	0.095	0.080	0.976	0.031
Spot freight rate	0.259	0.211	0.943	0.011

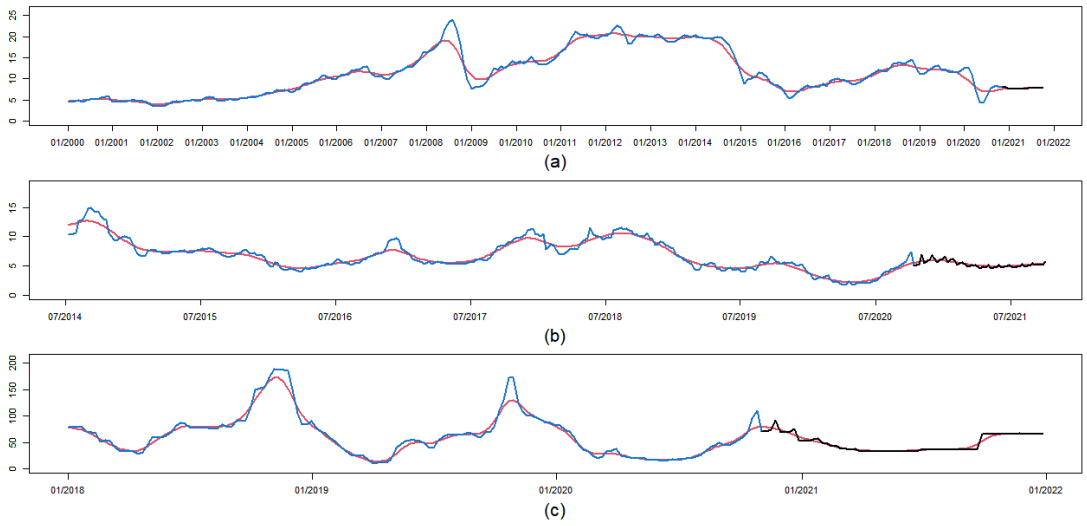

Figure 3-3. Estimated results of time-dependent mean (m_t)

Note: Panels (a), (b), and (c) show the time-dependent mean of the JCC price, the JKM price and the spot freight rate, respectively. The x-axis indicates the whole estimation period, while the y-axis indicates the price. The Red line represents the time-dependent mean. The Blue line represents the real price during the in-sample period. The Black line represents the price of futures, which will mature during the out-of-sample period. The unit of both the JCC and the JKM price is $/MMBtu. The unit of spot freight rate is thousand $/day.

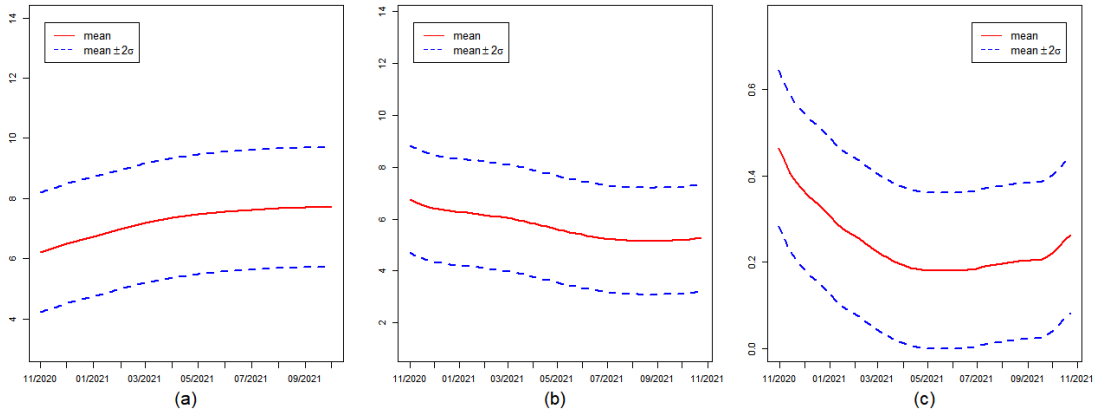

Figure 3-4. Forecast prices during out-of-sample period (unit: $/MMBtu)

Note: Panels (a), (b), and (c) show the forecast results of the JCC price, the JKM price, and the spot freight rate, respectively.[7] The x-axis indicates the out-of-sample period, and the y-axis indicates the price ($/MMBtu).

3.5 Results

Based on the price forecast results in Section 3.4, we conduct a case study in this section in order to evaluate the efficiency of the three different benchmarks for LTC pricing, and the risk-profit tradeoffs for the importer and the exporter. The case study we have chosen is a trade between a Japanese importer and an Australian exporter. They sign an LTC on October 29, 2020. The first settlement of the LTC will be conducted on October 30, 2021. According to the terms of the LTC, gas will be delivered in equal volumes on a weekly basis. In order to account for the seasonality of LNG consumption, we assume

[7] We unify the unit of the spot freight rate with the unit of other prices as $/MMBtu. The unit of original data on the spot freight rate is thousand $/day. As reported by Baltic Exchange, the voyage cycle of the BLNG 1 route is around 26 days (including port waiting time). A standard LNG tanker on this route can carry approximately 160 thousand cubic meters (5.853 million MMBtu) of LNG. Thus, one thousand $/day can be equally converted to $\frac{26}{5853}$ $/MMBtu. All of the information on the BLNG 1 route is available at https://www.balticexchange.com/en/data-services/routes.html

that the peak season consists of two periods: a) the period from the 1st week up to the 12th week after October 29, 2020; b) the period from the 40th week to the 52nd week. The slack season begins from the 13th week to 39th week after October 29, 2020.

The detailed information related to the parameters of the equilibrium model is shown in Table 3-2. As for the risk aversion parameter γ^h, we estimate that its order of magnitude is 10^{-2}. The exporter's risk aversion parameter γ^s is three times that of the importer's, denoted by γ^b. A detailed discussion of the risk aversion parameter is shown in Appendix B-2. In the following study, we will treat γ^h as a range between $10^{-3.5}$ to $10^{0.5}$, based on its order of magnitude. With this range, a risk aversion-based sensitivity analysis will be conducted in order to understand the effect of various risk aversion levels.

Table 3-2. Value of parameters in the model

Parameters	Value
$\sum_{t=1}^{T} d_t$	150 million MMBtu[8]
$\bar{p}^{CPM}$	9 $/MMBtu
Q^s	300 million MMBtu
Q^b	7.212 million MMBtu per week[9]
d_t in the peak season	4 million MMBtu per week
d_t in the slack season	1.852 million MMBtu per week

[8] We assume that this importer is a small gas retailer. In 2020, Japanese LNG imports were 3.67 billion MMbtu (UN Comrade, 2020). This retailer only takes up 4% of the shares in the Japanese consumption market.

[9] As reported by the U.S. Energy Information Administration, the annual regasification capacity of Japan in 2020 was 10 billion MMbtu, which is 2.7 times the level of Japanese LNG imports. Here we set 2.5 times the importer's domestic supply (150 million MMbtu) as its annual regasification capacity. Equivalently, the weekly regasification capacity is 7.212 million MMbtu.

3.5.1 Trade volume and LTC based price

We first analyze how LTC and spot trade volumes change with a given agent's risk aversion. Figure 3-5 (a), (b), and (c) present the impact of risk aversion on the LTC and spot trade volumes. Generally, the results suggest that the change trend of LTC and spot trade volumes under the oil price benchmark are consistent with those observed under the JKM price benchmark. LTC dominates the trade between importer and exporter when risk aversion is relatively low. The importer resells the LNG as much as possible within the spot market while meeting the demand of the consumer market. With an increase in risk aversion, the proportion of spot trade volume begins to increase, and eventually dominates the LNG trade. At the same time, the importer's resale in the spot market keeps declining.

The difference in trade volumes among different benchmarks is that the oil-indexed LTC volume is less sensitive to the agents' levels of risk aversion. As shown in Figure 3-5 (a), when the risk aversion increases from -3 to -2.5, the oil-indexed LTC volume remains 300 million MMBtu, but the JKM-indexed LTC declines to 260 million MMBtu. When the risk aversion ranges from -1.75 to 0.5, the JKM-indexed LTC is absent, but the oil-indexed LTC remains. In addition, the low sensitivity of the oil-indexed LTC to risk aversion leads to low spot trade volume. From Figure 3-5 (b) and (c), we can find that the spot trade volume between the importer and the exporter (as well as the importer's spot resale) under the oil price benchmark is less than the volume traded under the JKM price benchmark. This indicates that using the JKM price as the LTC pricing benchmark can promote the LNG spot trade.

Figure 3-5 (d) shows the relationships between the base price of the LTC and the risk aversion. We can observe that the base price of the LTC is significantly different

among the three benchmarks. The base price of the oil-indexed LTC turns out to be very high when risk aversion is larger than -0.5. With a risk aversion of 0.5, it reaches the highest value of 55 $/MMBtu. The base price of the JKM-indexed LTC remains stable, however, with a slight decline from 7.11 (6.3) $/MMbtu to 6.5 (5.9) $/MMbtu in the CIF (FOB) case.

The results of the LTC's base price provide an intuitive judgment, that is, the JKM price is more efficient as an LTC pricing benchmark compared to the oil price. The reason is that the JKM-indexed LTC performs better in risk-sharing. For an ideal LTC with the perfect risk-sharing, the TOP clause should fully impose the price risk on the exporter. This implies that the base price should be a risk-neutral price expectation, which is essentially a reflection of the total supply and demand in the market. In terms of the assumption that both the importer and the exporter are price takers, any change in risk aversion should not affect the price expectation. Apparently, the base price of the JKM-indexed LTC is more in line with the criteria of a stable risk-neutral expectation.

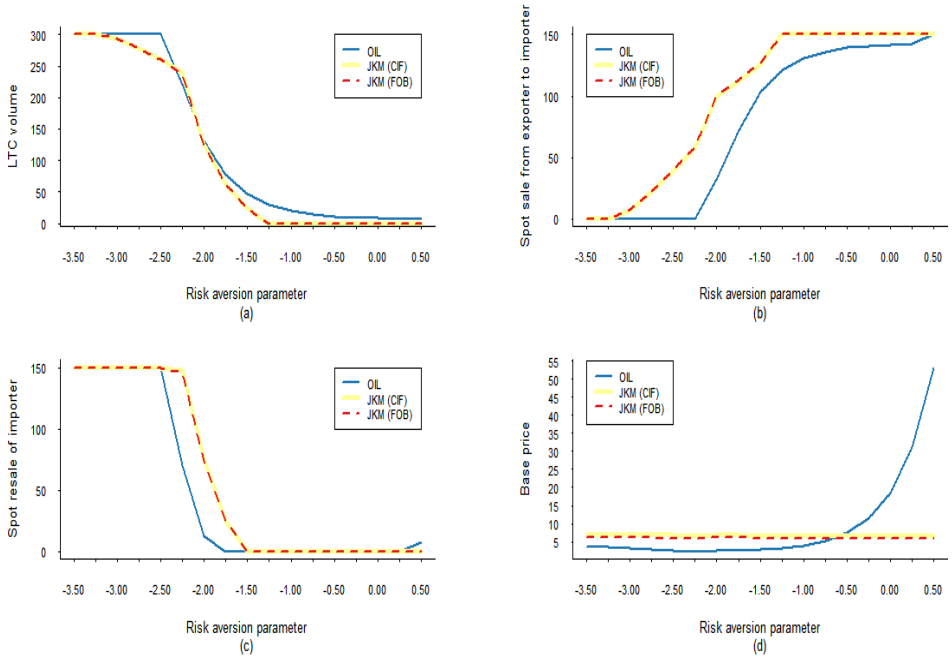

Figure 3-5. LNG trade volumes and base price of LTC

Note: Panel (a) shows the LTC volumes. Panel (b) shows the spot LNG sales from the exporter to the importer. Panel (c) shows the spot resales of the importer. Panel (d) shows the base price of the LTC. The x-axis indicates the risk aversion parameter γ^h, which is denoted as $\log\gamma^h$. Given a certain γ^h, the risk aversion parameter of importer γ^b is equal to γ^h, and that of exporter γ^s is $3\gamma^h$. The unit of the y-axis in panels (a), (b), and (c) is million MMBtu. The unit of y-axis in panel (d) is \$/MMBtu.

3.5.2 Hedging position and hedging effectiveness

We next discuss the hedging function of LTCs priced under different benchmarks. While analyzing the LTC base price, we find that TOP clauses under any benchmark cannot perfectly share the risks between counterparties. This can be evidenced by the fact that the base price still changes with risk aversion, even when using the JKM as the benchmark. This result is consistent with reality, as no price benchmark can perfectly reflect supply and demand in the market. This also means that the exporter

does not completely bear the price risk. Specifically, the base price contains the risk compensation for the exporter, resulting in a part of the price risk being transferred to the importer. Hence, the role of the LTC as a hedging instrument becomes critical to the importer. Suppose that an importer resells an amount of LNG while purchasing an LTC. These two opposite transactions will form a hedging instrument so as to offset the transferred price risk from the exporter, thereby ensuring that the risk-sharing function of the LTC remains in place. Therefore, it is of practical significance to discuss benchmark efficiency from the perspective of an LTC's hedging function.

According to the KKT conditions of the importer's optimization problem in the equilibrium model, we can get the following expression with regard to LTC purchasing volume of a given importer ($q^{b,LTC}$):

$$q^{b,LTC} = \frac{\bar{p}^{CPM} - E(\tilde{p}^{LTC} + (1-\kappa)\tilde{f}^{LTC}) - \sum_{t=1}^{T} \lambda_t^b - \rho^b + \sum_{t=1}^{T-1} \mu_t^b}{\gamma^b \cdot Var(\tilde{p}^{LTC})} + \sum_{t=1}^{T} \frac{-q_t^{b,SPM+} Cov(\tilde{p}^{LTC}, \tilde{p}_t^{SPM}) + q_t^{b,SPM-} Cov(\tilde{p}^{LTC}, \tilde{p}_t^{SPM} - \tilde{f}_t^{SPM})}{Var(\tilde{p}^{LTC})}, \ if \ q^{b,LTC} > 0. \quad (3.22)$$

On the right-hand side of equation (3.22), the first term indicates the speculative position of the LTC, and the second term represents the hedging position. $\frac{Cov(\tilde{p}^{LTC}, \tilde{p}_t^{SPM})}{Var(\tilde{p}^{LTC})}$ and $\frac{Cov(\tilde{p}^{LTC}, \tilde{p}_t^{SPM} - \tilde{f}_t^{SPM})}{Var(\tilde{p}^{LTC})}$ are the best hedging ratios for importer to hedge its spot resales ($q_t^{b,SPM-}$) and spot purchase from the exporter ($q_t^{b,SPM+}$), respectively. It should be noted that an LTC is different from futures or forward contracts. The unidirectionality of an LTC (only the exporter sells the LTC to the importer) determines that the importer can never hold a short position. This implies that the hedging of an LTC against spot trades is not complete for the importer. Equation (3.22) shows us that the necessary

condition to form hedging between the LTC and a spot trade is that both LTC volume and the hedging position are positive. This can be further split into two conditions: a) when the LTC pricing benchmark is negatively correlated with the spot price, the hedging position against $q_t^{b,SPM+}$ should be larger than that against $q_t^{b,SPM-}$; b) when the benchmark is positively correlated with the spot price, the hedging position against $q_t^{b,SPM+}$ should be smaller than that against $q_t^{b,SPM-}$. Based on the price forecast results in Section 3.4, $Cov(\tilde{p}^{LTC}, \tilde{p}_t^{SPM})$ and $Cov\left(\tilde{p}^{LTC}, \tilde{p}_t^{SPM} - \tilde{f}_t^{SPM}\right)$ are negative in most cases under the oil price benchmark, and are positive under the JKM price benchmark (see Appendix B-3). In order to construct a hedge between the LTC and the spot trade, the importer should ensure that condition a) is met while using the oil price benchmark, or that condition b) is met while using the JKM price benchmark. We have displayed the importer's hedging positions in an LTC and the corresponding hedging effectiveness in Figure 3-6 (a) and (b), respectively.

Figure 3-6 (a) describes the relationship between the importer's hedging position and the agents' risk aversion. We can observe that the oil-indexed LTC offers a hedging position under a high level of risk aversion (from -1.75 to 0.5), and that the JKM-indexed LTC offers a hedging position under a low level of risk aversion (from -3.75 to -1.75). This result verifies the incomplete hedging instrument that the LTC is.

More importantly, for a spot trade of the same scale, the oil-indexed LTC provides fewer hedging positions than the JKM-indexed one. For example, when the risk aversion parameter is 0.5, the importer's net spot trade volume is 142.7 million MMBtu (a positive value indicates a purchase) under the oil price benchmark. When the risk aversion parameter is -3, the importer's net spot trade volume is -142.9 million MMBtu (a negative value indicates a sale) under the JKM FOB benchmark. Although the

importer has the same spot trade scale in each of the two cases, the oil-indexed LTC provides 1.3 million MMBtu, while the JKM FOB provides 62.2 million MMBtu as the hedging position. The reason for this result is that the best hedge ratios under the oil price benchmark are much smaller than those under the JKM FOB benchmark. As the variance of LTC price $Var(\tilde{p}^{LTC})$ between two benchmarks is close (i.e., 0.99 for an oil-indexed LTC, and 1.07 for the JKM FOB-indexed one), the smaller absolute value of covariance $Cov(\tilde{p}^{LTC}, \tilde{p}_t^{SPM})$ and $Cov(\tilde{p}^{LTC}, \tilde{p}_t^{SPM} - \tilde{f}_t^{SPM})$ under the oil price benchmark (see Appendix C) leads to a smaller optimal hedge ratio. The difference in the covariance further indicates that there is a lack of correlation between the oil price and the spot LNG price.

Figure 6 (b) shows the relationship between hedging effectiveness (HE) of an LTC and risk aversion. The HE is defined as the reduction of spot trade risk though the introduction of hedging positions (Cotter and Hanly, 2012):

$$HE = -\frac{SD(spot\ return + return\ from\ Hedge\ position) - SD(spot\ return)}{SD(spot\ return)} \quad (23)$$

Under a low level of risk aversion (from -3.5 to -1.75), the JKM-indexed LTC can construct an effective hedging portfolio with spot trades for the importer. The maximum HE (64%) is reached at a risk aversion level of -2.25. As risk aversion is larger than -2.25, the HE of the JKM-indexed LTC decreases. This can be explained by the decrease in both LTC volume and in the importer's spot resale. This result implies that the demand for risk hedging is reduced as the importer significantly increases spot purchases from the exporter in order to satisfy domestic consumption. As risk aversion increase from -1.75, the HE declines to zero, as no LTC exists under the JKM benchmark. As for the oil price benchmark, the HE of the LTC is almost zero. This result indicates that the oil-indexed LTC is ineffective in providing hedging for the

importer. These results confirm that JKM price is more efficient than the oil price as the benchmark for LTC pricing, as the JKM-indexed LTC can be an effective hedging instrument for the importer.

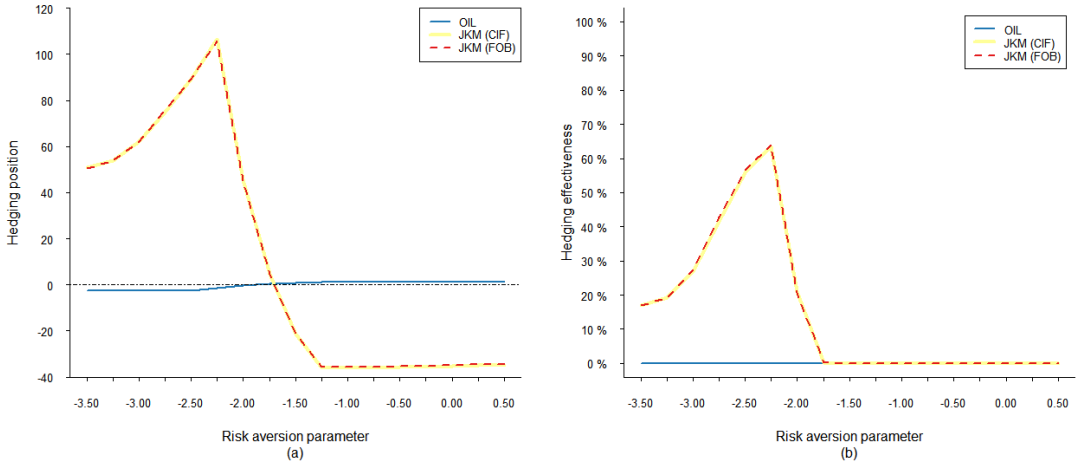

Figure 3-6. Importer's hedging position on an LTC and hedging effectiveness.

Note: Panel (a) describes the hedging position, and panel (b) describes the effectiveness of the hedging position. The x-axis indicates the risk aversion parameter γ^h, which is denoted as $\log \gamma^h$. Given a certain γ^h, the risk aversion parameter of importer γ^b is equal to γ^h, and that of exporter γ^s is $3\gamma^h$. The unit of the y-axis in panel (a) is million MMBtu.

3.5.3 Tradeoff between profits and risks

The previous two sections describe the JKM price as an efficient benchmark for LTCs. In this section, we will explore whether this benchmark is feasible. The adoption of this pricing measure relies on whether the benchmark can improve profit and lower the corresponding risks of the importer and exporter. In this study, we apply the coefficient of variance (CV) to represent the tradeoffs for the importer and the exporter between expected profit and profit-related risk. A smaller CV implies a better risk-profit tradeoff for both the importer and the exporter.

Figure 3-7 (a) and (b) show the change in CV of the importer and the exporter respectively. In the risk aversion range between -3.5 and -1.75 (low risk aversion), the CV of an importer under the JKM benchmark is always less than that under the oil price benchmark. For the exporter, the JKM benchmark also preforms better than the oil price benchmark in most cases. This indicates that the JKM benchmark is beneficial to both the importer and the exporter under conditions of low risk aversion. This is because, on the one hand, the JKM benchmark contributes to a higher LTC base price—which helps the exporter to transfer more price risk onto the importer. On the other hand, the JKM benchmark provides an effective hedging mechanism for the importer to offset the transferred price risk.

In the risk aversion range between -1.75 and -0.5 (moderate risk aversion), the oil price performs better than the JKM price as a benchmark of LTC pricing, since the CV of the importer and the exporter under the oil price benchmark is less than under the JKM benchmark. The reason for this is that the JKM-indexed LTC cannot provide effective hedging, although the LTC volume exists. This result implies that the JKM-indexed LTC is similar to the oil-indexed one, and should be viewed as an option within an LNG trade portfolio for risk diversification. It is known that less correlated assets among a portfolio perform better in risk diversification. Therefore, the oil price is the better choice for LTC pricing in this case.

In the risk aversion range between -0.5 and 0.5 (high risk-aversion), the CV of the importer under the JKM benchmark is significantly smaller than that under the oil price benchmark. The oil price benchmark, however, is more favorable for the exporter. The reason for this is that the JKM-indexed LTC is zero, while that a few amounts of oil-indexed LTC still exist. It implies that oil-indexed LTC is available to transfer exporter's

price risks while JKM-indexed one is not. With this high risk-averse attitude, the exporter needs to transfer more price risks, thereby driving a drastic increase in the base price of the oil-indexed LTC. As the oil-indexed LTC cannot provide an effective hedging option for the importer, the LTC that the importer purchased becomes an expensive sunk cost, which leads to profit losses for the importer.

Overall, these results show that the choice of an LTC pricing benchmark depends on the risk aversion of both the importer and the exporter. The JKM benchmark can benefit both the importer and the exporter under low levels of risk aversion. The oil price benchmark can be more suitable for both parties under conditions of moderate risk aversion (-1.75 ~ -0.5), due to its better risk diversification. Notably, the oil price benchmark is significantly inefficient to price the LTC in the high risk-aversion case (-0.5 ~ 0.5). Due to the decoupling of oil prices and the LNG spot price, the risk-sharing function of the oil-indexed LTC fails, and instead becomes a tool for the exporters to transfer price risk. The high risk-aversion of the exporter results in a high base price of the LTC, under which, the importer bears expensive gas-importing costs. For the importer, the essence of building an efficient pricing benchmark is to prevent the transfer of price risk. From this perspective, using the JKM price as the LTC pricing benchmark is helpful.

In addition, we find that there is no obvious difference in LNG trade volumes, base prices, or hedging effectiveness of LTCs when using either the JKM CIF price or using the JKM FOB price as the benchmark. The freight liability transferred from the exporter to the importer has little effect on the pricing efficiency. Consequently, we can conclude that the freight rate is not a determining factor in influencing price transparency.

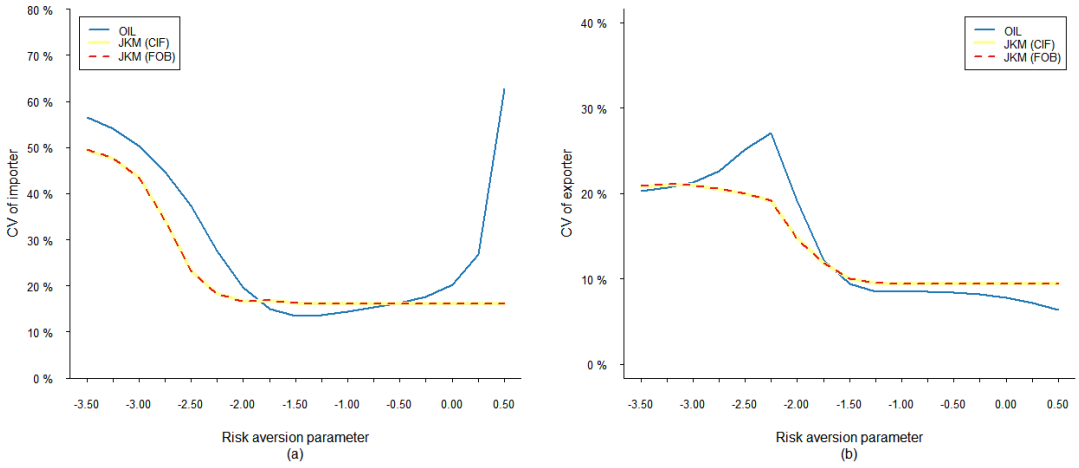

Figure 3-7. Coefficient of variance (CV) of expected profit

Note: Panel (a) describes the CV of a given importer's expected profit, and panel (b) describes the CV of the exporter's expected profit. The x-axis indicates the risk aversion parameter γ^h, which is denoted as $\log \gamma^h$. Given a certain γ^h, the risk aversion parameter of importer γ^b is equal to γ^h, and that of exporter γ^s is $3\gamma^h$.

3.6 Conclusion

In this chapter, we have established an LTC pricing equilibrium model that considers the risk aversion of an Asian LNG importer and an exporter, as well as price uncertainties. As an extension of the mean-variance utility framework, we highlight that a) natural gas is storable; and, b) the Asian LNG is traded at the CIF price. Based on the mean-reversion model and the kernel regression model, we forecast uncertain prices and capture their distributional characteristics. Based on this analysis, we simulate the corresponding stochastic inputs (that is, price expectation and covariance matrices) of the equilibrium model via the Monte Carlo method.

Using the equilibrium model, we conduct a risk aversion-related sensitivity analysis, and make a comparison between the oil price and the JKM price in order to

analyze their performance as a benchmark for LTC pricing. The major findings are as follows: a) the JKM price is more efficient than the oil price in establishing the pricing of an Asian long-term LNG contract; b) the JKM benchmark is a feasible price measure for the low risk-averse importer and exporter, as the JKM-indexed LTC functions better in risk sharing; c) the JKM benchmark can prevent the price risk transfer from an exporter to an importer, as it provides a more risk-neutral base price for the LTC.

Chapter 4. Interactions between shipping market and international iron ore trade — An equilibrium analysis

4.1 Introduction

In the international iron ore market, Asian countries, especially China, Korea, and Japan, are the major importers, accounting for 85.7% of global imports in 2016, while Australia and Brazil are the two major exporters, taking 77.33% global market in 2016 (World Steel Association Report, 2018). Due to its closer transport distance to Asia, Australia dominates Asian iron ore imports, accounting for 63.12% of the market in 2016 (World Steel Association Report, 2018). Notably, there is a great geographic difference between the iron ore consumption and the production. Iron ore supply relies heavily on marine transportation (Song et al., 2019). Exporters need to facilitate shipping in order to maintain a stable supply chain. A typical example is Brazil. Located far away from its major importers, Brazil has initiated a series of shipping strategies to compete with Australia in the East Asian market. For example, Brazilian miners (the Valley and Companhia Siderrgica Nacional) deployed very large bulk ships (400,000 tonnes Valemax) and have cooperated since 2012 with Chinese shipping giants, such as

China Merchants Group and China Ocean Shipping Company. They also built self-owned specialized terminals in order to increase iron ore sea handling capacity and reduce shipping cost in the East Asian trade. However, these strategies seem to be ineffective. As evidence, from 2012 to 2015, the iron ore exported from Brazil to East Asian countries grew by only 10.2%, while Australian exports increased by 54.6%. This raises a doubt as to whether it is worthwhile for Brazil miners to strive to improve the sea transportation of iron ore. To resolve this, it is critical to investigate the interactions between the markets for iron ore shipping and trade, thereby understanding the impact of shipping on iron ore trade.

Whether transportation (shipping) market affects international trade has been broadly discussed empirically, while the findings are equivocal. Nguyen and Tongzon (2010) indicated that these studies ignored some potential influences from factors such as the adverse economic changes (e.g., higher cost) and transport demand constraint. This motivates us to explore an alternative approach which enables to incorporate these influences in investigating the relationship between shipping and international trade. The computable equilibrium modeling, which is one of the efficient approaches to open the “black box” where the market mechanics are hidden (Robson et al., 2018), can be an ideal tool.

Many equilibrium models have been developed for policy and strategy analyses in international resource commodity markets. Most of the models focus on the natural gas market and the electricity market as their trades have increased significantly in recent decades, while iron ore attracts very limited attention. Even though these models have considered various market characteristics of natural gas and electricity market, they are not applicable here, as a) they cannot reflect some important characteristics of the iron

ore trade (e.g., heterogenous commodity and CFR trade price[10]); b) they cannot deliberate the interactions between markets for the shipping and the trade.

In this chapter, we present an equilibrium model of the iron ore trade taking into account two major characteristics. One is that iron ores are heterogenous across exporters due to ore's grade[11] (Warell, 2018), which means different prices for different grades. To reflect the importers' choice of iron ores from different exporters, we use a constant elasticity of substitution (CES) utility function to describe the consumer demand of iron ores. The other is that iron ore is traded at the CFR price, which means exporters are responsible for the shipping cost. The differences in shipping cost to importers can affect an exporter's production efficiency (Qing et al., 2017). Therefore, we propose a capacity allocation model for it. With this model, the trade volume from each exporter is not limited to its production capacity, but restricted by the allocated production capacities to importers, namely, export capacities.

More importantly, we endogenize the shipping cost in the model. With reference to the integrated modeling framework, which incorporates fleet assignment problem with cargo flow assignment (Xia et al., 2015; Lin and Chang, 2018), we propose a two-stage transportation optimization problem. It allows us to explore the potential influences of shipping on iron ore trade.

Due to the existence of integer variables (e.g., the number of ships), this model is formulated as a Discretely Constrained Mixed Complementarity Problem (DC-MCP),

[10] CFR indicates that the production cost and freight rate are included in the trade price. It implies that the exporter is responsible for the freight rate to the port of destination. Today, the iron ore pricing relies on the benchmark consisting of the major CFR pricing indices (e.g., Platts Iron Ore Index).

[11] The grade of iron ore refers to the iron content per unit volume or weight of ores. According to the report of the United States Geological Survey in 2017, the average iron ore grade in Australia was 48% against 52.2% in Brazil.

for which we design a solution procedure. In particular, we look for its near complementarity solutions by applying a mixed-integer nonlinear programming (MINLP) formulation and convexification techniques. We evaluate the performance of our model by comparing it to two models with canonical spatial equilibrium setups. Results suggest our model is better at simulating the iron ore trade. Furthermore, we find that shipping can dampen the impact of a trade shock on trade volume, although this effect is insignificant. And the dampening effect is different across exporters at a high freight rate level.

The rest of this chapter is organized as follows: in section 4.2, we summarize the existing literature relevant to this study. Section 4.3 develops a mixed complementarity-based equilibrium model. Section 4.4 provides the solution procedure for the proposed model. In section 4.5, a numerical study is conducted based on real data. Finally, in section 4.6, we conclude our findings.

4.2 Literature review

This study relates to three strands of literature: a) international resource market equilibrium; b) iron ore market/trade study; c) interaction between transportation and trade.

In recent years, due to the rapid growth of natural gas trade volumes, many computable equilibrium models have been established for the natural gas market (e.g., Gabriel et al., 2005; Egging et al., 2010; Guo and Hawkes, 2018) and the electricity market (e.g., Weigt et al., 2006; Leuthold et al., 2012; Grimm et al., 2017). These models have been used to evaluate the impacts of factors including infrastructure expansion (Huppmann, 2013; Kunz et al., 2015), pricing scheme (Egerer et al., 2016;

Shi and Variam, 2017), and energy structure transition (Holz et al., 2016; Assembayeva et al., 2018). In contrast, few equilibrium models exist in iron ore market analysis. The only one we found is conducted by Toweh and Newcomb (1991), who presented a spatial equilibrium model of the iron ore market to estimate competitive prices and efficient trade flows through ex-post-computed transport cost.

We noticed that the said model was built upon the assumption of perfect competition, which does not reflect the real market. As Wu et al. (2016) noted, iron ore trade is commonly recognized as an oligopoly market of exporters and a competitive market of importers. This argument is supported by Germeshausen et al. (2018), which investigated whether market power exists in the international iron ore market. It conducted a stochastic frontier analysis to estimate the Lerner index and suggested that this market is imperfectly competitive since iron ore exporters exercise their market power. Although existing natural gas/electricity models have described a similar market structure, they are not applicable to the iron ore market, as they are based on assumptions of homogeneous commodity and FOB [12] price (Asche et al., 2017; Simshauser, 2018). In the existing literature on iron ore market analysis, iron ore is generally regarded as a heterogenous commodity whose price is CFR and, as Warell (2018) pointed out, for which it is hard to establish a uniform price. Thus, it calls for a different modelling paradigm than the "law of one price", which is adopted in describing the natural gas/electricity demand (Grimm et al., 2017). Zhu et al. (2019) discovered significant impact on exporters' market power when pricing regime changes from annual benchmark (FOB price) into spot price benchmark (CFR price). We will take into account both characteristics distinctive for iron ore trade, i.e., heterogeneity

[12] FOB: free on board, where the importer must pay the freight rate to the port of destination.

and CFR trade prices.

The existing equilibrium models of resource markets assume exogenous cost and thereby cannot reflect the interaction between transportation (shipping) and trade. This interaction has been well addressed empirically in literature (e.g., Nguyen and Tongzon, 2010; Bernhofen 2016; Bottasso et al., 2018; Bai and Lam, 2019, Angelopoulos et al., 2020), but there is no consensus on whether transportation affects trade. Nguyen and Tongzon (2010) conducted a causality analysis between transportation and foreign trade in Australia. The result indicates that international trade growth can affect the growth of transportation but not the other way around. Recent studies point to the opposite direction. For example, Bai and Lam (2019) studied the international trade of liquefied petroleum gas (LPG). They found that LPG trade is highly correlated with freight rate, applying a structural equation model incorporating factors such as fleet size and freight rate. In the perspective of market information transmission, Angelopoulos et al. (2020) applied a novel dynamic factor model and suggested that a price discovery relationship exists between freight and commodity markets. In addition, few studies attempted to answer the question using equilibrium models with endogenous transportation cost. Asturias (2020) developed a spatial computable general equilibrium (SCGE) model for two countries, in which the transportation cost is endogenized by a three-stage entry game of shippers. Using this model, they tested the effects of symmetric increase of tariffs in both China and the United States and found that trade barriers can increase shipping cost. Brancaccio et al. (2020) proposed a spatial equilibrium model in which the endogenous transportation cost is determined by a generalized Nash bargaining between exporters and ships. It found that the transport sector can attenuate the difference in comparative advantage across countries, generate network effects, and dampen the impact of shocks on trade flows. Sun et al. (2020) incorporated a cargo flow

assignment model to a SCGE model to study the impact of opening a new route on the global trade. These studies attempt to endogenize transportation cost from different perspectives, but they haven't looked into the inherent characteristics of shipping, e.g., fleet structure and capacity, which matter greatly in the iron ore trade.

In this study, we build a computable equilibrium model for the iron ore market, considering its heterogeneity and CFR trade price. This new setup improves existing models and is applicable to other bulk resource markets with similar characteristics, including coal, grain, etc. When endogenizing shipping cost, we in particular include fleet capacity and structure. This enables us to thoroughly explore the influencing mechanism of shipping on iron ore trade.

4.3 Equilibrium model for iron ore trade

This section describes a multi-sector mixed complementarity-based equilibrium model. Three major players in iron ore trade, namely exporters, importers, and carriers, are considered; each has one module dedicated to itself. Importer Module and Exporter Module are used to determine the equilibrium trade volume and prices though a Cournot competition of exporters, incorporating a CES-based inverse demand function. Carrier Module models the iron ore shipping market by assuming perfect competition among carriers in all market segments. Commodity/shipment flow and fleet deployment in different market segments are determined through a transportation optimization model. We also introduce a port selection problem to transform trade volume into cargo handling volume at port, which helps determine the transport volume in the transportation optimization model. Market clearing and consistency conditions are also presented to connect the three modules and ensure equilibrium.

To start, an overview of these players is provided, followed by the definition of notations and, finally, the model comprising three modules.

4.3.1 Overview of the players

In general, three major players can be recognized in the international iron ore trade:

Importers — The importing countries of iron ore. We assume that importers are price takers. Due to the heterogeneity of iron ore (Warell, 2018), importers maximize their utility, representing their preferences, by determining the iron ore imports from various exporters.

Exporters — The iron ore exporting countries. They compete with each other while trading with importers. The competition intensity depends on the number of exporters and their market shares. Due to different trading costs (including shipping cost) with the importers, exporters need to allocate their production capacities.

Iron ore carriers — Shipping service providers. They operate in the shipping market of multiple segments. A segment is defined as one ship size on one shipping route between a pair of origin and destination ports (Dinwoodie et al., 2014). Demand in each segment is derived from the allocation of trade volume when the overall shipping cost is minimized. In existing literature, it is generally accepted that the dry bulk shipping market is perfectly competitive (Peng, 2016), in which numerous carriers provide a homogenous service and thus an individual carrier hardly owns any market power. Therefore, we can assume each ship as an independent carrier and the carriers (i.e. ships) compete perfectly with each other in each market segment.

It should be noted that port operators are also one of the players. They provide cargo handling service for importers/exporters and berthing service for carriers. Unlike the above three players who are the independent decision makers, we implicitly include ports in the cost functions.

4.3.2 Notations

We present a system of subscripts referring to different variables of the model. An importer is denoted by $c \in C$, with C being the set of importers. Exporter is indexed by $m \in M$, with M being the set of exporters. In addition, a destination port is denoted by $d \in D(c)$ with $D(c)$ being the set of destination ports of importer $c \in C$. An origin port is indicated by $o \in O(m)$, with $O(m)$ being the set of origin ports of exporter $m \in M$. As explained before, each ship is considered as an independent carrier, we can classify carriers by ship size. A certain carrier type of same ship size is denoted by $k \in K$, with K being the set of carriers.

Table 4-1, 4-2, and 4-3 display the variables of importers, exporters, carriers, and destination/origin ports respectively. Table 4-4 gives the parameters. A bar on a variable *x, i.e.,* $\bar{x}$, indicates that the variable is exogenous.

Table 4-1. Importer & exporter variables

Variables	Description
U_c	Utility of importer *c* while trading with different exporters.
DC_c	Iron ore import volume of importer *c*. ($DC_c > 0$)
IC_c	Purchasing budget of importer *c*.
π_{mc}	Profit of exporter *m* from trading with importer *c*.
QM_m	Export volume of exporter *m*. ($QM_m > 0$)
QTC_m	Iron ore production capacity of exporter m.
Q_{mc}	Trade volume between exporter m and importer c. ($Q_{mc} > 0$)
P_{mc}	Iron ore trading price between exporter *m* and importer *c*. ($P_{mc} > 0$)

Table 4-2. Carrier variables

Variables	Description
SC	Total shipping cost of the international iron ore trade.
$QS_{m_o c_d}$	Iron ore shipment volume from origin port *o* of exporter *m* to destination port *d* of importer *c*.
$N_{km_o c_d}$	Number of *k*-type ships sailing from origin port *o* of exporter *m* to destination port *d* of importer *c*. ($N_{km_o c_d} \geq 0$)
$FK_{km_o c_d}$	Freight rate of *k*-type ships on the route between port *o* of exporter *m* and port *d* of importer *c*.
NC_k	Total number of *k*-type ships in the shipping market.
W_k	Average deadweight of *k*-type ships.
OD_k	Annual operating time of *k*-type ships.
V_k	Average speed of *k*-type ships.
$L_{m_o c_d}$	Route distance from port *o* of exporter *m* to port *d* of importer *c*.
MV_{mc}	Annual minimum voyages arranged between exporter *m* and importer *c*.

Table 4-3. Port variables

Variables	Description
CHC_c	Total cargo handling charges that importer *c* pays for discharging services at all of its destination ports.
QD_{c_d}	Discharging volume at destination port *d* of importer *c*. ($QD_{c_d} > 0$)
PD_{c_d}	Cargo handling price at port *d* of importer *c*. ($PD_{c_d} > 0$)
DSD_{c_d}	Unit berthing fee at destination port d of importer c.
CHM_m	Total cargo handling charges that exporter *m* pays for loading services provided by all origin ports.
QO_{m_o}	Loading volume at origin port *o* of exporter *m*. ($QO_{m_o} > 0$)
PO_{m_o}	Cargo handling price at port *o* of exporter *m*. ($PO_{m_o} > 0$)
DSO_{m_o}	Unit berthing fee at origin port o of exporter m.

Table 4-4. Parameters in the model

Parameters	Description
δ_{mc}^{d}	Share parameter used to determine the share of trade volume from exporter *m* to importer *c*. $\delta_{mc}^{d} \in (0,1)$, $\sum_{m \in M} \delta_{mc}^{d} = 1$.
σc_c	Parameter of substitution elasticity $\sigma c_c = 1 - \frac{1}{ec_c}$, where ec_c ($ec_c > 1$) is substitution elasticity among trade volumes trading from exporters to importer *c*.
AC_m	Efficiency parameter in CET function.
δ_{mc}^{s}	Share parameter used to determine the share of export capacities from exporter *m* to importer *c*. $\delta_{mc}^{s} \in (0,1)$, $\sum_{c \in C} \delta_{mc}^{s} = 1$.
σm_m	Parameter of transformation elasticity. $\sigma m_m = 1 - \frac{1}{em_m}$, where em_m ($em_m < 0$) is transformation elasticity among export capacities allocated by exporter *m* to importers.
AD_c	Efficiency parameter of CES function.
$\delta_{c_d}^{DP}$	Share parameter used to determine the share of imports discharging at port *d* of importer *c*. $\delta_{c_d}^{DP} \in (0,1)$, $\sum_{d \in D(c)} \delta_{c_d}^{DP} = 1$.
σd_c	Parameter of substitution elasticity. $\sigma d_c = 1 - \frac{1}{ed_c}$, where ed_c ($ed_c > 1$) is substitution elasticity among ports of importer *c*.
AO_m	Efficiency parameter of CES function.
$\delta_{m_o}^{OP}$	Share parameter used to determine the share of exports loading at port *o* of exporter *m*. $\delta_{m_o}^{OP} \in (0,1)$, $\sum_{o \in O(m)} \delta_{m_o}^{OP} = 1$.
σo_m	Parameter of substitution elasticity. $\sigma o_m = 1 - \frac{1}{eo_m}$, where eo_m ($eo_m > 1$) is substitution elasticity among ports of exporter *m*.

4.3.3 Module description

Figure 4-1 shows the structure of our model. We design three modules to represent strategies of importers, exporters, and carriers. Importer Module is an importer's utility maximization problem. With perfect information, the inverse demand function is available for exporters, based on which an exporter maximizes its profit through determining its trade volume, i.e., Exporter Module. In Carrier Module, to maximize its profit, a carrier arranges appropriate ship capacities to meet shipment volumes from

the origin ports to the destination ports. To determine the shipment volume, we need to know the discharging/loading volume of a port. We introduce a port selection problem where the import/export volumes are allocated to different ports. The equilibrium is ensured by the market clearing conditions, i.e., trade volume = shipment volume. In the following sections, we will describe the three modules and the allocation problem respectively.

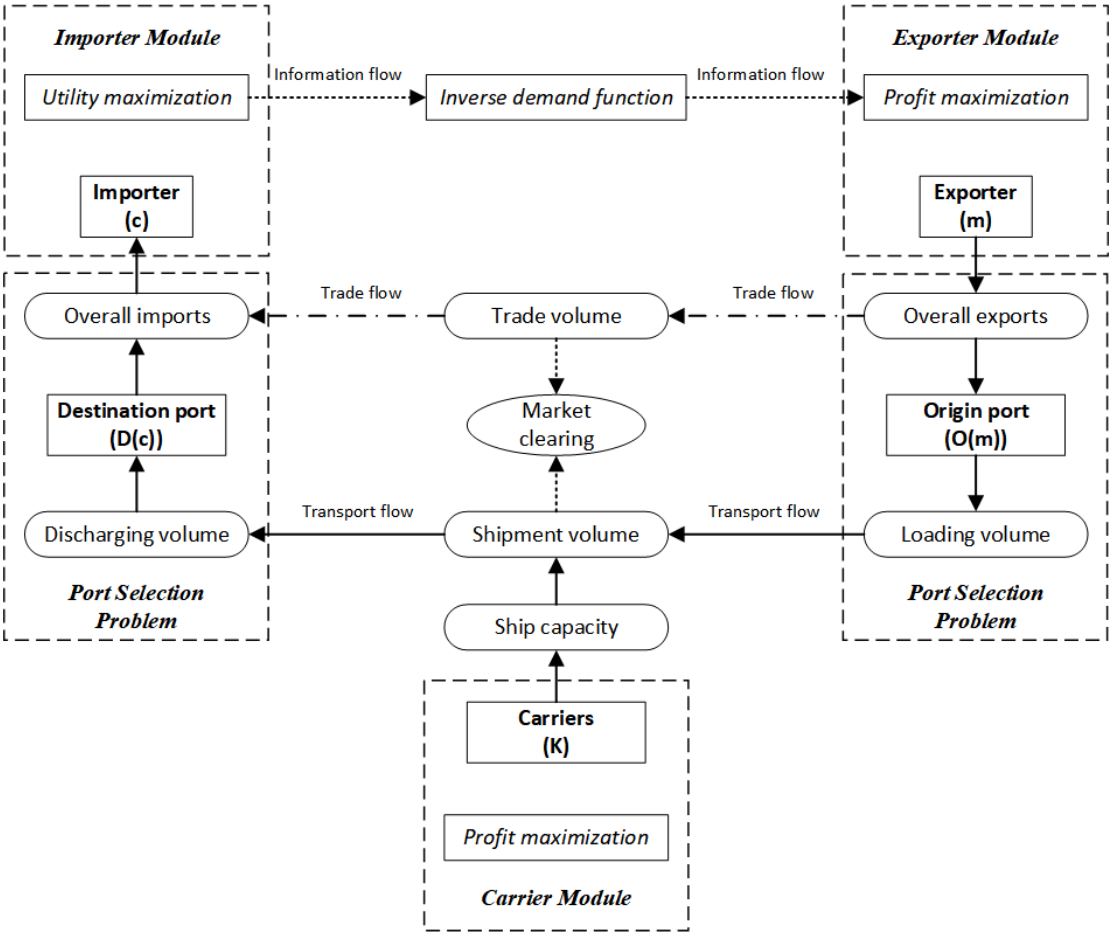

Figure 4-1. Structure of iron ore trade equilibrium model

4.3.3.1 Importer module

Importer Module illustrates the rational behaviors of importers in the international iron ore trade. Each importer has a given purchasing budget. Since they are price takers and

iron ores from different exporters are not perfect substitutes because of heterogeneity, each importer maximizes its utility by choosing appropriate proportions of iron ores from different exporters within its budget constraint. For an importer c, its utility maximization can be described as follows:

$$\max_{Q_{mc}} U_c = \left(\sum_{m \in M} \delta_{mc}^{d} {Q_{mc}}^{\sigma c_c} \right)^{1/\sigma c_c} \tag{4.1}$$

Subject to

$$\sum_{m \in M} P_{mc} Q_{mc} = \overline{IC}_c \quad (\gamma_c^U) \quad \forall\, c, \tag{4.1.a}$$

where γ_c^U ($\gamma_c^U\ free$) is the shadow price corresponding to constraint (4.1.a). The parameter of elasticity σc_c ($\sigma c_c = 1 - \frac{1}{ec_c}$) satisfies $\sigma c_c \in (0,1)$ since $ec_c > 1$.

In order to represent the imperfect substitution relationship among different exporters, (4.1) is constructed as a Constant Elasticity of Substitution (CES) utility function. Constraint (1a.1) indicates the budget constraint of importer c. Because the utility function satisfies the strict convex preference, we can derive a unique inverse demand function $P_{mc}(\cdot)$ to describe the relationship between trade price and volume based on the corresponding First Order Conditions (FOCs). Therefore, for a given trade between exporter m and importer c, the inverse demand function can be shown as the equation (4.2).

$$P_{mc} = P_{mc}(Q_{mc}, Q_{m'c}) = \frac{\overline{IC}_c \delta_{mc}^{d} {Q_{mc}}^{\sigma c_c - 1}}{\delta_{mc}^{d} {Q_{mc}}^{\sigma c_c} + \sum_{m' \in M \backslash m} \delta_{m'c}^{d} {Q_{m'c}}^{\sigma c_c}} \quad \forall\, m, c, \tag{4.2}$$

where $\sigma c_c = 1 - \frac{1}{ec_c}$ along with $ec_c > 1$, $\sigma c_c \in (0,1)$, $m'(m' \in M \backslash m)$ is a rival of exporter $m \in M$.

4.3.3.2 Exporter module

Wu et al. (2016) suggested that iron ore exporters participate in an imperfect competition. To understand their competitive pattern, we employ the conjectural variance approach (Wogrin et al., 2013), which is flexible in describing the market structure ranging from a Cournot competition to perfect competition. Given that competition among exporters varies in different iron ore markets because of heterogeneous cost and spatial difference (Zhu et al., 2019), we assume that exporters' competitions are not based on their overall exports, but on market-specific trade volume. Therefore, for each exporter m trading with importer c, it competes for quantity of output to maximize its own profits, which can be described as:

$$\max_{Q_{mc}} \ \pi_{mc} = [P_{mc}(Q_{mc}, Q_{m'c}) - PC_c - TC_{mc}]Q_{mc} \tag{4.3}$$

Subject to

$$Q_{mc} \leq QC_{mc} \quad (\gamma_{mc}^{QC}) \quad \forall\, m, c, \tag{4.3.a}$$

$$\sum_{m\in M}\sum_{c\in C}\frac{Q_{mc}}{\overline{MV}_{mc}} \leq \sum_{k\in K}\overline{NC}_k\overline{W}_k \quad (\gamma^{NC}), \tag{4.3.b}$$

where PC_c ($PC_c > 0$) is the average cargo handling price at the destination ports of importer c, TC_{mc} is the unit trade cost between m and c, QC_{mc} is the endogenous export capacity of exporter m to importer c ($QC_{mc} > 0$), γ_{mc}^{QC} and γ^{NC} ($\gamma_{mc}^{QC}, \gamma^{NC} \geq 0$) are the shadow prices corresponding to constraints (4.3.a) and (4.3.b).

In the objective function (4.3), $P_{mc}(Q_{mc}, Q_{m'c}) - PC_c$ indicates the FOB price offered by exporter m to importer c. TC_{mc} can be further split into following cost items:

$$TC_{mc} = \overline{CQ}_m + F_{mc} + PM_m \quad \forall\, m, c, \tag{4.4}$$

where $\overline{CQ}_m$ is the unit production cost of exporter m, F_{mc} ($F_{mc} > 0$) is the average freight rate from exporter m to importer c, PM_m ($PM_m > 0$) is the average cargo handling price at origin ports of exporter m. Constraint (4.3.a) specifies that trade volume (Q_{mc}) should be less than the export capacity. Constraint (4.3.b) guarantees that the overall fleet capacity can meet the shipping demand.

Since TC_{mc} is linear, and $P_{mc}Q_{mc}$ is concave given that $Q_{m'c}$ is fixed and $\sigma c_c \in (0,1)$, the KKT conditions of (4.3) are sufficient for optimality, which can be shown in (4.5) - (4.7):

$$0 \le Q_{mc} \perp \left[-(P_{mc} - PC_c - TC_{mc}) - \frac{\partial P_{mc}(Q_{mc}, Q_{m'c})}{\partial Q_{mc}} Q_{mc} + \gamma_{mc}^{QC} + \frac{\gamma^{NC}}{\overline{MV}_{mc}}\right] \ge 0 \quad \forall m, c, \tag{4.5}$$

$$0 \le \gamma_{mc}^{QC} \perp [QC_{mc} - Q_{mc}] \ge 0 \quad \forall m, c, \tag{4.6}$$

$$0 \le \gamma^{NC} \perp \left[\sum_K \overline{NC}_k \bar{W}_k - \sum_{m \in M} \sum_{c \in C} \frac{Q_{mc}}{\overline{MV}_{mc}}\right] \ge 0. \tag{4.7}$$

Given that production capacity ($\overline{QTC}_m$) is exogenous, the export capacity (QC_{mc}) can be regarded as the production capacity allocated to each importer. The relationships between the $\overline{QTC}_m$ and QC_{mc} is subject to the Production Possibility Frontier (PPF), which can be presented through a Constant Elasticity of Transformation (CET) function (Lin and Jia, 2018). Exporters need to maximize their trade revenue under zero profit condition ($P_{mc} - PC_c = TC_{mc}$) under the constraint of PPF. The endogenous export capacity from an exporter *m* to an importer *c* then can be derived from the following optimization problem:

$$\max_{QC_{mc}} TRR_m = \sum_{c \in C} TC_{mc}\, QC_{mc} \tag{4.8}$$

Subject to

$$\overline{QTC}_m = AC_m \left(\sum_{c \in C} \delta_{mc}^{s} {QC_{mc}}^{\sigma m_m} \right)^{1/\sigma m_m} \quad \left(\gamma_m^{QTC}\right) \quad \forall\, m, \tag{4.8.a}$$

where TRR_m denotes the revenue of exporter *m* while the FOB price equals to the unit trade cost, γ_m^{QTC} ($\gamma_m^{QTC}\ free$) is the shadow price corresponding to constraint (4.8.a). Based on FOCs of (2f), the export capacity of exporter *m* to importer *c* is given as:

$$QC_{mc} = \frac{\overline{QTC}_m}{AC_m} \left(\frac{\delta_{mc}^{s}}{TC_{mc}}\right)^{em_m} \left(\sum_{c \in C} {\delta_{mc}^{s}}^{em_m} {TC_{mc}}^{1-em_m} \right)^{-\frac{1}{\sigma m_m}} \quad \forall\, m, c. \tag{4.9}$$

Now we incorporate the conjectural variations into exporter profit maximization problem. These parameters represent an exporter's conjecture for the react of its rivals when itself adjusts its output or price (Perry, 1982). For exporter *m* and its rival $m'(m' \in M \backslash m)$, all trading with importer *c*, the conjectural variation is expressed as:

$$\mu_{mm'c} = \frac{\partial Q_{m'c}}{\partial Q_{mc}} \quad \forall\, m, m', c. \tag{4.10}$$

In equation (4.5), the first derivative of the inverse demand function associated with trade volumes of exporters and their conjectural variations, is given as:

$$\frac{\partial P_{mc}(Q_{mc}, Q_{m'c})}{\partial Q_{mc}} = P'_{mc}(Q_{mc}, Q_{m'c}, \mu_{mm'c}) \quad \forall\, m, c. \tag{4.11}$$

Given that the conjectural variations are constant, the competition pattern among exporters who trade with importer c, can be determined. Substitute equation (4.11) into equation (4.5), we can obtain the necessary condition for the optimal solution of

problem (4.3) as:

$$0 \le Q_{mc} \perp \left[PC_c + TC_{mc} + \gamma_{mc}^{QC} + \frac{\gamma^{NC}}{\overline{MV}_{mc}} - \frac{\sigma c_c}{\overline{IC}_c} P_{mc} \sum_{m' \in M'} P_{m'c} \cdot (Q_{m'c} - \mu_{mm'c} Q_{mc}) \right] \ge 0, \quad \forall\, m, c. \tag{4.12}$$

The optimal trade volumes can be solved by KKT conditions (4.6), (4.7) and (4.12).

4.3.3.3 Carrier module

Both importers and exporters have the incentive to minimize iron ore shipping cost. Here, we propose a two-stage transportation optimization model. In the first stage, a cargo flow assignment model is applied to determine the minimum-cost shipment volume ($QS_{m_o c_d}$) along different routes.

$$\min_{QS_{m_o c_d}} SC = \sum_{m \in M} \sum_{o \in O(m)} \sum_{c \in C} \sum_{d \in D(c)} (F_{mc} + \overline{PO}_{m_o} + \overline{PD}_{c_d}) QS_{m_o c_d} \tag{4.13}$$

Subject to

$$\sum_{c \in C} \sum_{d \in D(c)} QS_{m_o c_d} = QO_{m_o} \quad (\gamma_{m_o}^{SEA1}) \ \forall\, m, o, \tag{4.13.a}$$

$$\sum_{m \in M} \sum_{o \in O(m)} QS_{m_o c_d} = QD_{c_d} \quad (\gamma_{c_d}^{SEA2}) \ \forall\, c, d, \tag{4.13.b}$$

$$\sum_{o \in O(m)} \sum_{d \in D(c)} QS_{m_o c_d} = Q_{mc} \quad (\gamma_{mc}^{SEA3}) \ \forall\, m, c, \tag{4.13.c}$$

where SC denotes the overall shipping cost, $\gamma_{m_o}^{SEA1}, \gamma_{c_d}^{SEA2}$ and γ_{mc}^{SEA3} ($\gamma_{m_o}^{SEA1}, \gamma_{c_d}^{SEA2}\ and\ \gamma_{mc}^{SEA3}\ free$) are the shadow prices of constraint (4.13.a), (4.13.b) and (4.13.c).

In the objective function, the shipping cost consists of overall freight charges (F_{mc}) and cargo handling charges ($\overline{PO}_{m_o}, \overline{PD}_{c_d}$) at both origin and destination ports. Constraint (4.13.a) indicates that the sum of all shipment volumes ($QS_{m_o c_d}$) exiting origin port $o \in O(m)$ equals to its loading volume (QO_{m_o}). Constraint (4.13.b) illustrates that the discharging volume (QD_{c_d}) of destination port $d \in D(c)$ should be equal to the sum of all shipment volumes ($QS_{m_o c_d}$) to said destination port. Constraint (4.13.c) indicates a balance between the trade flow and the shipment flow from exporter *m* to importer *c*.

Since it is a linear program, the KKT conditions (3b) - (3e) are necessary and sufficient for optimality as:

$$0 \leq QS_{m_o c_d} \perp \left[F_{mc} + \overline{PO}_{m_o} + \overline{PD}_{c_d} - \gamma_{m_o}^{SEA1} - \gamma_{c_d}^{SEA2} - \gamma_{mc}^{SEA3}\right] \geq 0 \quad \forall m, o, c, d, \tag{4.14}$$

$$\gamma_{m_o}^{SEA1} \perp \left[\sum_{c \in C} \sum_{d \in D(c)} QS_{m_o c_d} - QO_{m_o}\right] = 0 \quad \forall m, o, \tag{4.15}$$

$$\gamma_{c_d}^{SEA2} \perp \left[\sum_{m \in M} \sum_{o \in O(m)} QS_{m_o c_d} - QD_{c_d}\right] = 0 \quad \forall c, d, \tag{4.16}$$

$$\gamma_{mc}^{SEA3} \perp \left[\sum_{o \in O(m)} \sum_{d \in D(c)} QS_{m_o c_d} - Q_{mc}\right] = 0 \quad \forall m, c. \tag{4.17}$$

Notice that the freight rate is correlated with the fleet structure placed on a route. Therefore, in the second stage, importers/exporters need to determine fleet deployment, namely, arranging the most appropriate combination of ship sizes, so as to minimize the freight charges as:

$$\min_{n_{km_oc_d}} FC_{mc} = \sum_{k\in K}\sum_{o\in O(m)}\sum_{d\in D(c)} FK_{km_oc_d} N_{km_oc_d} \bar{W}_k \left\lceil \frac{\overline{OD}_k \bar{V}_k}{2\bar{L}_{m_oc_d}} \right\rceil \tag{4.18}$$

Subject to

$$\sum_{k\in K} N_{km_oc_d} \bar{W}_k \left\lceil \frac{\overline{OD}_k \bar{V}_k}{2\bar{L}_{m_oc_d}} \right\rceil = QS_{m_oc_d} \quad (\gamma_{m_oc_d}^{SHIP1}) \quad \forall\, m, o, c, d, \tag{4.18.a}$$

$$\sum_{m\in M}\sum_{o\in O(m)}\sum_{c\in C}\sum_{d\in D(c)} N_{km_oc_d} \le \overline{NC}_k \quad (\gamma_k^{SHIP2}) \quad \forall\, k, \tag{4.18.b}$$

where FC_{mc} indicates freight charges for iron ore shipping between exporter m and importer c, $\gamma_{m_oc_d}^{SHIP1}$ ($\gamma_{m_oc_d}^{SHIP1}$ free) and γ_k^{SHIP2}($\gamma_k^{SHIP2} > 0$) are the shadow prices of constraints (4.18.a) and (4.18.b). $\left\lceil \frac{\overline{OD}_k \bar{V}_k}{2\bar{L}_{m_oc_d}} \right\rceil$ indicates the annual voyages of *k*-type ships between port $o \in O(m)$ and port $d \in D(c)$.

In iron ore shipping, a ship is always fully loaded in the head haul and ballast (non-load) in the back haul (Wu et al, 2018). Constraint (4.18.a) ensures the balance between the capacities of all ships and the shipment volume from the port $o \in O(m)$ to the port $d \in D(c)$. Constraint (4.18.b) indicates that the number of *k*-type ships is restricted by the total number of ships of the same type available in the shipping market. Because (4.18) is a linear program, KKT conditions (4.19) - (4.21) ensure optimality, as follows:

$$\begin{aligned} 0 \le N_{km_oc_d} \perp \left[FK_{km_oc_d} \bar{W}_k \left\lceil \frac{\overline{OD}_k \bar{V}_k}{2\bar{L}_{m_oc_d}} \right\rceil - \bar{W}_k \left\lceil \frac{\overline{OD}_k \bar{V}_k}{2\bar{L}_{m_oc_d}} \right\rceil \gamma_{m_oc_d}^{SHIP1} + \gamma_k^{SHIP2} \right] \\ \ge 0 \quad \forall\, k, m, o, c, d, \end{aligned} \tag{4.19}$$

$$\gamma_{m_oc_d}^{SHIP1} \perp \left[\sum_{k\in K} N_{km_oc_d} \bar{W}_k \left\lceil \frac{\overline{OD}_k \bar{V}_k}{2\bar{L}_{m_oc_d}} \right\rceil - QS_{m_oc_d} \right] = 0 \quad \forall\, m, o, c, d, \tag{4.20}$$

$$0 \leq \gamma_k^{SHIP2} \perp \left[\overline{NC}_k - \sum_{m \in M} \sum_{o \in O(m)} \sum_{c \in C} \sum_{d \in D(c)} N_{km_oc_d} \right] \geq 0 \quad \forall\, k. \tag{4.21}$$

With the above two-stage optimization models, demand in shipping market is converted into the number of k-type ships ($N_{km_oc_d}$) on each route. To align with the demand, we split the iron ore shipping market into different segments by ship type on the same route. On the supply side of each market segment, there is a perfect competition existing among carriers. Freight rate should be equal to the marginal cost of carriers as:

$$FK_{km_oc_d} = \frac{\overline{CT}_k \cdot 2\bar{L}_{m_oc_d}}{\bar{W}_k} + \overline{DSO}_{m_o} + \overline{DSD}_{c_d} \quad \forall\, m, o, c, d. \tag{4.22}$$

To simplify the model, we set an exogenous $\overline{CT}_k$ to describe the economies of scale caused by the ship size differences. Then carrier cost can be expressed as a linear function of shipment volume. In (4.22), carrier's marginal cost in a single voyage is a function of unit ship operating cost (e.g., bunker, discount, and crew) and unit berthing fee at ports ($\overline{DSO}_{m_o}$, $\overline{DSD}_{c_d}$).

4.3.3.4 Port selection problem

To obtain loading/discharging volumes (i.e., QO_{m_o}/QD_{c_d}) in Carrier Module, we formulate the port selection mechanism of importers/exporters as a volume allocation problem, assuming imperfect substitution among ports (Notteboom, 2009). For importer c and its destination port $d \in D(c)$, this cargo allocation problem can be specified as (4a).

$$\min_{QD_{c_d}} CHC_c = \sum_{d \in D(c)} \overline{PD}_{c_d} QD_{c_d} \tag{4.23}$$

Subject to

$$DC_c = AD_c \left(\sum_{d \in D(c)} \delta_{c_d}^{DP} {QD_{c_d}}^{\sigma d_c} \right)^{1/\sigma d_c} \quad (\gamma_c^{DP}) \quad \forall\, c, \tag{4.23.a}$$

where CHC_c denotes the cargo handling charges that importer *c* pays to its destination ports, γ_c^{DP} ($\gamma_c^{DP}\ free$) is the shadow price of constraint (4.23.a). Equation (4.23) is a linear objective function which minimizes the overall cargo handling charges of importer *c*. Constraint (4.23.a) is a CES function which describes the imperfect substitution among different ports of importer *c*.

Based on the FOCs for optimality of problem (4.23), we can obtain the discharging volume at destination port d of importer c as:

$$QD_{c_d} = \frac{DC_c}{AD_c} \left(\frac{\delta_{c_d}^{DP}}{\overline{PD}_{c_d}} \right)^{ed_c} \left[\sum_{d \in D(c)} (\delta_{c_d}^{DP})^{ed_c} {\overline{PD}_{c_d}}^{1-ed_c} \right]^{\frac{-1}{\sigma d_c}} \quad \forall\, c, d. \tag{4.24}$$

The average cargo handling price PC_c can be given as:

$$PC_c = \frac{CHC_c}{DC_c} = \frac{1}{AD_c} \left[\sum_{d \in D(c)} (\delta_{c_d}^{DP})^{ed_c} {\overline{PD}_{c_d}}^{1-ed_c} \right]^{1-\frac{1}{\sigma d_c}} \quad \forall\, c. \tag{4.25}$$

Similarly, for exporters, the minimization of cargo handling charges can be described as:

$$\min_{QO_{m_o}} CHM_m = \sum_{o \in O(m)} \overline{PO}_{m_o} QO_{m_o} \tag{4.26}$$

Subject to

$$QM_m = AO_m \left(\sum_{o \in O(m)} \delta_{m_o}^{OP} {QO_{m_o}}^{\sigma o_m} \right)^{\frac{1}{\sigma o_m}} \quad (\gamma_m^{OP}) \quad \forall\, m, \tag{4.26.a}$$

where CHM_m is the cargo handling charges that exporter m pays to origin ports, γ_m^{OP} ($\gamma_m^{OP}\ free$) is the shadow price of constraint (4.26.a).

The loading volume at origin port o of exporter m is formulated as:

$$QO_{m_o} = \frac{QM_m}{AO_m} \left(\frac{\delta_{m_o}^{OP}}{\overline{PO}_{m_o}} \right)^{eo_m} \left[\sum_{o \in O(m)} (\delta_{m_o}^{OP})^{eo_m} {\overline{PO}_{m_o}}^{1-eo_m} \right]^{\frac{-1}{\sigma o_m}} \quad \forall\, m, o. \tag{4.27}$$

The average cargo handling price PM_m can be given as:

$$PM_m = \frac{CHM_m}{QE_m} = \frac{1}{AO_m} \left[\sum_{o \in O(m)} (\delta_{m_o}^{OP})^{eo_m} {\overline{PO}_{m_o}}^{1-eo_m} \right]^{1-\frac{1}{\sigma o_m}} \quad \forall\, m. \tag{4.28}$$

4.3.3.5 Market-clearing and consistency conditions

To connect the modules, the following consistency and market clearing conditions are proposed:

$$QM_m = \sum_{c \in C} Q_{mc} \quad \forall\, m, \tag{4.29}$$

$$DC_c = \sum_{m \in M} Q_{mc} \quad \forall\, c, \tag{4.30}$$

$$P_{mc}^* = P_{mc}(Q_{mc}^*) = \frac{\overline{IC}_c \delta_{mc}^d {Q_{mc}^*}^{\sigma c_c - 1}}{\sum_{m \in M} \delta_{mc}^d {Q_{mc}^*}^{\sigma c_c}} \quad \forall\, m, c, \tag{4.31}$$

$$F_{mc} = \frac{FC_{mc}}{Q_{mc}} \quad \forall\, m, c. \tag{4.32}$$

Market clearing condition (4.29) indicates that the exports of an exporter are the sum of its trade to each importer. Market clearing condition (4.30) requires that the imports of an importer are the sum of its trade with each exporter. Market-clearing condition (4.31) is to calculate the equilibrium iron ore price (P_{mc}). Consistency condition (4.32) is the price function of average freight rate.

4.4 Solution procedure

The above model can be transformed into a Mixed Complementarity Problem (MCP) with KKT conditions of each module. Notice that the number of ships ($n_{km_oc_d}$) is an integer variable, therefore, it is a discretely constrained MCP (DC-MCP). Gabriel (2017) proposed that, the generic MCP can be transformed into a mixed-integer nonlinear program (MINLP) though the median function-based formulation. Refer to this, our model is reformulated as a MINLP. The complex nonlinearity of CES/CET functions in our model leads to the nonconvexities of transformed MINLP, we then need convexify those CES/CET-based nonconvexities, and apply OA/ER/AP (Outer-Approximation/Equality-Relaxation/Augmented-Penalty) algorithm to solve the MINLP model.

4.4.1 MINLP formulation of DC-MCP

Given the function $f: R^n \to R^n$, a nonnegative vector $x = (x_1, x_2, x_3, \dots, x_{n_x}) \in R^{n_x}$ and a vector $y = (y_1, y_2, y_3, \dots, y_{n_y}) \in R^{n_y}$, we consider a MCP as follows:

Find the entire vectors (x, y)

$$0 \le f_i(x,y) \perp x_i \ge 0, \qquad i \in I_x = \{1,\dots,n_x\}, \tag{4.33}$$

$$0 = f_j(x,y), y_j \; free, \qquad j \in I_y = \{1,\dots,n_y\}. \tag{4.34}$$

Consider some integer elements in vector x, they should satisfy the (p1) with the following discrete restrictions:

$$x_s \in [0,+\infty), \qquad s \in S_x \subseteq I_x, \tag{4.35}$$

where S_x is the set of indices for integer variables. The solution of DC-MCP is a pair of vectors (x,y) that can solve (4.33), (4.34) and (4.35).

The MCP (4.33 and 4.34) can be equivalently transformed into a problem to find the zero of median function $H: R^n \to R^n$ (Gabriel, 2017). Here, we redefine H as a minimum function to fit our model, as:

$$H_i(x,y) = [x_i, f_i(x,y)], \qquad i \in I_x = \{1,\dots,n_x\}, \tag{4.36}$$

$$H_j(x,y) = f_j(x,y), y_j \; free, \qquad j \in I_y = \{1,\dots,n_y\}. \tag{4.37}$$

Based on the concept of function H, we consider the following problem:

$$\min_{x,y} \|H(x,y)\|_1 \tag{4.38}$$

Subject to

$$x_i \in R_+ \quad i \in I_x \setminus S_x, \tag{4.38.a}$$

$$x_i \in Z_+ \quad i \in S_x, \tag{4.38.b}$$

$$y_j \in R \quad j \in I_y, \tag{4.39.c}$$

where $\|\cdot\|_1$ is the L1 vector norm, $\|H(x,y)\|_1 = \sum_{i\in I_x}|H_i(x,y)| + \sum_{j\in I_y}|H_j(x,y)|$. The objective function of (4.38) indicates the minimization of the Manhattan Distance

of $H(x,y)$. Constraints (4.38.a) and (4.38.c) ensure the positive and free variables, respectively. Constraint (4.38.b) ensures the integer variables. Suppose the optimal solution of (4.38) is the vector pair (x^*, y^*), it's not difficult to show that the optimal solution of (4.38) can solve the DC-MCP (4.33, 4.34 and 4.35) if its objective function value equals to *zero*. By considering the complementarity between x_i and f_i in equation (4.36), three cases regarding $H_i(x,y)$ for each $i \in I_x$ can be recognized as follows:

Case1: If $x_i - f_i(x,y) > 0$, then $H_i(x,y) = f_i(x,y)$

Case2: If $x_i - f_i(x,y) < 0$, then $H_i(x,y) = x_i$

Case3: If $x_i - f_i(x,y) = 0$, then $H_i(x,y) = x_i = f_i(x,y)$

For equation (4.37), we have $H_j(x,y) = f_j(x,y)$ holding for each $j \in I_y$.

Accordingly, the following disjunctive inequalities can be derived based on the above cases concerning $H_i(x,y)$:

$$-M(1-b_i) \le x_i - f_i(x,y) \le Mb_i \quad i \in I_x, \tag{4.40.a}$$

$$-Mb_i \le H_i(x,y) - x_i \le Mb_i \quad i \in I_x, \tag{4.40.b}$$

$$-M(1-b_i) \le H_i(x,y) - f_i(x,y) \le M(1-b_i) \quad i \in I_x, \tag{4.40.c}$$

where b_i is a binary variable for each $i \in I_x$. M is a suitably large, positive constant. It is easy to find that ***Case 1*** holds only if $b_i = 1$. When $b_i = 1$, (p7) implies that $x_i - f_i(x,y) \ge 0$, (p8) is redundant and (p9) implies that $H_i(x,y) - f_i(x,y) = 0$. Similarly, ***Case 2*** holds only if $b_i = 0$. For ***Case 3***, given $x_i - f_i(x,y) = 0$, (p7) is feasible when $b_i = 0 \; or \; 1$. When $b_i = 0$, (p8) shows that $H_i(x,y) = x_i = f_i(x,y)$ and (p9) is redundant. When $b_i = 1$, (p8) is redundant and (p9) shows that $H_i(x,y) = f_i(x,y) = x_i$. Hence, ***Case 3*** holds if $b_i = 0 \; or \; 1$. s for $H_j(x,y)$, there are always the equalities:

$$H_j(x,y) - f_j(x,y) = 0, \quad j \in I_y. \tag{4.40.d}$$

By adding (p7), (p8), (p9) and (p10) as the constraints, we can transform the objective function of (4.38) to a smooth form.

Here we introduce two pairs of nonnegative vectors (α^+, α^-) and (β^+, β^-), where $\alpha^+, \alpha^- \in R^{n_x}$ and $\beta^+, \beta^- \in R^{n_y}$. The minimum function H can be formulated as $H_i(x,y) = \alpha_i^+ - \alpha_i^-$ $(i \in I_x)$ and $H_j(x,y) = \beta_j^+ - \beta_j^-$ $(j \in I_y)$ respectively. Then, the smooth form of (4.38) can be shown as follows:

$$\min_{x,y,\alpha_i^+,\alpha_i^-,\beta_j^+,\beta_j^-,b_i} \sum_{i \in I_x} (\alpha_i^+ + \alpha_i^-) + \sum_{j \in I_y} (\beta_j^+ + \beta_j^-) \tag{4.41}$$

Subject to

$$-M(1-b_i) \le x_i - f_i(x,y) \le Mb_i \quad i \in I_x, \tag{4.41.a}$$

$$-Mb_i \le \alpha_i^+ - \alpha_i^- - x_i \le Mb_i \quad i \in I_x, \tag{4.41.b}$$

$$-M(1-b_i) \le \alpha_i^+ - \alpha_i^- - f_i(x,y) \le M(1-b_i) \quad i \in I_x, \tag{4.41.c}$$

$$\beta_j^+ - \beta_j^- - f_j(x,y) = 0 \quad j \in I_y, \tag{4.41.d}$$

$$x_i \in R_+ \qquad i \in I_x \setminus S_x, \tag{4.41.e}$$

$$x_i \in Z_+ \qquad i \in S_x, \tag{4.41.f}$$

$$y_j \in R \qquad j \in I_y, \tag{4.41.g}$$

$$b_i \in \{0,1\} \qquad i \in I_x, \tag{4.41.h}$$

$$\alpha_i^+, \alpha_i^- \ge 0 \quad i \in I_x, \tag{4.41.i}$$

$$\beta_j^+, \beta_j^- \geq 0 \quad j \in I_y. \tag{4.41.j}$$

Due to nonlinear formulations existed in $f_j(x, y)$ of our model, problem (4.41) is a mixed integer nonlinear program (MINLP). Gabriel (2017) has proved that the optimal solution $(x^*, y^*, \alpha_i^{+*}, \alpha_i^{-*}, \beta_j^{+*}, \beta_j^{-*}, b_i^*)$ to problem (4.41) contains a vector pair (x^*, y^*) which can solve the DC-MCP (4.33, 4.34 and 4.35) when the objective function value of (4.41) equals to *zero*. Hence, the DC-MCP (4.33, 4.34 and 4.35) can be transformed into a MINLP (4.41).

According to the definition of DC-MCP, the solution (x^*, y^*) satisfies the discrete constraints and also the complementarities. For a large-scale DC-MCP (4.33, 4.34 and 4.35), the MINLP (4.41) generally is its relaxation problem since the complementarities (4.33 and 4.34) need to be relaxed so as to satisfy the discrete constraint (4.35). Therefore, the optimal objective function value of (4.41) is larger than zero, which implies that (x^*, y^*) is an approximate solution. When the optimal objective function value of (4.41) is smaller, the (x^*, y^*) is closer to the solution of the DC-MCP (4.33, 4.34 and 4.35).

In order to ensure that (x^*, y^*) can solve the DC-MCP (4.33, 4.34 and 4.35), it is necessary to find the global optimal solution of MINLP (4.41). As a large-scale problem, there is no exact algorithm developed to solve the MINLP (4.41) yet. From this model, it can be observed that the integer variables (both $N_{km_oc_d}$ and b_i) in (4.41) are separable[13]. With this feature, we apply the Outer Approximation (OA) algorithms to

[13] In a slight abuse of notation, suppose x is a continuous variable, y is an integer variable, and f(x,y) is a function. If y in f(x, y) can be separated by an univariant function h(y), as f(x, y)=g(x)+h(y), we call the integer variable y is separable.

obtain a near optimal solution of (4.41) within the acceptable tolerance, which has been demonstrated to be efficient in computing time for many instances of separable MINLP (Floudas, 1995).

However, since the complexity of CES/CET functions lead to the nonconvexity in $f_i(x, y)$, the global (approximate) optimum of (p11) cannot be guaranteed with general *decomposition strategy* algorithms, e.g., Generalized Benders Decomposition (GBD) and Outer Approximation (OA) algorithms (Kesavan, et al., 2004). Therefore, we need further reformulate these nonconvexities in (p11) to match with the requirements of the selected algorithm.

4.4.2 Reformulation of the CES/CET-based nonconvexity

The nonconvexity in MINLP (4.41) is caused by CES functions and CET functions. The CES-based nonconvexity is from the KKT conditions in exporter module. The CET-based nonconvexity is from the first order conditions of cost minimization problem in production capacity allocation.

4.4.2.1 CES-based nonconvexity

Among KKT conditions of exporter module, the complementarity relationship in (4.12) can be abstracted as the following nonlinear format:

$$0 \le q_i \perp \left[u_i - \sum_{i' \in I_x \setminus i} \overline{\sigma} \cdot p_i p_{i'} q_{i'} + \sum_{i' \in I_x \setminus i} \overline{\sigma} \cdot \overline{\mu}_{ii'} \cdot p_i p_{i'} q_i \right] \ge 0, \quad \forall\, i \in I_x. \quad (4.42)$$

where q_i, u_i and p_i are positive variables, $\overline{\sigma}$ and $\overline{\mu}_{ii'}$ are positive constant. Inequality (4.42) is transformed into a group of constraints in MINLP (4.41) shown as follows:

$$\begin{cases} q_i - u_i + \sum_{i' \in I_x \setminus i} \overline{\sigma} \cdot p_i p_{i'} q_{i'} - \sum_{i' \in I_x \setminus i} \overline{\sigma} \cdot \overline{\mu}_{ii'} \cdot p_i p_{i'} q_i \le M \cdot b_i \\ -q_i + u_i - \sum_{i' \in I_x \setminus i} \overline{\sigma} \cdot p_i p_{i'} q_{i'} + \sum_{i' \in I_x \setminus i} \overline{\sigma} \cdot \overline{\mu}_{ii'} \cdot p_i p_{i'} q_i \le M(1 - b_i) \\ -M \cdot b_i \le \alpha_i^+ - \alpha_i^- - q_i \le M \cdot b_i \\ \alpha_i^+ - \alpha_i^- - u_i + \sum_{i' \in I_x \setminus i} \overline{\sigma} \cdot p_i p_{i'} q_{i'} - \sum_{i' \in I_x \setminus i} \overline{\sigma} \cdot \overline{\mu}_{ii'} \cdot p_i p_{i'} q_i \le M(1 - b_i) \\ -\alpha_i^+ + \alpha_i^- + u_i - \sum_{i' \in I_x \setminus i} \overline{\sigma} \cdot p_i p_{i'} q_{i'} + \sum_{i' \in I_x \setminus i} \overline{\sigma} \cdot \overline{\mu}_{ii'} \cdot p_i p_{i'} q_i \le M(1 - b_i) \\ \forall\, i, i' \in I_x,\ \ i \ne i', \end{cases}$$

(4.43)

where M is positive, $b_i \in \{0,1\}$, $\alpha_i^+ \in \alpha^+$ and $\alpha_i^- \in \alpha^-$. The nonlinear terms $\overline{\sigma} \cdot p_i p_{i'} q_{i'}$ and $\overline{\sigma} \cdot \overline{\mu}_{ii'} \cdot p_i p_{i'} q_i$ are nonconvex. We can firstly linearize the (4.13) by introducing two positive variables $\phi_{ii'}$ and $\omega_{ii'}$ to replace the nonlinear terms, as:

$$\phi_{ii'} = \overline{\sigma} \cdot p_i p_{i'} q_{i'}, \tag{4.44.a}$$

$$\omega_{ii'} = \overline{\sigma} \cdot \overline{\mu}_{ii'} \cdot p_i p_{i'} q_i, \ \ \forall\, i, i' \in I_x, i \ne i'. \tag{4.44.b}$$

Since $\overline{\sigma}$ and $\overline{\mu}_{ii'}$ are positive, the right-hand sides of equations (4.44) and (4.45) are posynomials which can be convexified though an exponential transformation, as:

$$\phi_{ii'} = \overline{\sigma} \cdot e^{\tau_i^p + \tau_{i'}^p + \tau_{i'}^q}, \tag{4.45.a}$$

$$\omega_{ii'} = \overline{\sigma} \cdot \overline{\mu}_{ii'} \cdot e^{\tau_i^p + \tau_{i'}^p + \tau_i^q}, \tag{4.45.b}$$

$$\tau_i^p = ln\, p_i\,, \tag{4.45.c}$$

$$\tau_i^q = ln\, q_i\,, \ \ \forall i, i' \in I_x, i \ne i', \tag{4.45.d}$$

where τ_i^p and τ_i^q are free. It is easy to prove that the right-hand sides of (4.45.a) and

(4.45.b) are convex, $ln\ p_i$ and $ln\ q_i$ are concave. Thus, the constraint group (4.43) can be reformulated as the following convex format:

$$\begin{cases} q_i - u_i + \sum_{i' \in I_x \setminus i} \phi_{ii'} - \sum_{i' \in I_x \setminus i} \omega_{ii'} \le M \cdot b_i \\ -q_i + u_i - \sum_{i' \in I_x \setminus i} \phi_{ii'} + \sum_{i' \in I_x \setminus i} \omega_{ii'} \le M(1 - b_i) \\ -M \cdot b_i \le \alpha_i^+ - \alpha_i^- - q_i \le M \cdot b_i \\ \alpha_i^+ - \alpha_i^- - u_i + \sum_{i' \in I_x \setminus i} \phi_{ii'} - \sum_{i' \in I_x \setminus i} \omega_{ii'} \le M(1 - b_i) \\ -\alpha_i^+ + \alpha_i^- + u_i - \sum_{i' \in I_x \setminus i} \phi_{ii'} + \sum_{i' \in I_x \setminus i} \omega_{ii'} \le M(1 - b_i) \\ \overline{\sigma} \cdot e^{\tau_i^p + \tau_{i'}^p + \tau_{i'}^q} - \phi_{ii'} = 0 \\ \overline{\sigma} \cdot \overline{\mu}_{ii'} \cdot e^{\tau_i^p + \tau_{i'}^p + \tau_i^q} - \omega_{ii'} = 0 \\ \tau_i^p - \ln p_i = 0 \\ \tau_i^q - \ln q_i = 0 \\ \phi_{ii'}, \omega_{ii'} \in R_+,\ \ \tau_i^p, \tau_i^q \in R \\ \forall i, i' \in I_x, i \ne i'. \end{cases} \tag{4.46}$$

4.4.2.2 CET production frontier-based nonconvexity

In exporter module, we endogenize the export capacity through a cost minimization problem under the constraint of CET production frontier. The FOC of this problem can be abstracted as the following format:

$$z_j = \overline{\rho} \cdot \overline{\delta}_j \cdot {t_j}^{-\overline{e}} \left(\sum_{j \in I_y} \overline{\delta}_j \cdot {t_j}^{1-\overline{e}} \right)^{\frac{\overline{e}}{1-\overline{e}}}, \quad \forall\, j, \tag{4.47}$$

where z_j and t_j are positive variables, $\overline{\rho}$ and $\overline{\delta}_j$ are positive constants, and $\overline{e}$ is a negative constant. The equation (4.47) can be transformed into a constraint of MINLP (4.41), which is shown as:

$$\beta_j^+ - \beta_j^- - z_j + \overline{\rho} \cdot \overline{\delta}_j \cdot {t_j}^{-\overline{e}} \left(\sum_{j \in I_y} \overline{\delta}_j \cdot {t_j}^{1-\overline{e}} \right)^{\frac{\overline{e}}{1-\overline{e}}} = 0, \ \ \forall j, \tag{4.48}$$

where $\beta_j^+ \in \beta^+, \ \beta_j^- \in \beta^-$. The nonlinear term in the equality (4.48) is nonconvex. To convexify the (4.48), we firstly introduce a positive variable ψ, by

$$\psi = \sum_{j \in I_y} \overline{\delta}_j \cdot {t_j}^{1-\overline{e}}, \tag{4.49.a}$$

$$\beta_j^+ - \beta_j^- - z_j + \overline{\rho} \cdot \overline{\delta}_j \cdot {t_j}^{-\overline{e}} \psi^{\frac{\overline{e}}{1-\overline{e}}} = 0, \ \ \forall j. \tag{4.49.b}$$

It can be proved that the right-hand side of (4.49a) is convex when $\overline{e} < 0$. Since the nonlinear term in (4.49b) is a posynomial, which can be convexified through an exponential transformation, as:

$$\beta_j^+ - \beta_j^- - z_j + \overline{\rho} \cdot \overline{\delta}_j \cdot exp\left(-\overline{e} \cdot \theta_j^t + \frac{\overline{e}}{1-\overline{e}} \cdot \theta^{\psi}\right) = 0, \tag{4.50.a}$$

$$\theta_j^t = ln\left(t_j\right), \tag{4.50.b}$$

$$\theta^{\psi} = ln\left(\psi\right), \ \ \forall j, \tag{4.50.c}$$

where θ_j^t and θ^{ψ} are free. Based on (4.49.a), (4.50.a), (4.50.b) and (4.50.c), the constraint (4.48) can be reformulated as a group of convex constraints:

$$\begin{cases} \beta_j^+ - \beta_j^- - k_j + \overline{\rho} \cdot \overline{\delta}_j \cdot \exp\left(-\overline{e} \cdot \theta_j^t + \dfrac{\overline{e}}{1-\overline{e}} \cdot \theta^\psi\right) = 0 \\ \theta_j^t - \ln(t_j) = 0 \\ \theta^\psi - \ln(\psi) = 0 \\ \sum\limits_{j \in I_y} \overline{\delta}_j \cdot {t_j}^{1-\overline{e}} - \psi = 0 \\ \psi \in R_+, \quad \theta_j^t, \theta^\psi \in R \\ \forall\, j \in I_y. \end{cases} \tag{4.51}$$

By convexifying these non-convex terms, MINLP (4.41) can be reformulated as a convex MINLP. The OA/ER/AP algorithm proposed by Viswanathan et al. (1990) can be applied to solve the reformulated MINLP. The global optimal solution contains the vector pair (x^*, y^*), which is the relaxed solution to DC-MCP (4.33, 4.34 and 4.35).

4.5 Numerical study

In this section, we apply our model to simulate the international iron ore trade. After introducing the case, data, and parameter estimation, we first evaluate the performance of our model by comparing it to the models (Model 1 and Model 2) with exogenous shipping freight rate and production capacity constraint in Section 4.5.3. Then, we investigate the impact of shipping when an outside shock is present in Section 4.5.4. Our model is solved with DICOPT Solver of GAMS. Model 1 and Model 2 are solved with PATH Solver of GAMS.

4.5.1 Case introduction

According to the database released by UN Comtrade in 2016, China, Japan and South Korea accounted for 81.7% of total international iron ore import in 2015. Australia and Brazil took up over 81% of the global export in the same year. Therefore, the trade among them is going to be our case study, as shown in Table 4-5.

Table 4-5. Main importers and exporters in iron ore trade

Set	Subscripts	Element	Explanation	Abbreviation
C	c	$c1$	China	CHN
		$c2$	Japan	JPN
		$c3$	South Korea	SK
M	m	$m1$	Brazil	BRA
		$m2$	Australia	AUS

In Brazil, the main iron ore loading ports include Port of PDM, Port Victoria (e.g., Tubarao) and Port Rio de Janeiro (e.g., CSN terminal). The majority of Australian iron ore is exported from the ports located on the west coast, e.g., Port Dampier and Port Headland under Pilbara Port Authority. Some of the ports, with considerable export volumes, are owned and operated by iron ore miners (e.g., Port Walcott). Hence, we distinguish Australian port authority (Pilbara) managed ports from miner operated ports. For discharging ports in China, simply, we divide them into three groups by geographical proximity, which are North China, Central China and South China. As for Japan and South Korea, we assume either has one single iron ore port because their discharging ports are quite concentrated. Table 4-6 shows the details of origin/destination ports considered in our model.

Table 4-6. Origin/destination ports of main exporters/importers

Set	Subscripts	Element	Explanation
$O(m1)$	o	$o1$	Port of Ponta da Madeira (PDM)
		$o2$	Ports of Victoria (main Tubarao and Ponta do Ubu)
		$o3$	Ports of Rio de Janeiro (main CSN, CPBS and GIT) [(a)]
$O(m2)$	o	$o4$	Pilbara port authority (main Dampier and Port Headland)
		$o5$	Other non-authority ports (e.g., Walcott and Cape Preston)
$D(c1)$	d	$d1$	Ports in North China
		$d2$	Ports in Yangtze River Delta (Central China)
		$d3$	Ports in South China
$D(c2)$	d	$d4$	Ports of Japan
$D(c2)$	d	$d5$	Ports of South Korea

Note: CSN: the terminal of Companhia Siderrgica Nacional; CPBS: the terminal of the Companhia

Portuaria Baia de Sepetiba; GIT: Guaiba Island Terminal.

The Capesize ship is the most adopted ship type for transporting iron ore. The tonnage of Capesize ships varies greatly. To simply, we classify them (carrier types) into three groups shown in table 4-7. Note that Brazil can employ large-size ships, while Australia cannot, due to its port depth limitation.

Table 4-7. Types of Capesize ships in iron ore shipping market

Set	Subscripts	Element	Explanation
K	k	$k1$	Small size—150,000-200,000 dwt
		$k2$	Medium size—200,000-300,000 dwt
		$k3$	Large size—300,000-400,000 dwt

4.5.2 Data and parameter estimation

The data applied in this study is collected from multiple sources. Due to the delayed update, e.g., CSN and GIT terminals in Brazil, the data we used in this study are from the year of 2015.

Iron ore purchasing budgets and export capacities are derived from *UN Comtrade*. Iron ore production costs are collected from *MySteel.com*. Port charges are obtained from corresponding websites of Port Authorities. Fleet capacities and average DWTs are obtained from *Shipping Intelligence Network*. Sea routes and distances are from *Sea-Distances.org*. Ship operating cost, speed, and average annual operating days are provided by the *COSCO Bulk*. Detailed values of above data can be found in the Appendix C-1.

In the study, we need estimate the parameters of CES functions. We adopt a linear regression approach proposed by Gallaway et al. (2003) to estimate the parameters of importer CES utility and exporter CET production possibility frontier. This estimation

is based on monthly trade volumes between ODs and their corresponding CFR prices, covering the period from January 2014 to December 2016, from *MySteel.com*.

The parameters of CET PPF are estimated with the Kmenta approximation approach adopted by Koesler and Schymura (2015). Same data source of the same time period as above.

The parameters of CES functions in the import/export volume allocation problem are also estimated based on Kmenta approximation approach. Iron ore loading/discharging volumes are collected for the origin/destination ports presented in Table 4-6. Those of Brazilian ports are collected from *LBH Group*. Those of Australian ports is obtained from *trade statistics of Western Australia Port Authorities.* Discharging volumes of Chinese ports are from *China's Customs Statistics*. Again, monthly records from the same time period.

We also need to estimate the conjectural variations of exporters. Here, we apply the approach proposed by Santis et al. (2002). Detailed information regarding parameter estimation can be found in the Appendix C-2.

4.5.3 Model performance

Assuming freight rate, fleet, and production capacity are the same, we compare our model, namely Model 0, with two spatial equilibrium models in canonical settings (Model 1 and Model 2). Table 4-8 illustrates the differences. Model 1 stands for a standard international resource market model, subject to exogenous shipping cost and production capacity constraint. Model 2 is built upon Model 1, where the production capacity constraint is replaced by export capacity constraint generated from production capacity allocation.

Table 4-8. Differences among three equilibrium models

Model	Constraints on trade volumes	Shipping cost
Model 0	Export capacity generated from production capacity allocation (Constraint 4.3.a)	Endogenous
Model 1	Production capacity ($\sum_{c\in C} Q_{mc} \leq \overline{QTC}_m$)	Exogenous
Model 2	Export capacity generated from production capacity allocation (Constraint 4.3.a)	Exogenous

Note: Model 0 represents our model.

Table 4-9 compares the trade volumes simulated by these three models with real data. Two models (Model 0 and Model 2) with export capacity constraints generate almost identical results. It indicates that the endogenous shipping cost does not affect the accuracy in simulating trade volumes. The results between Model 0 (Model 2) and Model 1 are different. In terms of total trade volume, the relative error of Model 0 (Model 2) is -1.17% against 1.74% of Model 1. The result of Model 0 (Model 2) is slightly better than that of Model 1. However, as for trade volumes between different OD pairs, the relative errors of Model 0 (Model 2) range from -0.83% (AUS-CHN) to 14.04% (BRA-SK), which is much smaller than the range of Model 1, from -10.02% (BRA-SK) to 60.63% (AUS-SK). This indicates that the models subject to export capacity constraint (Constraint 4.3.a) perform better.

Table 4-9. Comparison of iron-ore trade volumes between different ODs

OD pair	Trade volume[a] (Q_{mc})						
	Real data of 2015[b]	Model 0	Model 1	Model 2	Relative error of Model 0	Relative error of Model 1	Relative error of Model 2
BRA-CHN	1784.47	1695.59	1650.26	1695.63	-4.98%	-7.52%	-4.98%
BRA-JPN	345.48	330.78	323.64	330.78	-4.25%	-6.32%	-4.25%
BRA-SK	97.04	110.66	87.32	110.66	14.04%	-10.02%	14.04%
AUS-CHN	6283.92	6231.92	6211.17	6231.78	-0.83%	-1.16%	-0.83%
AUS-JPN	875.04	891.87	938.04	891.87	1.92%	7.20%	1.92%
AUS-SK	574.70	582.92	923.13	582.92	1.43%	60.63%	1.43%
Total trade volume	9960.65	9843.75	10133.56	9843.64	-1.17%	1.74%	-1.17%

Note: (a) The unit of trade volume is 10^5 tonnes. (b) The trade volume data in 2015 is collected from Mysteel.com.

Table 4-10 compares the capacity constraint, price, and profit of Model 0 and 1. The results of Model 1 show that the production capacities of both Australia and Brazil have no restriction on the trade volume (i.e., shadow price is 0), which implies that Australia and Brazil compete for trade volumes under sufficient production capacities. Assuming production capacity allocation, the results of Model 0 (Mode 2) illustrate that Australia restricts its exports to Japan and South Korea, as corresponding shadow prices are positive (i.e., 1.43 for JPN and 4.48 for SK). This explains why Model 1 exhibits a large discrepancy in trade volumes between Australia and South Korea/Japan. In addition, it is also found that both exporters' profits are higher in Model 0 (Model 2). This suggests that, facing the difference in trade cost, competitive exporters can effectively make up losses in profits through production capacity allocation.

Table 4-10. Capacity restriction, price and profit between Model 0 and Model 1

Indicator	Model 0 (Model 2)	Model 1
Export capacity restriction[a]	1.434 (AUS-JPN)	NA
	4.48 (AUS-SK)	
Production capacity restriction	NA	0
BRA-CHN trade price[b]	64.96	65.74
BRA-JPN trade price	77.02	75.44
BRA-SK trade price	80.06	72.79
AUS-CHN trade price	59.09	59.56
AUS-JPN trade price	61.31	59.43
AUS-SK trade price	59.13	39.83
BRA's profit[c]	73665.78	71058.56
AUS's profit	228390.81	222376.8

Note: (a) Export capacity/production capacity restriction is represented by the shadow price of export/production capacity constraint (4.3.a) on the trade volume in the two models. (b) The unit of trade price is US dollars per tonne ($/tonne). (c) The unit of profit is 10^5 US dollars.

4.5.4 Impact of shipping on iron ore trade

In this section, we investigate the impact of shipping on the iron ore trade. We assume a sudden change in importers' demand, which can be brought by various shocks, such as trade friction or unforeseen global events (e.g., COVID-19). In addition, some state strategies, such as the Belt & Road initiative, can also lead to this change through influencing the global production network (Chhetri et al., 2020; Cheong, 2020). We simulate this kind of shock through changing the importers' purchasing budgets and compare the results from Model 0 and Model 2, which consider endogenous cost and exogenous cost respectively. Their difference will reflect the impact of shipping on iron ore trade.

We assume a 30% reduction in all importers' purchasing budget. Table 4-11 shows

the changes in trade volume based on Model 0 and Model 2. Brazil and Australia both reduced their export volumes, and the total trade volume thus decreases by 27.4% in Model 0 and 28% in Model 2. Brazil's export volume reduced 29.6% in Model 0 and 30.5% in Model 2, and they are 26.8% and 27.3% for Australia. Overall, the reduction of trade volume from Model 0 is less than Model 2, which suggests that the iron ore shipping can dampen the effect on the trade volume caused by budget reduction. The dampening effect can be explained by the decline of freight rate in Model 0. As Table 4-11 shows, the average freight rates from Brazil and Australia decrease by 3.2% and 4.0% respectively in Model 0. The reduction of freight rate is caused by the decrease in trade volume, which in turn enables the exporters to reduce trade prices. The trade price in Model 0 decreases by 2.1% for Brazil and by 4.0% for Australia, against 1.1% and 3.2% in Model 2. Lower trade prices lead to the less impact from budget reduction in Model 0. However, it should be noted that this dampening effect is insignificant. With a 30% decline in importers' budget, the difference between two models' results is only 0.6% in total trade volume, 0.9% in Brazil exports and 0.5% in Australia exports.

Table 4-11. Indicator changes after 30% budget reduction at the low freight rate level

Indicator		100% budget Model 0 / Model 2	70% budget Model 0	70% budget Model 2	Difference in change of trade volume between two models
Total trade volume		9843.74	**-27.4%**	-28.0%	0.6%
Export volume	BRA	2137.02	**-29.6%**	-30.5%	0.9%
	AUS	7706.72	**-26.8%**	-27.3%	0.5%
Average Freight rate	BRA-EA	12.51	**-3.2%**	0.0%	NA
	AUS-EA	5.44	**-4.0%**	0.2%	NA
Trade price	BRA-EA	67.57	**-2.1%**	-1.1%	NA
	AUS-EA	59.33	**-4.0%**	-3.2%	NA

Note: (a) The unit of Total trade volume and Export volume: 10^5tonnes. (b) The unit of Average freight rate and Trade price: $/tonne.

Aforementioned results are estimated at a lower freight rate level ($12.51/tonne from Brazil; $5.44/tonne from Australia), due to low voyage cost[14]. As freight rate can affect shipping demand (Li et al., 2019), we further estimate the trade volume by doubling voyage cost, which will lead to increased freight rates ($22.91/tonne from Brazil; $9.28/tonne from Australia). The finding suggests that the dampening effect is still insignificant at higher freight rates. As shown in Table 4-12, with 30% budget reduction, the difference in total trade volume between two models is 0.7%, which is close to the 0.6% at low freight rate. However, we find that the dampening effect varies at different freight rate levels. The difference in Brazil's export volume between Model 0 and Model 1 is 3.9% at higher freight rates, much higher than 0.9% at lower freight rates. In contrast, the difference in Australia's export between two models is 0.0%, lower than 0.5% at the low freight rate level. This is caused by the difference in fleet structure on the two trade routes.

Table 4-12. Indicator change after 30% budget reduction at the high freight rate level

Indicator		100% budget Model 0 / Model 2	70% budget Model 0	70% budget Model 2	Difference in change of trade volume between two models
Total trade volume		8796.91	**-27.4%**	-28.1%	0.7%
Export volume	BRA	1517.07	**-26.7%**	-30.6%	3.9%
	AUS	7279.84	**-27.5%**	-27.6%	0.0%
Average Freight rate	BRA-EA	22.91	**-7.3%**	0.0%	NA
	AUS-EA	9.28	**-3.1%**	0.2%	NA
Trade price	BRA-EA	79.76	**-2.5%**	-0.5%	NA
	AUS-EA	66.03	**-3.9%**	-3.0%	NA

Note: (a) The unit of Total trade volume and export volume: 10^5tonnes. (b) The unit of Average freight rate and trade price: $/tonne.

[14] The unit voyage cost at low freight rate level (unit: $/tonne per nautical mile): $104 for small-sized ships, $128 for medium-sized ships, and $150 for large-sized ships.

As mentioned in Section 4.5.2, large ships are only used by Brazil as Australian ports can't accommodate them due to water depth. Figure 4-2 shows the changes in fleet structure at different freight rate levels. When the importers' purchasing budget is reduced by 30%, it can be found that the proportion of large ships in Brazil's fleet increases by 25.2% at high freight rate level, much higher than 13.8% at low freight rate level. This causes a larger decline (-7.3%) in freight rate from Brazil, compared to -3.2% at the lower freight rate level. In contrast, for Australia's fleet, at a higher freight rate, the proportion of medium ships increases by 26.3%, 35.1% at the lower freight rate. It leads to a less decline (-3.1%) in freight rate from Australia, compared to -4.0% at the low freight rate level. Because of the difference in the change of freight rate, shipping has various effects on lessening the decrease in export volume from Brazil and Australia.

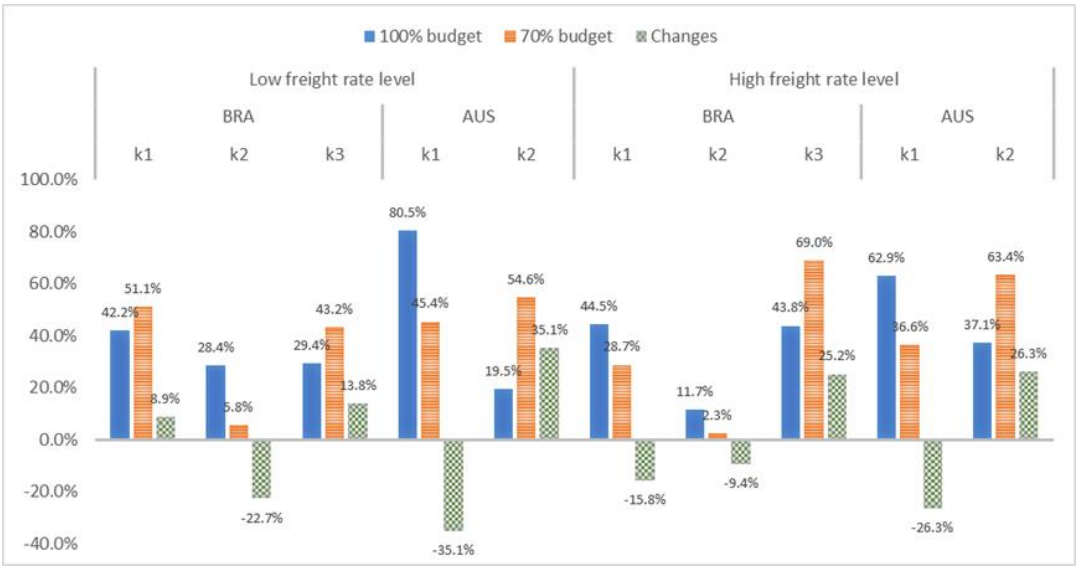

Figure 4-2. Changes in fleet structure caused by 30% budget reduction

Note: (a) k1, k2, k3 denotes the small-sized ships, medium-sized ships, and large-sized ships, respectively. (b) Vertical axis indicates the proportion of different ship sizes in the fleet of an exporter.

In summary, although shipping plays a role in dampening the effect from a sudden shock on the iron ore trade, overall, it is not significant. With different freight rates, the dampening effects on exporters varies, which can mainly be attributed to the difference in fleet structure on trade routes. In particular, when freight rate is high, shipping can absorb the shock to Brazil's iron ore export to some extent. This finding answers the research question we propose at the beginning: Strategies for shipping facilitation (e.g., building large ships) as a way to reduce shipping cost can be good for Brazil's miners only when the freight rate stays high.

4.6 Conclusion

In this chapter, we have established a computable equilibrium model to analyze the impact of shipping on the international iron ore trade. This model incorporates a more plausible utility-derived demand function, and a more generalized description on oligopolistic market structure. We also assume the allocation of production capacity of exporters and endogenize shipping cost. This allows us to shape the interactions between the shipping market and the iron ore trade in an equilibrium framework.

The existence of integer variables in Carrier Module makes it difficult to solve this model, since traditional MCP algorithms are not applicable with discrete constraints. To overcome this, we have proposed a solution procedure, transforming the model into a nonconvex MINLP. An exponential transformation is applied to convexify the nonconvexities with posynomial features in the MINLP. The final convex MINLP is solved by OA/ER/AP algorithm.

Based on real data from 2015, we evaluate the efficiency of this model by comparing it with models assuming exogenous shipping cost and production capacity

constraint. The findings suggest that production capacity allocation can make up for profit loss brought by exporter competition. From a numerical analysis, we find that shipping can dampen the effect of budget reduction on iron ore trade volume, but the effect is small. In addition, as fleet structure varies across different routes, shipping has different magnitudes of dampening effects on trade volume decrease, which is more evident when freight rate remains high.

5. Conclusion of this thesis and future study

5.1 Conclusion of this thesis

In this thesis, we have studied three issues of trade via computable equilibrium models, and obtained some results that cannot be achieved via gravity models. The first study (Chapter 2) focused on the impacts of tariff reduction on major economic indices. In addition to the trade creation emphasized by the gravity model-based research, we found that the tariff reduction can stabilize the exchange rate and tame the inflation. The second study (Chapter 3) concerned the pricing mechanism in the long-term contract of Asian LNG. We found that an inefficient pricing mechanism (e.g., oil indexation) can lead to a high price of the long-term contract. This finding implies that the trade price estimated by gravity models may not match the reality due to little consideration of the pricing mechanism. The third study (Chapter 4) concentrated on the interactions between shipping and trade sectors. We found that the shipping sector can dampen the effect of budget reduction on trade. It indicates that the trade models with exogenous transportation costs (e.g., gravity models) probably overestimate the impacts of policies or sudden shocks on the trade volume. With the aforementioned

three studies, this thesis has proved that the computable equilibrium model still has great potential in the research of international trade. Despite enormous empirical studies based on the gravity model, the computable equilibrium model is still a necessary complement, particularly to those weaknesses of the gravity model in analyzing policies' wider economic impacts, trade prices, and endogenous interactions between trade and influencing factors.

We have built computable equilibrium models in this thesis based on various economic equilibrium theories[15]. In Chapter 2, as the research objective is a national economy system involving multiple markets, we build the computable equilibrium model based on the general equilibrium theory. In Chapter 3 and Chapter 4, as our focus is a single commodity market (i.e., natural gas market or iron ore market), the computable equilibrium models that we applied to these two studies are built upon the partial equilibrium theory. Due to the multi-nation trade and explicit consideration of freight rate, the computable equilibrium models in Chapter 3 and Chapter 4 can be regarded as spatial equilibrium models.

This thesis contributes to the computable equilibrium models from the following two perspectives. Firstly, we proposed a simulation approach for stochastic prices of the computable equilibrium model in Chapter 3. Through effectively capturing the distributional characteristics of those stochastic prices, this approach can reduce the difficulty in dealing with the price uncertainty in the computable equilibrium modeling. Second, we designed a solution procedure for the equilibrium model containing discrete variables in Chapter 4. It allows computable equilibrium models with more flexible

[15] Tieben (2009) discussed the specific concepts of economic equilibrium theories from various perspectives. See details in this book.

variable selection in describing the real world.

5.2 Research limitations and future studies

In this thesis, there exist several limitations that should be overcome in the future studies.

In Chapter 2, we failed to examine the impact of tariff reduction on the trade of China with her major partners along the Belt and Road. To achieve this, we need to aggregate the Chinese trade with those partners into her total imports/exports. This is not a hard nut to crack from the modeling perspective. We only need to introduce additional CES/CET functions in the CGE model to represent the substitution relationships of trade partners in Chinese imports/exports. The main obstacle is the data available for estimating parameters, as it requires the data on trade volumes of 17 commodities between China and her trade partners over decades of years.

In Chapter 2 and Chapter 4, we conducted the static comparative analysis which ignores the dynamics features of policy's impacts. For example, we have known that tariff reduction can promote resident consumption from Chapter 2. Due to the differences in the production cycle among commodities, such a consumption increase caused by the tariff reduction may various across commodities. The consumption of some commodities may increase immediately, while others may need time to respond to the tariff reduction. For policymakers, capturing these temporal characteristics of tariff reduction impacts is critical for selecting the timing of tariff reduction. Therefore, it is of great value to extend these two studies via dynamic modeling.

In Chapter 3, we examined the difference between CIF and FOB prices in pricing LNG long-term contracts. The result has shown that there is little difference between

these two prices. The possible reason for this result could be the exogenous freight rate in the model. Inspired by findings in Chapter 4, incorporating shipping carriers' decisions into the equilibrium model of Chapter 3 may lead to more interesting implications. Another line of this direction is to endogenize transportation cost via modeling the transport sector from different perspectives. In Chapter 4, we have modeled the shipping sector via using a two-stage problem incorporating cargo flow assignment and fleet deployment. The advantage of this modeling setting is that it focuses on the cargo flows, thereby being suitable for either dry bulk or container shipping. Its disadvantage is that it ignores the unique characteristics of shipping markets. Modeling the shipping sector based on its characteristics may give us some new insights into the nexus between shipping and trade.

In addition, we ignored the political factors in this thesis. Recent practice has shown that the political relationships across countries significantly affect international trade. We will further extend the computable equilibrium model by incorporating political factors. Based on that extended model, we will quantify the impact of international politics on trade.

References

Abada, Ibrahim, Andreas Ehrenmann, and Yves Smeers. "Modeling gas markets with endogenous long-term contracts." *Operations research* 65, no. 4 (2017): 856-877.

Alim, Abdullahi, Peter R. Hartley, and Yihui Lan. "Asian spot prices for LNG and other energy commodities." *The Energy Journal* 39, no. 1 (2018).

Anderson, James E. "The gravity model." *Annu. Rev. Econ.* 3, no. 1 (2011): 133-160.

Anderson, James E., and Eric Van Wincoop. "Gravity with gravitas: A solution to the border puzzle." *American economic review* 93, no. 1 (2003): 170-192.

Angelopoulos, Jason, Satya Sahoo, and Ilias D. Visvikis. "Commodity and transportation economic market interactions revisited: New evidence from a dynamic factor model." *Transportation Research Part E: Logistics and Transportation Review* 133 (2020): 101836.

Asche, Frank, Atle Oglend, and Petter Osmundsen. "Modeling UK natural gas prices when gas prices periodically decouple from the oil price." *The Energy Journal* 38, no. 2 (2017).

Assembayeva, Makpal, Jonas Egerer, Roman Mendelevitch, and Nurkhat Zhakiyev. "A spatial electricity market model for the power system: The Kazakhstan case study." *Energy* 149 (2018): 762-778.

Ason, Agnieszka. Scenarios for Asian long-term LNG contracts before and after COVID-19. No. 160. OIES Paper: NG, 2020.

Asturias, Jose. "Endogenous transportation costs." *European Economic Review* 123 (2020): 103366.

Australia, Western Port Authority. *Trade statistics*. The Authority., 2015.

Awokuse, Titus O. "Causality between exports, imports, and economic growth: Evidence from transition economies." *Economics letters* 94, no. 3 (2007): 389-395.

Bai, Xiwen, and Jasmine Siu Lee Lam. "A copula-GARCH approach for analyzing dynamic conditional dependency structure between liquefied petroleum gas freight rate, product price arbitrage and crude oil price." *Energy Economics* 78 (2019): 412-427.

Bao, Te, Yun Dai, and Shuai Liu. "Trade Liberalization and Trade and Capital Flows: Evidence from China Pilot Free Trade Zones." *Available at SSRN 3534587* (2020).

Batten, Jonathan A., Cetin Ciner, and Brian M. Lucey. "The dynamic linkages between crude oil and natural gas markets." Energy Economics 62 (2017): 155-170.

Bessembinder, Hendrik, and Michael L. Lemmon. "Equilibrium pricing and optimal hedging in electricity forward markets." *the Journal of Finance* 57, no. 3 (2002): 1347-1382.

Bernhofen, Daniel M., Zouheir El-Sahli, and Richard Kneller. "Estimating the effects of the container revolution on world trade." *Journal of International Economics* 98 (2016): 36-50.

Bloom, Nicholas, Mirko Draca, and John Van Reenen. "Trade induced technical change? The impact of Chinese imports on innovation, IT and productivity." *The review of economic studies* 83, no. 1 (2016): 87-117.

Bottasso, Anna, Maurizio Conti, Paulo Costacurta de Sa Porto, Claudio Ferrari, and Alessio Tei. "Port infrastructures and trade: empirical evidence from Brazil." Transportation Research Part A: Policy and Practice 107 (2018): 126-139.

Brancaccio, Giulia, Myrto Kalouptsidi, and Theodore Papageorgiou. "Geography, transportation, and endogenous trade costs." *Econometrica* 88, no. 2 (2020): 657-691.

Brigida, Matthew. "The switching relationship between natural gas and crude oil prices." *Energy Economics* 43 (2014): 48-55.

Brown, Stephen PA, and Mine K. Yucel. "What drives natural gas prices?." *The Energy Journal* 29, no. 2 (2008).

Cai, Jun, Kai Xin, and Yahong Zhou. "A dynamic panel data approach and HCW's method: Assessing the effect of China (Shanghai) Free Trade Zone on local GDP." *Journal of Management Science and Engineering* 6, no. 3 (2021): 249-267.

Caliendo, Lorenzo, and Fernando Parro. "Estimates of the Trade and Welfare Effects of NAFTA." *The Review of Economic Studies* 82, no. 1 (2015): 1-44.

Chen, Elynn Y., and Rong Chen. "Modeling dynamic transport network with matrix factor models: with an application to international trade flow." *arXiv preprint arXiv:1901.00769* (2019).

Cheong, Inkyo. "Assessment of the Economic Background of the OBOR." *Journal of International Logistics and Trade* 15, no. 2 (2017): 72-82.

Chepeliev, Maksym, Robert McDougall, and Dominique van der Mensbrugghe. "Including fossil-fuel consumption subsidies in the GTAP data base." *Journal of Global Economic Analysis* 3, no. 1 (2018): 84-121.

Chhetri, Prem, Mathews Nkhoma, Konrad Peszynski, Anjali Chhetri, and Paul Tae-Woo Lee. "Global logistics city concept: a cluster-led strategy under the belt and road initiative." *Maritime Policy & Management* 45, no. 3 (2018): 319-335.

Chhetri, Prem, Victor Gekara, Shaorong Li, and Jun Yeop Lee. "Changing global production network and its implication on Belt and Road Initiative." *Journal of International Logistics and Trade* 18, no. 1 (2020): 13-14.

China Customs Statistical Yearbook of 2018.

Comtrade, U. N. "International Trade Statistics Database (2016)." (2018).

Cotter, John, and Jim Hanly. "Hedging effectiveness under conditions of asymmetry." *The european Journal of finance* 18, no. 2 (2012): 135-147.

De Santis, Roberto A. "A computable general equilibrium model for open economies

with imperfect competition and product differentiation." *Journal of Economic Integration* (2002): 311-338.

Deardoff, A. "Determinants of bilateral trade: Does Gravity Model work in a classical world." (1998).

Devarajan, Shantayanan, Delfin S. Go, Sherman Robinson, and Karen Thierfelder. "Tax policy to reduce carbon emissions in a distorted economy: Illustrations from a South Africa CGE model." *The BE Journal of Economic Analysis & Policy* 11, no. 1 (2011).

Dinwoodie, John, Melanie Landamore, and Patrick Rigot-Muller. "Dry bulk shipping flows to 2050: Delphi perceptions of early career specialists." *Technological Forecasting and Social Change* 88 (2014): 64-75.

Distances, Sea. "Sea Distances." *Org:[sn]* (2015).

Dixon, Peter, and Maureen T. Rimmer. *Forecasting and policy analysis with a dynamic CGE model of Australia*. Centre of Policy Studies (CoPS), 1998.

Eaton, Jonathan, and Samuel Kortum. "Technology, geography, and trade." *Econometrica* 70, no. 5 (2002): 1741-1779.

Egerer, Jonas, Jens Weibezahn, and Hauke Hermann. "Two price zones for the German electricity market—Market implications and distributional effects." *Energy Economics* 59 (2016): 365-381.

Egging, Ruud, Franziska Holz, and Steven A. Gabriel. "The World Gas Model: A multi-period mixed complementarity model for the global natural gas market." *Energy* 35, no. 10 (2010): 4016-4029.

Egging, Ruud, Alois Pichler, Øyvind Iversen Kalvø, and Thomas Meyer Walle–Hansen. "Risk aversion in imperfect natural gas markets." *European Journal of Operational Research* 259, no. 1 (2017): 367-383.

Erdős, Péter. "Have oil and gas prices got separated?." *Energy Policy* 49 (2012): 707-718.

Feijoo, Felipe, Daniel Huppmann, Larissa Sakiyama, and Sauleh Siddiqui. "North American natural gas model: Impact of cross-border trade with Mexico." Energy 112 (2016): 1084-1095.

Fiscal Yearbook of China-2013.

Floudas, Christodoulos A. *Nonlinear and mixed-integer optimization: fundamentals and applications*. Oxford University Press, 1995.

Ftiti, Zied, Kais Tissaoui, and Sahbi Boubaker. "On the relationship between oil and gas markets: a new forecasting framework based on a machine learning approach." *Annals of Operations Research* (2020): 1-29.

Gabriel, Steven A. "Solving discretely constrained mixed complementarity problems using a median function." *Optimization and Engineering* 18, no. 3 (2017): 631-658.

Gabriel, Steven A., Supat Kiet, and Jifang Zhuang. "A mixed complementarity-based equilibrium model of natural gas markets." *Operations Research* 53, no. 5 (2005): 799-818.

Gallaway, Michael P., Christine A. McDaniel, and Sandra A. Rivera. "Short-run and long-run industry-level estimates of US Armington elasticities." *The North American Journal of Economics and Finance* 14, no. 1 (2003): 49-68.

Geng, Jiang-Bo, Qiang Ji, and Ying Fan. "The impact of the North American shale gas revolution on regional natural gas markets: Evidence from the regime-switching model." *Energy Policy* 96 (2016): 167-178.

Germeshausen, Robert, Timo Panke, and Heike Wetzel. "Firm characteristics and the ability to exercise market power: empirical evidence from the iron ore market." *Empirical Economics* (2018): 1-25.

Gersema, Gerke, and David Wozabal. "An equilibrium pricing model for wind power futures." *Energy Economics* 65 (2017): 64-74.

Gersema, Gerke, and David Wozabal. "Risk-optimized pooling of intermittent renewable energy sources." *Journal of banking & finance* 95 (2018): 217-230.

Glendinning, Caroline, and Martin Powell, eds. *Partnerships, New Labour and the governance of welfare*. Policy Press, 2002.

Glomsrød, Solveig, and Wei Taoyuan. "Coal cleaning: a viable strategy for reduced carbon emissions and improved environment in China?." *Energy Policy* 33, no. 4 (2005): 525-542.

Grimm, Veronika, Lars Schewe, Martin Schmidt, and Gregor Zöttl. "Uniqueness of market equilibrium on a network: A peak-load pricing approach." *European Journal of Operational Research* 261, no. 3 (2017): 971-983.

Guo, Yingjian, and Adam Hawkes. "Simulating the game-theoretic market equilibrium and contract-driven investment in global gas trade using an agent-based method." *Energy* 160 (2018): 820-834.

Hartley, Peter R., Kenneth B. Medlock III, and Jennifer E. Rosthal. "The relationship of natural gas to oil prices." The Energy Journal 29, no. 3 (2008).

Holz, Franziska, Philipp M. Richter, and Ruud Egging. "The Role of Natural Gas in a Low-Carbon Europe: Infrastructure and Supply Security." *Energy Journal* 37 (2016).

Huppmann, Daniel. "Endogenous production capacity investment in natural gas market equilibrium models." *European Journal of Operational Research* 231, no. 2 (2013): 503-506.

Ivus, Olena, and Aaron Strong. "Modeling approaches to the analysis of trade policy: computable general equilibrium and gravity models." Handbook on International Trade Policy 44 (2007).

Jarreau, Joachim, and Sandra Poncet. "Export sophistication and economic growth: Evidence from China." *Journal of development Economics* 97, no. 2 (2012): 281-292.

Johansen, Leif. *A multi-sector study of economic growth*. Vol. 21. North-Holland Publishing Company, 1960.

Kesavan, Padmanaban, Russell J. Allgor, Edward P. Gatzke, and Paul I. Barton. "Outer approximation algorithms for separable nonconvex mixed-integer nonlinear programs." *Mathematical Programming* 100, no. 3 (2004): 517-535.

Keuning, Steven J., and Willem A. de Ruuter. "Guidelines to the construction of a social accounting matrix." *Review of income and wealth* 34, no. 1 (1988): 71-100.

Kleinert, Jörn, and Julia Spies. *Endogenous transport costs in international trade*. No. 74. IAW Diskussionspapiere, 2011.

Koesler, Simon, and Michael Schymura. "Substitution elasticities in a constant elasticity of substitution framework–empirical estimates using nonlinear least squares." *Economic Systems Research* 27, no. 1 (2015): 101-121.

Kunz, Friedrich, and Alexander Zerrahn. "Benefits of coordinating congestion management in electricity transmission networks: Theory and application to Germany." Utilities Policy 37 (2015): 34-45.

Leuthold, Florian U., Hannes Weigt, and Christian von Hirschhausen. "A large-scale spatial optimization model of the European electricity market." *Networks and spatial economics* 12, no. 1 (2012): 75-107.

Li, Feng, Dong Yang, Shuaian Wang, and Jinxian Weng. "Ship routing and scheduling problem for steel plants cluster alongside the Yangtze River." *Transportation Research Part E: Logistics and Transportation Review* 122 (2019): 198-210.

Li, Kevin X., Mengjie Jin, Guanqiu Qi, Wenming Shi, and Adolf KY Ng. "Logistics as a driving force for development under the belt and road initiative–the Chinese model for developing countries." *Transport Reviews* 38, no. 4 (2018): 457-478.

Li, Yan, Julien Chevallier, Yigang Wei, and Jing Li. "Identifying price bubbles in the US, European and Asian natural gas market: Evidence from a GSADF test approach." *Energy Economics* 87 (2020): 104740.

Lin, Boqiang, and Zhijie Jia. "Impact of quota decline scheme of emission trading in China: A dynamic recursive CGE model." *Energy* 149 (2018): 190-203.

Lin, Dung-Ying, and Yu-Ting Chang. "Ship routing and freight assignment problem for liner shipping: Application to the Northern Sea Route planning problem." *Transportation Research Part E: Logistics and Transportation Review* 110 (2018): 47-70.

Lovcha, Yuliya, and Alejandro Perez-Laborda. "Dynamic frequency connectedness between oil and natural gas volatilities." *Economic Modelling* 84 (2020): 181-189.

Lu, Jing, Xiuyang Pan, and Zuoling Xie. "Unity versus Collaboration: Construction of China's Belt and Road Free Trade Agreement 2.0 Network." *Pacific Economic Review* 25, no. 2 (2020): 250-271.

Nag, Biswajit, and Chandrima Sikdar. "Welfare implication of India-ASEAN FTA: An analysis using GTAP model." *Indian Institute of Foreign Trade Working Paper No. EC-11-06* (2011).

Naranpanawa, Athula, and Rashmi Arora. "Does trade liberalization promote regional disparities? Evidence from a multiregional CGE model of India." *World development* 64 (2014): 339-349.

Network, Clarksons Shipping Intelligence. " Dry bulk ship list." (2018).

Neumann, Anne, and Christian Von Hirschhausen. "Natural gas: an overview of a lower-carbon transformation fuel." *Review of Environmental Economics and Policy* 9, no. 1 (2015): 64-84.

Nguyen, Hong-Oanh, and Jose Tongzon. "Causal nexus between the transport and logistics sector and trade: The case of Australia." *Transport policy* 17, no. 3 (2010): 135-146.

Notteboom, Theo E. "Complementarity and substitutability among adjacent gateway ports." *Environment and Planning A* 41, no. 3 (2009): 743-762.

Palti-Guzman, Leslie. "The Future of Asia's Natural Gas Market: The Need for a Regional LNG Hub." *asia policy* 13, no. 3 (2018): 101-126.

Peng, Zixuan, Wenxuan Shan, Feng Guan, and Bin Yu. "Stable vessel-cargo matching in dry bulk shipping market with price game mechanism." *Transportation Research Part E: Logistics and Transportation Review* 95 (2016): 76-94.

Perry, Martin K. "Oligopoly and consistent conjectural variations." *The Bell Journal of*

Economics (1982): 197-205.

PETROLEUM–BP, British. "Statistical Review of World Energy. 2020." (2012).

Qi, Tianyu, Niven Winchester, Valerie J. Karplus, Da Zhang, and Xiliang Zhang. "An analysis of China's climate policy using the China-in-Global Energy Model." *Economic Modelling* 52 (2016): 650-660.

Qing, Qiankai, Tianhu Deng, and Hongwei Wang. "Capacity allocation under downstream competition and bargaining." *European Journal of Operational Research* 261, no. 1 (2017): 97-107.

Ramberg, David J., and John E. Parsons. "The weak tie between natural gas and oil prices." *The Energy Journal* 33, no. 2 (2012).

Ramos, Francisco F. Ribeiro. "Exports, imports, and economic growth in Portugal: evidence from causality and cointegration analysis." *Economic modelling* 18, no. 4 (2001): 613-623.

Robson, Edward N., Kasun P. Wijayaratna, and Vinayak V. Dixit. "A review of computable general equilibrium models for transport and their applications in appraisal." *Transportation Research Part A: Policy and Practice* 116 (2018): 31-53.

Rosyadi, Saiful Alim, and Tri Widodo. "Impact of Donald Trump's tariff increase against Chinese imports on global economy: Global Trade Analysis Project (GTAP) model." *Journal of Chinese Economic and Business Studies* 16, no. 2 (2018): 125-145.

Rudolph, Stephan. "The gravity equation with micro-founded trade costs." (2009).

Scarf, Herbert E., and Terje Hansen. *The computation of economic equilibria*. No. 24. Yale University Press, 1973.

Sen, Sunanda. "International trade theory and policy: a review of the literature." (2010).

Sesini, Marzia, Sara Giarola, and Adam D. Hawkes. "The impact of liquefied natural gas and storage on the EU natural gas infrastructure resilience." *Energy* 209 (2020): 118367.

Shi, Xunpeng, and Hari MP Variam. "East Asia's gas-market failure and distinctive economics—A case study of low oil prices." *Applied energy* 195 (2017): 800-809.

Shi, Xunpeng, and Yifan Shen. "Macroeconomic uncertainty and natural gas prices: Revisiting the Asian Premium." *Energy Economics* 94 (2021): 105081.

Shoven, John B., and John Whalley. "A general equilibrium calculation of the effects of differential taxation of income from capital in the US." (1972).

Simshauser, Paul. "On intermittent renewable generation & the stability of Australia's National Electricity Market." *Energy Economics* 72 (2018): 1-19.

Siriwardana, Mahinda, and Jinmei Yang. "GTAP model analysis of the economic effects of an Australia–China FTA: Welfare and sectoral aspects." *Global Economic Review* 37, no. 3 (2008): 341-362.

Song, Yunting, Nuo Wang, and Anqi Yu. "Temporal and spatial evolution of global iron ore supply-demand and trade structure." *Resources Policy* 64 (2019): 101506.

Stern, Jonathan. "International gas pricing in Europe and Asia: A crisis of fundamentals." *Energy Policy* 64 (2014): 43-48.

Stern, Jonathan. "Comparative History of Oil and Gas Markets and Prices: is 2020 just an extreme cyclical event or an acceleration of the energy transition?." (2020).

Sun, Zhuo, Ran Zhang, Yuan Gao, Zhongxing Tian, and Yi Zuo. "Hub ports in economic shocks of the melting Arctic." *Maritime Policy & Management* (2020): 1-24.

National Statistics Bureau of China. "The Balance of Payments Statement (2012)." *China Statistical Yearbook-2013*.

National Statistics Bureau of China. "The Flows-of-Funds Table (2012)." *China Statistical Yearbook-2014*.

National Statistics Bureau of China. "The Input-Output Table (2012)." *Chinese Statistical Yearbook - 2015*.

Tieben, Bert. *The concept of equilibrium in different economic traditions: A historical investigation*. No. 449. Rozenberg Publishers, 2009.

Toweh, Solomon H., and Richard T. Newcomb. "A spatial equilibrium analysis of world iron ore trade." *Resources Policy* 17, no. 3 (1991): 236-248.

Tseng, Chung-Li, and Graydon Barz. "Short-term generation asset valuation: a real options approach." *Operations Research* 50, no. 2 (2002): 297-310.

Van Ha, Pham, Tom Kompas, Hoa Thi Minh Nguyen, and Chu Hoang Long. "Building a better trade model to determine local effects: A regional and intertemporal GTAP model." *Economic Modelling* 67 (2017): 102-113.

Vivoda, Vlado. "Natural gas in Asia: Trade, markets and regional institutions." *Energy Policy* 74 (2014): 80-90.

Wang, TianTian, Dayong Zhang, and David Clive Broadstock. "Financialization, fundamentals, and the time-varying determinants of US natural gas prices." *Energy Economics* 80 (2019): 707-719.

Wang, Xueqin, Yiik Diew Wong, Kevin X. Li, and Kum Fai Yuen. "Transport research under Belt and Road Initiative: current trends and future research agenda." *Transportmetrica A: Transport Science* 17, no. 4 (2021): 357-379.

Wårell, Linda. "An analysis of iron ore prices during the latest commodity boom." *Mineral Economics* 31, no. 1-2 (2018): 203-216.

Weigt, Hannes, Karen Freund, and Till Jeske. "Nodal Pricing of the European Electricity Grid-A Welfare Economic Analysis for Feeding-in Offshore Wind Electricity." *Available at SSRN 1137383* (2006).

Wogrin, Sonja, Benjamin F. Hobbs, Daniel Ralph, Efraim Centeno, and J. Barquín. "Open versus closed loop capacity equilibria in electricity markets under perfect and oligopolistic competition." *Mathematical Programming* 140, no. 2 (2013): 295-322.

Wong, Woan Foong. "The round trip effect: Endogenous transport costs and international trade." *University of Oregon* (2018).

World Steel Association. "World Steel in Figures 2018 Now Available." *World Steel Association: Brussels, Belgium* (2018).

Wu, Jinxi, Jie Yang, Linwei Ma, Zheng Li, and Xuesi Shen. "A system analysis of the development strategy of iron ore in China." *Resources Policy* 48 (2016): 32-40.

Wu, Lingxiao, Kai Pan, Shuaian Wang, and Dong Yang. "Bulk ship scheduling in industrial shipping with stochastic backhaul canvassing demand." *Transportation Research Part B: Methodological* 117 (2018): 117-136.

Xia, Jun, Kevin X. Li, Hong Ma, and Zhou Xu. "Joint planning of fleet deployment, speed optimization, and cargo allocation for liner shipping." *Transportation Science* 49, no. 4 (2015): 922-938.

Yang, Dong, Liping Jiang, and Adolf KY Ng. "One Belt one Road, but several routes: A case study of new emerging trade corridors connecting the Far East to Europe." *Transportation Research Part A: Policy and Practice* 117 (2018): 190-204.

Yang, Shanping, and Inmaculada Martinez-Zarzoso. "A panel data analysis of trade creation and trade diversion effects: The case of ASEAN–China Free Trade Area." *China Economic Review* 29 (2014): 138-151.

Yii, Kwang-Jing, Kai-Ying Bee, Wei-Yong Cheam, Yee-Lee Chong, and Ching-Mei Lee. "Is transportation infrastructure important to the One Belt One Road

(OBOR) Initiative? Empirical evidence from the selected Asian countries." *Sustainability* 10, no. 11 (2018): 4131.

Yotov, Yoto V., Roberta Piermartini, José-Antonio Monteiro, and Mario Larch. *An advanced guide to trade policy analysis: The structural gravity model*. Geneva: World Trade Organization, 2016.

Zhai, Fan, and Thomas Hertel. *Impacts of the Doha Development Agenda on People's Republic of China: The Role of Complementary Education Reforms*. No. 73. ERD Working Paper Series, 2005.

Zhang, Dayong, and Qiang Ji. "Further evidence on the debate of oil-gas price decoupling: A long memory approach." *Energy Policy* 113 (2018a): 68-75.

Zhang, Dayong, Min Shi, and Xunpeng Shi. "Oil indexation, market fundamentals, and natural gas prices: An investigation of the Asian premium in natural gas trade." *Energy Economics* 69 (2018b): 33-41.

Zhang, Dayong, Tiantian Wang, Xunpeng Shi, and Jia Liu. "Is hub-based pricing a better choice than oil indexation for natural gas? Evidence from a multiple bubble test." *Energy Economics* 76 (2018c): 495-503.

Zhao, Yanan. "Analysis of trade effect in Post-Tpp era: based on gravity model and Gtap model." *Applied Mathematics and Nonlinear Sciences* 5, no. 1 (2020): 61-70.

Zheng, Yuxin, and Mingtai Fan. "A Chinese CGE Model and Its Application to Policy Analysis." *Social Sciences Documentation Publishing House, Beijing* (1999).

Zhu, Xuehong, Weihang Zheng, Hongwei Zhang, and Yaoqi Guo. "Time-varying international market power for the Chinese iron ore markets." *Resources Policy* 64 (2019): 101502.

Zhuang, Jifang, and Steven A. Gabriel. "A complementarity model for solving stochastic natural gas market equilibria." *Energy Economics* 30, no. 1 (2008): 113-147.

Appendix A. Appendices of Chapter 2

Appendix A-1 Explanatory social accounting matrix (SAM) table

	Commodity	Activity	Labor	Capital	Resident	Enterprise	Government	Tariff	Rest of world	Investment & saving	Aggregate
Commodity		Intermediate input			Consumption of resident		Consumption of government			Domestic investment	Aggregate demand
Activity	Output consumed in domestic market								Export		Aggregate output
Labor		Demand for labor									Revenue of labor
Capital		Demand for capital									Revenue of capital
Resident			Earning of labor	Capital revenue of resident		Transfer payment from enterprise to resident	Transfer payment from government to resident		Transfer payment from foreign account to resident		Revenue of resident
Enterprise				Capital revenue of enterprise							Revenue of enterprise
Government		Net production tax			Individual income tax	Enterprise income tax		Import tariff	Transfer payment from foreign account to government		Revenue of government
Tariff	Import tariff										Import tariff
Rest of world	import			Capital revenue of foreign investor			Transfer payment from government to foreign account				Revenue of overseas account
Investment & saving					Resident saving	Enterprise saving	Government saving		Overseas net saving		Aggregate saving
Aggregate	Aggregate supply	Aggregate input	Expenditure of labor	Expenditure of capital	Expenditure of resident	Expenditure of resident	Expenditure of government	Import tariff	Expenditure of foreign account	Aggregate investment	

Appendix A-2 Detailed expression of the CGE model

Input-output module

For each production sector $a \in A$, we assume that to produce the quantity QA_a, two inputs are needed: labor and capital inputs (QVA_a) and intermediate inputs ($QINTA_a$). The outputs-input relation is assumed to follow a constant elasticity of substitution (CES) production function as follows:

$$QA_a = \alpha_a^q [\delta_a^q \cdot QVA_a^{\rho q_a} + (1 - \delta_a^q) \cdot QINTA_a^{\rho q_a}]^{1/\rho q_a}, \quad \text{(A1)}$$

where α_a^q is a productivity coefficient which can be treated as a constant in a short period, δ_a^q is the contribution of QVA_a to QA_a, and ρq_a is a parameter that specifies the substitution between the two inputs. Then the cost minimizing inputs combination should satisfy the following condition:

$$PVA_a / PINTA_a = \frac{\delta_a^q}{(1 - \delta_a^q)} \cdot \left(\frac{QINTA_a}{QVA_a}\right)^{(1-\rho q_a)}, \quad \text{(A2)}$$

where PVA_a and $PINTA_a$ are prices of QVA_a and $QINTA_a$. Assume average cost pricing, the price of the output PA_a should satisfy following condition:

$$PA_a \cdot QA_a = PVA_a \cdot QVA_a + PINTA_a \cdot QINTA_a. \quad \text{(A3)}$$

The labor and capital inputs QVA_a can also be treated as a product of labor QLD_a and capital QKD_a. Then, using a CES function to describe the input-output relationship, following equations can also be obtained:

$$PA_a \cdot QA_a = PVA_a \cdot QVA_a + PINTA_a \cdot QINTA_a. \quad \text{(A4)}$$

$$QVA_a = \alpha_a^{va}[\delta_a^{va} \cdot QLD_a^{\rho va_a} + (1 - \delta_a^{va}) \cdot QKD_a^{\rho va_a}]^{1/\rho va_a}, \quad \text{(A5)}$$

$$PVA_a \cdot QVA_a = WL(1 + tval_a) \cdot QLD_a + WK(1 + tvak_a) \cdot QKD_a, \quad \text{(A6)}$$

where α_a^{va} is also a productivity coefficient, QLD_a and QKD_a denote the inputs of labor and capital in the production of QVA_a. δ_a^{va} is the relative contribution of QLD_a to QVA_a. ρva_a is the substitution parameter between the two inputs; WL and WK are prices of labor and capital. $tval_a$ and $tvak_a$ are added-value tax rate of labor and capital respectively.

The production of the intermediate input ($QINTA_a$) is the aggregation of the intermediate input commodity $c \in C$. It can be modeled using Leontief production function:

$$QINTA_a = QINT_{ca}/ica_{ca}, \quad \text{(A7)}$$

$$PINTA_a = \sum_{c \in C} ica_{ca} \cdot PQ_C, \quad \text{(A8)}$$

where $QINT_{ca}$ indicates intermediate input commodity from commodity sector c to production sector a. ica_{ca} refers to the share of commodity c in $QINTA_a$. $PINTA_a$ is the price of $QINTA_a$. PQ_c is the price of commodity c.

The production output QA_a is supplied for both domestic consumption and export. A constant elasticity of transformation function (Jarreau and Poncet, 2012) is applied to describe the allocation of total production QA_a:

$$QA_a = \alpha_a^l[\delta_a^l \cdot QDA_a^{\rho l_a} + (1-\delta_a^l) \cdot QE_a^{\rho l_a}]^{1/\rho l_a}, \quad \text{(A9)}$$

$$PDA_a/PE_a = \frac{\delta_a^l}{(1-\delta_a^l)} \cdot (\frac{QE_a}{QDA_a})^{(1-\rho l_a)}, \quad \text{(A10)}$$

where α_a^l is a constant parameter to represent the technology level, δ_c^l is the contribution of QDA_a to QA_a, QDA_a indicates the supply in domestic market, QE_a denote the export. ρl_a ($\rho l_a > 1$) is the parameter of transformation elasticity, PDA_a and PE_a are prices of QDA_a and QE_a, respectively. The price relationship can be expressed as:

$$PA_a \cdot QA_a = PDA_a \cdot QDA_a + PE_a \cdot QE_a, \quad \text{(A11)}$$

$$PE_a = pwe_a \cdot EXR, \quad \text{(A12)}$$

where pwe_a is the export price in the international trade market, EXR denotes the exchange rate.

The total commodity consumption in the domestic market (QQ_C) is from two sources: the domestic produced commodity (QDC_c), and the imported commodity (QM_c). An Armington function is adopted to describe this relationship:

$$QQ_c = \alpha_c^q[\delta_c^q \cdot QDC_c^{\rho q_c} + (1-\delta_c^q) \cdot QM_c^{\rho q_c}]^{1/\rho q_c}, \quad \text{(A13)}$$

$$PDC_c/PM_c = \frac{\delta_c^q}{(1-\delta_c^q)} \cdot (\frac{QM_c}{QDC_c})^{(1-\rho q_c)}, \quad \text{(A14)}$$

where α_c^q is a constant parameter to represent the technology level, δ_c^q is the contribution of QDC_c to QQ_c, and ρq_c is the substitution parameter. PDC_c and PM_c are prices of QDC_c and QM_c, respectively. The price equations are:

$$PQ_c \cdot QQ_c = PDC_c \cdot QDC_c + PM_c \cdot QM_c, \quad \text{(A15)}$$

$$PM_c = pwm_c \cdot (1 + tm_c) \cdot EXR, \quad \text{(A16)}$$

where pwm_c is the import price of commodity, and tm_c is import tariff rate. In addition, we need to establish the connections between production sector a and commodity c. For a given industry $i = \{1,2,3, \dots ,17\}$, there is a consistent relationship between its production sector $a(i)$ and commodity sector $c(i)$:

$$QDA_{a(i)} = QDC_{c(i)}, \quad \text{(A17)}$$

$$PDA_{a(i)} = PDC_{c(i)}, \quad \text{(A18)}$$

These two equations ensure the equilibrium between supply and demand within national borders.

Cash flow module

This module describes the cash flows in the national accounting system using four accounts: Resident, Enterprise, Government and Rest of world (ROW).

Resident account

The income of the residents (YH) comes from several sources: a) wage income; b) domestic capital earnings; c) transfer payments from enterprises, government and the rest of the world.

$$YH = WL \cdot QLS + shif_{hk} \cdot WK \cdot QKS + transf_{hent} + transfr_{hgov} + transfr_{hrow} \cdot EXR \quad \text{(A19)}$$

where QLS is the total labor supply, QKS is total capital supply, $shif_{hk}$ is the residents'

proportion of total domestic capital revenue, $transf_{hent}$, $transf_{hgov}$, and $transf_{hrow}$ are transfer payments to resident from enterprise, government and rest of world, respectively. YH are used for either consumption or saving. Using mpc to represent the proportion of revenue for resident's consumption. $shrh_c$ denotes the share of commodity c in the resident's total consumption, the equation for total consumption of resident can be written as:

$$PQ_c \cdot QH_c = (1 - ti_h) \cdot shrh_c \cdot mpc \cdot YH, \tag{A20}$$

where QH_c indicates the commodity c consumed by resident, ti_h is rate of individual income tax. Then, resident savings ($HSAV$) can be written as:

$$HSAV = (1 - ti_h) \cdot YH - \sum_{c \in C} PQ_c \cdot QH_c. \tag{A21}$$

Enterprise account

Enterprise earns its revenue ($YENT$) from capital income according to its share ($shif_{entk}$) in the total domestic capital income:

$$YENT = WK \cdot QKS \cdot shif_{entk}. \tag{A22}$$

Then, $YENT$ minus $transf_{hent}$ is its saving:

$$ENTSAV = (1 - ti_{ent}) \cdot YENT - transf_{hent}, \tag{A23}$$

where $ENTSAV$ is saving of enterprise, and ti_{ent} is the enterprise income tax rate. The investment of the enterprise can be given as:

$$EINV = \sum_{c \in C} PQ_c \cdot QINV_c, \tag{A24}$$

where $EINV$ denote the investment of enterprise and $QINV_c$ is the investment for commodity c.

Government account

The government's revenue (YG) from many sources, include tax on wage and capital in the production activity (i.e., value-added tax), and personal income tax, enterprise income tax, import tariff, transfer payments from rest of the world ($transfr_{govrow}$), and debt or financial deficit ($YDEBT$):

$$\begin{aligned} YG = \sum_{a \in A} (tval_a \cdot WL \cdot QLD_a + tvak_a \cdot WK \cdot QKD_a) + YH \cdot ti_h + YENT \\ \cdot ti_{ent} + tm_c \cdot pwm_c \cdot QM_c + transfr_{govrow} \cdot EXR \\ + YDEBT. \end{aligned} \tag{A25}$$

Government expenditure (EG) includes consumption of commodities and transfer payments to the residents ($transfr_{hgov}$) and rest of the world ($transfr_{rowgov}$):

$$EG = \sum_{c \in C} PQ_c \cdot QG_c + transfr_{hgov} + transfr_{rowgov} \cdot EXR, \tag{A26}$$

where QG_c represents the commodity consumption of government. The government saving ($GOVSAV$) is shown as:

$$GOVSAV = YG - EG. \tag{A27}$$

Rest of world account

The earning of the ROW account ($YROW$) includes the total imports of the country, the domestic capital supplied for overseas investment, and the transfer payments from government to ROW:

$$YROW = \sum_{c \in C} (pwm_c \cdot QM_c \cdot EXR) + shif_{rowk} \cdot WK \cdot QKS + transfr_{rowgov} \cdot EXR, \quad \text{(A28)}$$

where $shif_{rowk}$ is the proportion of domestic capital in ROW account. In addition, $shif_{rowk} + shif_{hk} + shif_{entk} = 1$. The expenditure of ROW account includes the export of the country and the transfer payments from ROW to resident and government:

$$EROW = \sum_{a \in A} (pwe_a \cdot QE_a \cdot EXR) + transfr_{hrow} \cdot EXR + transfr_{govrow} \cdot EXR. \quad \text{(A29)}$$

Market equilibrium module

This module describes the equilibrium conditions for the commodity market, the labor market, capital market, international payment, and domestic investment & saving.

For commodity market

$$QQ_c = \sum_{a \in A} QINT_{ca} + QH_C + QINV_c + QG_c. \quad \text{(A30)}$$

For labor market

$$\sum_{a \in A} QLD_a = QLS\,. \quad \text{(A31)}$$

For capital market

$$\sum_{a \in A} QKD_a = QKS\,. \tag{A32}$$

For international payment

$$YROW = EROW + ROWSAV, \tag{A33}$$

where $ROWSAV$ is net saving of ROW account.

For domestic investment and saving

$$EINV + YDEBT = HSAV + ENTSAV + GOVSAV + ROWSAV \tag{A34}$$

In addition, this module also closes the CGE model via the Keynesian closure:

$$WL = \overline{WL}, \tag{A35}$$

$$WK = \overline{WK}, \tag{A36}$$

$$ROWSAV = \overline{ROWSAV}, \tag{A37}$$

$$YH = \overline{YH}, \tag{A38}$$

$$QINV_c = \overline{QINV_c}. \tag{A39}$$

These four closure conditions aim to set selected variables (e.g., WL) as exogenous ones (e.g., $\overline{WL}$). Eventually, we calculate the GDP and price of GDP ($PGDP$) via following two equations:

$$GDP = \sum_{c \in C} (QH_C + QINV_c + QG_c - QM_c) + \sum_{a \in A} QE_a, \tag{A40}$$

$$PGDP \cdot GDP = \sum_{c \in C} (PQ_c \cdot (QH_C + QINV_c + QG_c) - PM_c \cdot QM_c) + \sum_{a \in A} PE_a \cdot QE_a. \quad \text{(A41)}$$

Appendix A-3 Parameters of elasticity

No.	Activity ($a \in A$)	Commodity (c$\in C$)	ρl_a	ρq_c	ρva_a	ρq_a
1	a_1	c_1	0.6	1.28	2.05	0.1
2	a_2	c_2	0.7	1.22	2.05	0.1
3	a_3	c_3	0.7	1.21	2.05	0.1
4	a_4	c_4	0.7	1.19	2.05	0.1
5	a_5	c_5	0.5	1.26	2.05	0.1
6	a_6	c_6	0.5	1.26	2.05	0.1
7	a_7	c_7	0.5	1.22	2.05	0.1
8	a_8	c_8	0.5	1.22	2.05	0.1
9	a_9	c_9	0.5	1.22	2.05	0.1
10	a_{10}	c_{10}	0.7	1.22	2.05	0.1
11	a_{11}	c_{11}	0.5	1.18	2.05	0.1
12	a_{12}	c_{12}	0.3	1.26	2.05	0.1
13	a_{13}	c_{13}	0.9	1.36	2.05	0.1
14	a_{14}	c_{14}	0.6	1.36	2.05	0.1
15	a_{15}	c_{15}	0.6	1.36	2.05	0.1
16	a_{16}	c_{16}	0.6	1.36	2.05	0.1
17	a_{17}	c_{17}	0.6	1.36	2.05	0.1

Appendix B. Appendices of Chapter 3

Appendix B-1 Mixed complementarity problem of the equilibrium model

We present the mixed complementarity problem (MCP) of the proposed equilibrium model into in this Appendix. The MCP consists of KKT conditions of importer/exporter's optimization problem and the market clearing conditions.

The importer's KKT conditions are:

$$\begin{aligned}
&\forall\, q^{b,LTC},\ \ 0 \le q^{b,LTC} \\
&\qquad \perp -\bar{p}^{CPM} + E(\tilde{p}^{LTC}) + (1-\kappa)\bar{f}^{LTC} + \gamma^b q^{b,LTC} Var(\tilde{p}^{LTC}) \\
&\qquad + \gamma^b \sum_{t=1}^{T} \Big[q_t^{b,SPM+} Cov(\tilde{p}^{LTC}, \tilde{p}_t^{SPM}) \\
&\qquad - q_t^{b,SPM-} Cov\big(\tilde{p}^{LTC}, \tilde{p}_t^{SPM} - \tilde{f}_t^{SPM}\big)\Big] + \sum_{t=1}^{T} \frac{\lambda_t^b}{ord(T)} \\
&\qquad - \sum_{t=1}^{T-1} \frac{ord(t)\mu_t^b}{ord(T)} + \rho^b \ge 0
\end{aligned} \tag{B1}$$

$$
\begin{aligned}
\forall\, q_t^{b,SPM+},\ \ 0 \le q_t^{b,SPM+} \\
&\perp -\bar{p}^{CPM} + E(\tilde{p}_t^{SPM}) \\
&+ \gamma^b \Big[q_t^{b,SPM+} Var(\tilde{p}_t^{SPM}) \\
&- q_t^{b,SPM-} Cov\big(\tilde{p}_t^{SPM}, \tilde{p}_t^{SPM} - \tilde{f}_t^{SPM}\big) \Big] \\
&+ \frac{\gamma^b}{2} \Bigg[\sum_{t' \neq t} q_{t'}^{b,SPM+} Cov\big(\tilde{p}_t^{SPM}, \tilde{p}_{t'}^{SPM}\big) \\
&- \sum_{t' \neq t} q_{t'}^{b,SPM-} Cov\big(\tilde{p}_t^{SPM}, \tilde{p}_{t'}^{SPM} - \tilde{f}_{t'}^{SPM}\big) \Bigg] \\
&+ \gamma^b q^{b,LTC} Cov(\tilde{p}^{LTC}, \tilde{p}_t^{SPM}) + \lambda_t^b - \mu_t^b - \sum_{t'>t}^{T-1} \mu_{t'}^b + \rho^b \ge 0
\end{aligned}
\tag{B2}
$$

$$
\begin{aligned}
\forall\, q_t^{b,SPM-},\ \ 0 \le q_t^{b,SPM-} \\
&\perp \bar{p}^{CPM} - E\big(\tilde{p}_t^{SPM} - \tilde{f}_t^{SPM}\big) \\
&+ \gamma^b \Big[q_t^{b,SPM-} Var\big(\tilde{p}_t^{SPM} - \tilde{f}_t^{SPM}\big) \\
&- q_t^{b,SPM+} Cov\big(\tilde{p}_t^{SPM}, \tilde{p}_t^{SPM} - \tilde{f}_t^{SPM}\big) \Big] \\
&+ \frac{\gamma^b}{2} \Bigg[\sum_{t' \neq t} q_{t'}^{b,SPM-} Cov\big(\tilde{p}_t^{SPM} - \tilde{f}_t^{SPM}, \tilde{p}_{t'}^{SPM} - \tilde{f}_{t'}^{SPM}\big) \\
&- \sum_{t' \neq t} q_{t'}^{b,SPM+} Cov\big(\tilde{p}_t^{SPM} - \tilde{f}_t^{SPM}, \tilde{p}_{t'}^{SPM}\big) \Bigg] \\
&- \gamma^b q^{b,LTC} Cov\big(\tilde{p}^{LTC}, \tilde{p}_t^{SPM} - \tilde{f}_t^{SPM}\big) + \mu_t^b + \sum_{t'>t}^{T-1} \mu_{t'}^b - \rho^b \\
&\ge 0 \quad \forall t, t' \in \{1,2,\dots,T-1\}
\end{aligned}
\tag{B3}
$$

$$
\forall\, \lambda_t^b,\ \ 0 \le \lambda_t^b \perp Q^b - \frac{q^{b,LTC}}{ord(T)} - q_t^{b,SPM+} \ge 0 \quad \forall t \in \{1,2,\dots,T\}
\tag{B4}
$$

$$\forall\ \mu_t^b,\ \ 0 \le \mu_t^b \perp \frac{q^{b,LTC}}{ord(T)} + q_t^{b,SPM+} - q_t^{b,SPM-} + (ord(t)-1)\frac{q^{b,LTC}}{ord(T)} + \sum_{t'<t}\left(q_{t'}^{b,SPM+} - q_{t'}^{b,SPM-} - d_{t'}\right) - d_t \ge 0 \tag{B5}$$

$$\forall\ \rho^b,\ \ free\ \rho^b \perp q^{b,LTC} + \sum_{t=1}^{T}\left(q_t^{b,SPM+} - q_t^{b,SPM-}\right) - \sum_{t=1}^{T} d_t = 0 \tag{B6}$$

The exporter's KKT conditions are:

$$\forall\ q^{s,LTC},\ \ 0 \le q^{s,LTC} \perp -E(\tilde{p}^{LTC}) + \kappa\bar{f}^{LTC} + \gamma^s q^{s,LTC} Var(\tilde{p}^{LTC}) + \gamma^s \sum_{t=1}^{T} q_t^{s,SPM} Cov\left(\tilde{p}^{LTC}, \tilde{p}_t^{SPM} - \tilde{f}_t^{SPM}\right) + \lambda^s \ge 0 \tag{B7}$$

$$\forall\ \lambda^s,\ \ 0 \le \lambda^s \perp Q^s - q^{s,LTC} - \sum_{t=1}^{T} q_t^{s,SPM} \ge 0 \tag{B8}$$

$$\tilde{p}^{LTC} = p_0^{LTC} + \delta(\tilde{p}_T^{OIL} - \bar{p}_0^{OIL}) + (1-\delta)\left[\left(\tilde{p}_T^{SPM} - \kappa\tilde{f}_T^{SPM}\right) - \left(\bar{p}_0^{SPM} - \kappa\bar{f}_0^{SPM}\right)\right] \tag{B9}$$

The market clearing conditions are:

$$\forall\ p_0^{LTC},\ \ free\ p_0^{LTC} \perp q^{b,LTC} - q^{s,LTC} = 0 \tag{B10}$$

$$\forall\ \ q_t^{b,SPM+},\ \ free\ q_t^{b,SPM+} \perp\ q_t^{b,SPM+} - q_t^{s,SPM} = 0 \tag{B11}$$

Appendix B-2 Estimation of importer/exporter's risk aversion parameter

According to Eq. (B1) and Eq. (B7) in Appendix B-1, we can derive the formulars to calculate the risk aversion parameter of importer (γ^b) and that of exporter (γ^s), which

are as follows:

$$\gamma^b = \frac{\bar{p}^{CPM} - E(\tilde{p}^{LTC}) - (1-\kappa)\bar{f}^{LTC} - \sum_{t=1}^{T}\frac{\lambda_t^b}{ord(T)} + \sum_{t=1}^{T-1}\frac{ord(t)\mu_t^b}{ord(T)} - \rho^b}{q^{b,LTC}Var(\tilde{p}^{LTC}) + \sum_{t=1}^{T} q_t^{b,SPM+}Cov(\tilde{p}^{LTC}, \tilde{p}_t^{SPM}) - \sum_{t=1}^{T} q_t^{b,SPM-}Cov(\tilde{p}^{LTC}, \tilde{p}_t^{SPM} - \tilde{f}_t^{SPM})}, \quad \text{(B12)}$$

$$\gamma^s = \frac{E(\tilde{p}^{LTC}) - \kappa\bar{f}^{LTC} - \lambda^s}{q^{s,LTC}Var(\tilde{p}^{LTC}) + \sum_{t=1}^{T} q_t^{s,SPM}Cov(\tilde{p}^{LTC}, \tilde{p}_t^{SPM} - \tilde{f}_t^{SPM})}, \quad \text{(B13)}$$

where $q^{b,LTC}$ and $q^{s,LTC}$ should be positive to ensure that the two equalities hold. Based on the market clearing conditions, $q^{b,LTC}$ equals to $q^{s,LTC}$, and $q_t^{b,SPM+}$ equals to $q_t^{s,SPM}$. Since $\tilde{p}^{LTC}$, $q^{b,LTC}$, $q_t^{b,SPM+}$, and $q_t^{b,SPM-}$ in the future are not observable, we cannot estimate an accurate value of γ^b and γ^s based on the Eq. (B12) and Eq. (B13). However, we can estimate the order of magnitude for γ^b and γ^s according to the actual situation in the current LNG market.

We assume that the LTC will go on with the oil-indexed pricing. On the basis of LTC-spot trade volume ratio reported by **GIIGNL Annual Report 2020**[16], we assume that the LTC volume possesses 70% and spot trade volume possesses 30% in the LNG transaction between the importer and the exporter. The importer does not resell LNG in the spot market. With this assumption, we can determine that $q^{b,LTC}$ ($q^{s,LTC}$) equals to 105 million MMBtu, $\sum_{t=1}^{T} q_t^{b,SPM+}$ ($\sum_{t=1}^{T} q_t^{s,SPM}$) equals to 45 million MMBtu, and $q_t^{b,SPM-}$ equals to 0.

As the oil price is less correlated with the LNG spot price (see Appendix B-3), we can ignore the term of $\sum_{t=1}^{T} q_t^{b,SPM+}Cov(\tilde{p}^{LTC}, \tilde{p}_t^{SPM})$ in Eq. (B12) and the term of

[16] GIIGNL Annual Report 2020 is available at https://giignl.org/system/files/publication/giignl_-_2020_annual_report_-_04082020.pdf/

$\sum_{t=1}^{T} q_t^{s,SPM} Cov\left(\tilde{p}^{LTC}, \tilde{p}_t^{SPM} - \tilde{f}_t^{SPM}\right)$ in Eq. (B13). Without considering the constraints we set the model, γ^b and γ^s can be approximately estimated by following formulars:

$$\gamma^b \approx \frac{\bar{p}^{CPM} - E(\tilde{p}^{LTC})}{q^{b,LTC} Var(\tilde{p}^{LTC})}, \tag{B14}$$

$$\gamma^s \approx \frac{E(\tilde{p}^{LTC}) - \bar{f}^{LTC}}{q^{s,LTC} Var(\tilde{p}^{LTC})}. \tag{B15}$$

We use the average LTC price during November, 2020 to replace $E(\tilde{p}^{LTC})$. This price was published by METI of Japan and equals to 6.8 \$/MMBtu. $\bar{p}^{CPM}$, $\bar{f}^{LTC}$ and $Var(\tilde{p}^{LTC})$ refers to the value we present in Section 5. Through Eq. (B14) and Eq. (B15), we can calculate that γ^s equals to 0.021 and γ^s equals to 0.061. The estimation results show: a) the order of magnitude for risk aversion parameter is around 10^{-2}; b) γ^s is around 3 times of γ^b.

Appendix B-3 Covariances between LTC and spot LNG prices under different benchmark

$t \in \{1,2,\dots,T\}$	Oil benchmark		JKM benchmark (CIF)		JKM benchmark (FOB)	
$T = 52$	$Cov1$	$Cov2$	$Cov1$	$Cov2$	$Cov1$	$Cov2$
1	-0.0027	0.0065	0.0078	0.0086	0.0079	0.0089
2	-0.0100	-0.0095	0.0215	0.0235	0.0210	0.0231
3	-0.0102	-0.0144	0.0292	0.0324	0.0297	0.0331
4	-0.0062	-0.0108	0.0271	0.0316	0.0277	0.0325
5	-0.0074	-0.0065	0.0207	0.0227	0.0198	0.0221
6	-0.0131	-0.0171	0.0265	0.0256	0.0249	0.0243
7	-0.0115	-0.0153	0.0224	0.0216	0.0207	0.0201
8	-0.0094	-0.0146	0.0221	0.0206	0.0203	0.0190
9	-0.0077	-0.0073	0.0256	0.0234	0.0236	0.0214
10	-0.0168	-0.0161	0.0270	0.0248	0.0254	0.0231
11	-0.0155	-0.0134	0.0313	0.0306	0.0301	0.0292
12	-0.0209	-0.0195	0.0235	0.0234	0.0215	0.0212
13	-0.0293	-0.0256	0.0310	0.0308	0.0287	0.0284

14	-0.0140	-0.0131	0.0267	0.0273	0.0238	0.0243
15	-0.0145	-0.0173	0.0296	0.0299	0.0258	0.0260
16	-0.0182	-0.0194	0.0458	0.0463	0.0419	0.0423
17	-0.0325	-0.0396	0.0413	0.0421	0.0388	0.0393
18	-0.0338	-0.0397	0.0533	0.0532	0.0524	0.0523
19	-0.0537	-0.0551	0.0611	0.0613	0.0602	0.0605
20	-0.0524	-0.0540	0.0720	0.0720	0.0728	0.0726
21	-0.0516	-0.0550	0.0676	0.0674	0.0680	0.0678
22	-0.0517	-0.0557	0.0798	0.0791	0.0796	0.0789
23	-0.0272	-0.0306	0.0812	0.0805	0.0821	0.0814
24	-0.0292	-0.0303	0.0943	0.0942	0.0959	0.0958
25	-0.0230	-0.0222	0.0922	0.0928	0.0935	0.0940
26	-0.0283	-0.0278	0.1053	0.1053	0.1065	0.1065
27	-0.0316	-0.0324	0.1006	0.1006	0.1014	0.1013
28	-0.0217	-0.0205	0.1085	0.1096	0.1093	0.1104
29	-0.0176	-0.0216	0.1277	0.1287	0.1275	0.1285
30	-0.0044	-0.0072	0.1381	0.1391	0.1376	0.1387
31	-0.0062	-0.0039	0.1612	0.1625	0.1618	0.1631
32	-0.0070	-0.0067	0.1669	0.1676	0.1682	0.1691
33	0.0024	0.0027	0.1747	0.1754	0.1748	0.1756
34	-0.0009	-0.0032	0.1935	0.1936	0.1942	0.1943
35	0.0022	0.0018	0.2177	0.2175	0.2191	0.2190
36	0.0096	0.0115	0.2262	0.2262	0.2275	0.2277
37	0.0045	0.0073	0.2426	0.2425	0.2437	0.2436
38	0.0099	0.0138	0.2502	0.2487	0.2523	0.2509
39	0.0133	0.0169	0.2764	0.2747	0.2779	0.2763
40	0.0104	0.0131	0.2998	0.2979	0.3004	0.2987
41	-0.0031	0.0034	0.3310	0.3288	0.3314	0.3295
42	-0.0016	-0.0004	0.3728	0.3710	0.3729	0.3715
43	-0.0006	-0.0008	0.4076	0.4069	0.4078	0.4076
44	0.0103	0.0072	0.4585	0.4582	0.4590	0.4594
45	0.0148	0.0137	0.5101	0.5094	0.5106	0.5108
46	0.0034	-0.0017	0.5564	0.5554	0.5559	0.5561
47	0.0080	0.0049	0.6152	0.6140	0.6141	0.6145
48	-0.0007	-0.0013	0.6842	0.6828	0.6832	0.6841
49	-0.0098	-0.0072	0.7713	0.7695	0.7708	0.7722
50	-0.0093	-0.0122	0.8557	0.8546	0.8559	0.8591
51	-0.0055	-0.0024	0.9490	0.9489	0.9488	0.9546
52	-0.0150	-0.0100	1.0583	1.0586	1.0586	1.0671

Note: $Cov1 = Cov(\tilde{p}^{LTC}, \tilde{p}_t^{SPM})$; $Cov2 = Cov\left(\tilde{p}^{LTC}, \tilde{p}_t^{SPM} - \tilde{f}_t^{SPM}\right)$.

Appendix C. Appendices of Chapter 4

Appendix C-1 Values of exogenous variables and parameters

Table C-1. Values of trade-related exogenous variables

Variable (unit)	Value		Data source
I_c (10^6 \$)	c1 (China)	478369.925	UN Comtrade database (2016)
	c2 (Japan)	80162.411	
	c3 (South Korea)	43098.036	
QTC_m (10^6 tons)	m1 (Brazil)	2408.6	UN Comtrade database (2016)
	m2 (Australia)	8394.5	
CQ_m (\$)	m1 (Brazil)	15.2	MySteel Database (2016)
	m2 (Australia)	17.5	

Table C-2. Values of carrier-related exogenous variables

Variable (unit)	Value		Data source
W_k (10^6 tons)	k1 (small-size ship)	1.8	Shipping Intelligence Network (2018)
	k2 (medium-size ship)	2.6	
	k3 (large-size ship)	3.8	
OD_k (days/year)	All ship type	280	COSCO Shipping (2018)
V_k (knot)	All ship type	12	COSCO Shipping (2018)
CT_k (\$/nautical mile)	k1 (small-size ship)	104	COSCO Shipping (2018)
	k2 (medium-size ship)	128	
	k3 (large-size ship)	150	
NC_k	k1 (small-size ship)	360	Shipping Intelligence Network (2016)
	k2 (medium-size ship)	120	
	k3 (large-size ship)	60	
MV_{mc}	m1-c1	4	Sea-Distances.Org
	m1-c2	4	
	m1-c3	4	
	m2-c1	12.5	
	m2-c2	12	
	m2-c3	12.5	

Table C-3. Values of port-related exogenous variables

Variable (unit)	Value		Data source
PD_{c_d} (\$)	d1(c1)	3.210	Estimation based on Port Charges Rules published by
	d2(c1)	3.210	Ministry of Transport of China
	d3(c1)	3.210	
	d4(c2)	3.852	Mizushima Port Authority
	d5(c3)	3.531	Kwang yang Port Authority
DSD_{c_d} (\$)	d1(c1)	0.556	Estimation based on Port Charges Rules published by
	d2(c1)	0.556	Ministry of Transport of China
	d3(c1)	0.556	
	d4(c2)	0.667	Mizushima Port Authority
	d5(c3)	0.611	Kwang yang Port Authority
PO_{m_o} (\$)	o1(m1)	2.010	Regulations of Terminals-Vale
	o2(m1)	2.010	
	o3(m1)	2.010	
	o4(m2)	3.480	Pilbara Ports Authority
	o5(m2)	3.480	Rio Tinto Ltd
DSO_{m_o} (\$)	o1(m1)	0.722	Regulations of Terminals-Vale
	o2(m1)	0.722	
	o3(m1)	0.722	
	o4(m2)	0.817	Pilbara Ports Authority
	o5(m2)	0.639	Rio Tinto Ltd

Table C-4. Values of conjectural variations

Parameter	Value	
$\mu_{mm'c}$	m1-m2-c1	0.696
	m1-m2-c2	0.687
	m1-m2-c3	0.463
	m2-m1-c1	-0.455
	m2-m1-c2	-0.340
	m2-m1-c3	-0.765

Table C-5. Values of parameters in utility function and production possibility frontier

Parameter		Value
CES utility function		
σc_c	c1	0.814
	c2	0.855
	c3	0.569
δ_{mc}^{d}	m1-c1	0.463
	m2-c1	0.537
	m1-c2	0.521
	m2-c2	0.479
	m1-c3	0.398
	m2-c3	0.602
CET production possibility frontier		
σm_m	m1	1.331
	m2	1.716
AC_m	m1	2.393
	m2	4.558
δ_{mc}^{s}	m1-c1	0.193
	m1-c2	0.334
	m1-c3	0.473
	m2-c1	0.091
	m2-c2	0.385
	m2-c3	0.524

Table C-6. Values of parameters in CES production function

Parameter	Value	
CES production function (destination port)		
σd_c	c1	0.396
	c2	1.000
	c3	1.000
AD_c	c1	2.492
	c2	1.000
	c3	1.000
$\delta_{c_d}^{DP}$	d1(c1)	0.539
	d2(c1)	0.319
	d3(c1)	0.142
	d4(c2)	1.000
	d5(c3)	1.000
CES production function (origin port)		
σo_m	m1	0.762
	m2	0.711
AO_m	m1	2.995
	m2	1.863
$\delta_{m_o}^{OP}$	o1(m1)	0.338
	o2(m1)	0.342
	o3(m1)	0.320
	o4(m2)	0.606
	o5(m2)	0.394

Appendix C-2 Parameter estimation in the model

Parameters in CES utility function

The parameter of elasticity σc_c and share parameters δ_{mc}^{d} in utility function (4.1) need to be estimated. Two exporters are included in the case study. For an importer *c*, we can derive the equation (B1) from its inverse demand functions:

$$\frac{P_{m1c}}{P_{m2c}} = \frac{\delta^d_{m1c} {Q_{m1c}}^{\sigma c_c - 1}}{\delta^d_{m2c} {Q_{m2c}}^{\sigma c_c - 1}}. \quad \text{(C1)}$$

The parameter estimation function is derived from the linearization of equation (C1), shown as:

$$Y = a0 + a1 \cdot X_c + \varepsilon, \quad \text{(C2)}$$

where Y equals to $\ln(\frac{P_{m1c}}{P_{m2c}})$, coefficient $a0$ equals to $\ln(\frac{\delta^d_{m1c}}{\delta^d_{m2c}})$, $a1$ ($a1 = \sigma c_c - 1$) is the coefficient with respective to (w.r.t) parameter of elasticity σc_c, ε is the error term.

Since the share parameters of δ^d_{mc} satisfies $\delta^d_{m1c} + \delta^d_{m2c} = 1$, δ^d_{mc} can be calibrated by following equations as long as σc_c is estimated:

$$\delta^d_{m1c} = \frac{P_{m1c} {Q_{m1c}}^{\sigma c_c - 1}}{P_{m1c} {Q_{m1c}}^{\sigma c_c - 1} + P_{m2c} {Q_{m2c}}^{\sigma c_c - 1}}, \quad \text{(C3)}$$

$$\delta^d_{m2c} = 1 - \delta^d_{m1c}. \quad \text{(C4)}$$

Parameters in CET/CES production functions

The parameters of CET PPF (constraint 4.8.a) in exporter module and those of CES functions (constraint 4.23.a and 4.26.a) in port selection problem are estimated through the same method. For clarity of expression, here we present the estimation function as a generic formation. A general form of CET/CES production function can be given as:

$$y = A\left(\sum_{i \in I} \delta_i {x_i}^{\sigma}\right)^{1/\sigma} \quad \forall\, i \in I, \quad \text{(C5)}$$

where y is the volume of composite goods, x_i is the volume of substitutable goods i in corresponding set I, σ is the parameter of substitution elasticity, A is the efficiency

parameter related to the level of technology, δ_i is share parameter of x_i, satisfying $\sum_{i\in I}\delta_i = 1$. Here we discuss the CET/CES functions composed by two and three substitutable goods. For multiple substitutable goods (over three goods), the corresponding CES/CET function is constructed as a nested form, which consists of multi-level two-goods CES functions. Parameter estimation of a nested CES/CET function is a process to estimate the parameters of two-goods function at each level. See details in Koesler and Schymura (2012).

The parameter estimation of function (C5) is based on the Kmenta approximation approach applied by Koesler and Schymura (2012). We write the equation (C5) as a logarithmic form:

$$\ln y = \ln A + \frac{1}{\sigma}\cdot \ln\left(\sum_{i\in I}\delta_i {x_i}^{\sigma}\right). \tag{C6}$$

We replace the function (C6) by its linear approximation in σ. This can be implemented through Taylor expansion at $\sigma = 0$. For two-goods CET/CES functions ($i \in \{1,2\} = I$), the linear estimation function is show as:

We replace the function (C6) by its linear approximation in σ. This can be implemented through Taylor expansion at $\sigma = 0$. For two-goods CET/CES functions ($i \in \{1,2\} = I$), the linear estimation function is show as:

$$Y = \ln A + \delta_1 \cdot X1 + \delta_2 \cdot X2 + \frac{1}{2}\sigma\delta_1\delta_2 \cdot X3 + \varepsilon, \tag{C7}$$

where $X1$ equals to $\ln x_1$, $X2$ equals to $\ln x_2$, $X3$ equals to $\left[\ln(\frac{x_1}{x_2})\right]^2$, and ε is the error term. All parameters in a two-goods CET/CES function can be directly estimated through ordinary least squares.

For three-goods CET/CES functions ($i \in \{1,2,3\} = I$), the linear estimation function is show as:

$$Y = \ln A + \delta_1 \cdot X1 + \delta_2 \cdot X2 + \delta_3 \cdot X3 + \frac{1}{2}\sigma\delta_1\delta_2 \cdot X4 + \frac{1}{2}\sigma\delta_2\delta_3 \cdot X5 + \frac{1}{2}\sigma\delta_3\delta_1 \cdot X6 + \varepsilon, \tag{C8}$$

where $X1$ equals to $\ln x_1$, $X2$ equals to $\ln x_2$, $X3$ equals to $\ln x_3$, $X4$ is $\left[\ln(\frac{x_1}{x_2})\right]^2$, $X5$ is $\left[\ln(\frac{x_2}{x_3})\right]^2$, $X6$ is $\left[\ln(\frac{x_3}{x_1})\right]^2$ and ε is the error term. All parameters in equation (B8) can also be directly estimated through ordinary least squares.

Parameters of conjectural variations

For two exporters in the numerical study, the inverse demand function (4.2) is shown as:

$$P_{mc} = P_{mc}(Q_{mc}, Q_{m'c}) = \frac{\overline{IC}_c \delta_m^d {Q_{mc}}^{\sigma c_c - 1}}{\delta_{mc}^d {Q_{mc}}^{\sigma c_c} + \delta_{m'c}^d {Q_{m'c}}^{\sigma c_c}}, \tag{C9}$$

where m' ($m' \in M \backslash m$) is a rival of exporter $m \in M = \{m1, m2\}$.

We introduce the Lerner Index to estimate the conjectural variations. The Lerner index should equal to the inverse of price elasticity derived from (C9), as:

$$LI_{mc} = \frac{\partial P_{mc}(Q_{mc}, Q_{m'c})}{\partial Q_{mc}} \cdot \frac{Q_{mc}}{P_{mc}} = \sigma c_c \cdot \frac{P_{m'c}}{\overline{IC}_c}(Q_{m'c} - \mu_{mm'c} Q_{mc}) - 1, \tag{C10}$$

where LI_{mc} is the Lerner index, $\mu_{mm'c}$ is the conjectural variation of exporter m to its rival in the trade with importer c ($\mu_{mm'c} = \frac{\partial Q_{m'c}}{\partial Q_{mc}}$).

Depending on the (C10), the estimation function can be given as:

$$Y = a1 \cdot X1 + a2 \cdot \mathrm{X2} + \varepsilon \tag{C11}$$

where Y equals to $\frac{\overline{IC}_c}{P_{m'c}}$, $X1$, X2 equal to $Q_{m'c}$ and Q_{mc} respectively, coefficient $a1$ equals to $\frac{\sigma c_c}{LI_{mc}+1}$, $a2$ equals to $-\frac{\sigma c_c}{LI_{mc}+1} \cdot \mu_{mm'c}$. The conjectural variation $\mu_{mm'c}$ should be $-\frac{a2}{a1}$. The equation (C11) can be estimated via ordinary least squares.